



저작자표시-비영리-변경금지 2.0 대한민국

이용자는 아래의 조건을 따르는 경우에 한하여 자유롭게

- 이 저작물을 복제, 배포, 전송, 전시, 공연 및 방송할 수 있습니다.

다음과 같은 조건을 따라야 합니다:



저작자표시. 귀하는 원저작자를 표시하여야 합니다.



비영리. 귀하는 이 저작물을 영리 목적으로 이용할 수 없습니다.



변경금지. 귀하는 이 저작물을 개작, 변형 또는 가공할 수 없습니다.

- 귀하는, 이 저작물의 재이용이나 배포의 경우, 이 저작물에 적용된 이용허락조건을 명확하게 나타내어야 합니다.
- 저작권자로부터 별도의 허가를 받으면 이러한 조건들은 적용되지 않습니다.

저작권법에 따른 이용자의 권리는 위의 내용에 의하여 영향을 받지 않습니다.

이것은 [이용허락규약\(Legal Code\)](#)을 이해하기 쉽게 요약한 것입니다.

[Disclaimer](#)

이학박사 학위논문

알츠하이머 병에서 Gamma-secretase 활성을
조절하는 인자 발굴 및 분자 기전 연구

**Identification of novel Gamma-secretase
regulators and its functions in Alzheimer's
disease**

2025년 2월

서울대학교 대학원

생명과학부

현준호

Identification of novel Gamma-secretase regulators and its functions in Alzheimer's disease

Advisor: Professor Yong-Keun Jung, Ph.D.

**Submitting a Ph.D. Dissertation of
Biological Sciences
February, 2025**

**Graduate School of Natural Sciences
Seoul National University
Biological Science Major**

Junho Hyun

**Confirming the Ph.D. Dissertation written by
Junho Hyun
December, 2024**

Chair _____ Jae Hong Seol _____ (Seal)

Vice Chair _____ Yong-Keun Jung _____ (Seal)

Examiner _____ Sukwoo Choi _____ (Seal)

Examiner _____ Dong-Gyu Jo _____ (Seal)

Examiner _____ Tae-In Kam _____ (Seal)

ABSTRACT

Identification of novel Gamma-secretase regulators and its functions in Alzheimer's disease

Junho Hyun

School of Biological Science

Seoul National University

Alzheimer's disease (AD) is characterized by the accumulation of amyloid-beta ($A\beta$), a process driven by the γ -secretase complex. While γ -secretase is critical for $A\beta$ generation, its regulation under pathological conditions such as hypoxic conditions and neuroinflammation remains poorly understood. In this study, I investigated two novel regulators of γ -secretase, pyruvate kinase M2 (PKM2) and nicotinamide phosphoribosyltransferase (NAMPT), uncovering distinct but convergent mechanisms that link stress-mediated gene expression and inflammatory pathways to amyloidogenic processing.

PKM2 was shown to regulate γ -secretase activity through transcriptional control of APH-1a, one of the core component of the γ -secretase complex. PKM2's nuclear dimeric form acted as a transcription co-activator, modulating APH-1a

transcription via histone modification and HDAC3 inhibition. In vitro and in vivo experiments confirmed PKM2's role in γ -secretase activation, A β production, and memory impairment in AD model mice. Importantly, PKM2's regulatory role is independent of its metabolic functions, emphasizing its transcriptional regulation in AD pathogenesis.

NAMPT, identified through a gain-of-function screening, was found to selectively enhance γ -secretase activity without affecting α - or β -secretases or Notch cleavage. NAMPT levels were elevated in AD mouse models and patient CSF, correlating with disease progression. Mechanistically, NAMPT interacted with IFITM3, a presenilin regulator, and extracellular NAMPT induced IFITM3 expression via NF- κ B signaling. These findings highlight NAMPT's dual role as a secreted inflammatory mediator and a γ -secretase regulator.

Together, this study identifies PKM2 and NAMPT as distinct but complementary γ -secretase regulators, integrating stress-mediated gene expression and inflammatory pathways into the pathogenesis of AD. These findings provide novel insights into γ -secretase modulation and propose both PKM2 and NAMPT as potential therapeutic targets for Alzheimer's disease.

Key Words: Alzheimer's disease, γ -secretase, Amyloid-beta (A β), PKM2, NAMPT, Hypoxic conditions, Neuroinflammation

Student Number: 2017-25409

CONTENTS

ABSTRACT.....	i
CONTENTS.....	iii
LIST OF FIGURES.....	viii
ABBREVIATION.....	xiii
BACKGROUND.....	1
CHAPTER I. PKM2 modulates γ-secretase activity through transcriptional regulation of APH1a	
I-1.Introduction.....	14
I-2.Results.....	17
PKM2 expression is elevated in the brains of AD patients and AD mouse models.....	17
PKM2 modulates γ -secretase activity without affecting other secretase activities.....	18
PKM2 modulates the assembly of the γ -Secretase complex.....	18

PKM2 modulates γ -secretase activity affecting both APP and Notc5 processing.....	19
Dimeric PKM2 modulates γ -secretase activity via transcription regulation....	20
PKM2 specifically modulates mRNA level of APH1a.....	21
PKM2 modulates APH-1a transcription via HDAC3 inhibition.....	22
PKM2 mediates γ -secretase activation in hypoxic neurons.....	23
Neuronal expression of PKM2 exacerbates A β production and memory decline in 3xTg AD mice.....	24
I-3. Discussion.....	73
I-4. Limitation of study.....	76

CHAPTER II. NAMPT upregulates γ -secretase activity under inflammation condition

II-1.Introduction.....	77
II-2. Results.....	79
NAMPT was identified as γ -secretase regulator through a cell-based gain-of-function γ -secretase reporter assay.....	79
Levels of NAMPT are elevated in brains of 3xTg AD model mice and AD patients.....	79

NAMPT modulates γ -secretase activity without affecting other secretase activities.	81
NAMPT is a Notch-sparing γ -secretase regulator.	82
Enzymatic activity of NAMPT is not associated with regulation of γ -secretase activity.	83
NAMPT does not alter levels of γ -secretase complex and components.....	84
NAMPT is mainly expressed in glial cells and is upregulated by LPS stimulation.....	85
NAMPT knockdown blocks the induction of AICD levels under LPS stimulation.....	85
NAMPT binds to IFITM3, a Presenilin regulator.....	86
NAMPT and IFITM3 are induced by LPS injection and mediate increase of γ -secretase activity in mice.....	87
Recombinant NAMPT induces increase of NAMPT and IFITM3 expression through NF- κ B signaling.....	88
NAMPT knockdown reduces IFITM3-associated γ -secretase complex levels without affecting overall complex abundance.....	89
II-3. Discussion.....	123
II-4. Limitation of study.....	126

Conclusion.....	128
Materials and Methods.....	130
Genome-wide functional screen using cDNA.....	130
SDS-PAGE and western blot.....	130
ELISA.....	131
In vitro AICD generation assays.....	131
BN-PAGE.....	131
γ -Secretase activity assay.....	131
β -secretase assays.....	132
α -secretase assays.....	132
qPCR.....	132
Glutaraldehyde cross-linking.....	133
X-ChIP.....	133
Behavior tests.....	134
Measurement of intracellular concentrations of pyruvate and ATP.....	135
Immunohistochemistry.....	135
Lentivirus generation.....	135
Stereotaxic injection.....	136

LIST OF FIGURES

Figure A. Schematic of the APP cleavage process.....	22
Figure B. A list of of Gamma-secretase inhibitor.....	24
Figure C. Gamma-secretase regulators.....	26
Figure I-1. PKM2 expression is elevated in the brains of AD patients.....	27
Figure I-2. PKM2 expression is elevated in the brains of AD mouse model.....	29
Figure I-3. PKM2 modulates gamma-secretase activity without affecting other secretase activities.....	31
Figure I-4. PKM2 modulates γ -secretase complex level via APH1a-NCT sub-complex.....	33
Figure I-5. PKM2 modulates APH1a-NCT sub-complex.....	35
Figure I-6. PKM2 regulates individual γ -secretase component levels, especially APH1a.....	37
Figure I-7. PKM2 modulates γ -secretase activity affecting Notch processing...	39
Figure I-8. Dimeric PKM2 regulates γ -secretase activity.....	41
Figure I-9. Pyruvate level in culture medium and cellular ATP level do not affect to γ -Secretase activity.....	43

Figure I-10. PKM2 specifically modulates level of APH1a mRNA.....45

Figure I-11. PKM2 modulates APH-1a transcription via HDAC3 inhibition....47

Figure I-12. PKM2 mediates γ -secretase activation in hypoxic primary neurons.....49

Figure I-13. PKM2 regulates γ -secretase component level in hypoxic primary neurons.....51

Figure I-14. PKM2 regulates gamma-secretase component level **under hypoxic stress**.....53

Figure I-15. Neuronal expression of PKM2 elevates APH1a protein expression in 3xTg AD mice.....55

Figure I-16. Neuronal expression of PKM2 aggravates A β generation in 3xTg AD mice.....57

Figure I-17. Neuronal expression of PKM2 accelerates A β burden and gliosis in 3xTg AD mice.....59

Figure I-18. Neuronal expression of PKM2 accelerates gliosis in 3xTg AD mice.....61

Figure I-19. Hippocampal knockdown of PKM2 dampens expression of γ -secretase components.....63

Figure I-20. Hippocampal knockdown of PKM2 reduces amyloid burden in 3xTg AD mice.....65

Figure I-21. Neuronal expression of PKM2 aggravates memory decline in 3xTg AD mice.....67

Figure I-22. Hippocampal knockdown of PKM2 rescues memory decline in 3xTg AD mice.....69

Figure I-23. Schematic diagram of PKM2's molecular mechanism in AD pathogenesis.....71

Figure II-1. Schematic diagram showing gain-of-function screening and isolation of NAMPT which increases reporter activity of γ -secretase.....110

Figure II-2. Levels NAMPT expression and γ -secretase components are elevated in 3xTg mouse brain.....112

Figure II-3. NAMPT expression level is elevated in the CSF and cortex of AD patients.....114

Figure II-4. Levels of NAMPT mRNA expression in 3xTg mice and AD patients.....116

Figure II-5. NAMPT affects γ -secretase activity without affecting other secretases.....118

Figure II-6. Expression of NAMPT enhances A β secretion after proteolytic processing of APP into the conditioned medium.....120

Figure II-7. NAMPT is a notch-sparing γ -secretase regulator..... 122

Figure II-8. The enzymatic activity of NAMPT is not associated with its effects on γ -secretase activity.....124

Figure II-9. Expression levels of NAMPT do not affect γ -secretase components and complex expression.....126

Figure II-10. NAMPT expression in glial cells is upregulated by LPS stimulation.....128

Figure II-11. NAMPT knockdown blocks the LPS-induced induction of AICD level.....130

Figure II-12. NAMPT binds to IFITM3, a presenilin regulator.....132

Figure II-13. LPS (i.p.) injection increases NAMPT and IFITM3 levels in the mouse brain and upregulates γ -secretase activity.....134

Figure II-14. Treatment with recombinant NAMPT protein increases levels of NAMPT and IFITM3 through NF-kB signaling.....136

Figure II-15. NAMPT knockdown interferes with the IFITM3-associated γ -secretase complex.....138

Figure II-16. Schematic diagram of the proposed molecular mechanism of
NAMPT in AD pathogenesis.....140

ABBREVIATION

A β	Amyloid beta
AD	Alzheimer's disease
AICD	APP intracellular domain
APH1	Anterior pharynx-defective phenotype 1
APP	Amyloid precursor protein
BACE1	β -site amyloid precursor protein cleaving enzyme
BN-PAGE	Blue native PAGE
CCR5	C-C chemokine receptor type 5
CSF	Cerebrospinal fluid
FBS	Fetal bovine serum
GFP	Green fluorescence protein
GOFS	Gain of function screening
HA	Hemagglutinin
IFITM3	Interferon-induced transmembrane protein 3
IL1 β	Interleukin-1 beta
IL6	Interleukin 6
IP	Immunoprecipitation
LPS	Lipopolysaccharide

NAD	Nicotinamide adenine dinucleotide
NAMPT	Nicotinamide phosphoribosyltransferase
NCT	Nicestrin
NICD	Notch intracellular domain
NMN	Nicotinamide mononucleotide
PBEF	Pre-B-cell colony-enhancing factor 1
PBS	Phosphate buffered saline
PEN2	Presenilin enhancer 2
PK	Pyruvate kinase
PS	Presenilin
shRNA	Small hairpin RNA
TLR4	Toll like receptor 4
TNF α	Tumor necrosis factor α

BACKGROUND

Overview of existing research on γ -secretase

Alzheimer's disease is characterized by the accumulation of amyloid beta ($A\beta$) aggregates in the brain. The formation and accumulation of $A\beta$ are critical in Alzheimer's pathology, and several mechanisms can lead to its increased presence, including enhanced production, reduced degradation, or facilitated propagation of $A\beta$ aggregates. Among these mechanisms, the production of $A\beta$ has been identified as a significant contributor, where γ -secretase plays a pivotal role as it is responsible for the final cleavage step of APP that results in $A\beta$ formation (Figure A.).

APP undergoes sequential cleavage steps involving multiple proteases: alpha-secretase, beta-secretase (BACE1), and γ -secretase. Alpha-secretase primarily generates non-amyloidogenic fragments by cleaving APP within the $A\beta$ domain, thereby preventing $A\beta$ formation. Beta-secretase (BACE1) initiates the amyloidogenic pathway by cleaving APP outside the $A\beta$ domain, creating a substrate for gamma-secretase. γ -secretase is crucial as it executes the final cleavage, determining the generation of $A\beta$ fragments. This step is especially important because γ -secretase cleavage not only determines whether $A\beta$ is produced but also influences the specific length of the $A\beta$ fragment, with longer fragments such as $A\beta_{42}$ being more prone to aggregation and neurotoxicity, thus playing a central role in Alzheimer's disease progression (Figure A.).

Challenges with BACE1 and γ -secretase inhibitors

Efforts to target the amyloidogenic pathway initially focused on BACE1 inhibitors, given their role in the early stages of APP cleavage. Several BACE1 inhibitors, such as Verubecestat and Lanabecestat, were developed with the aim of reducing A β production by blocking the initial cleavage step of APP. However, these inhibitors faced significant setbacks during clinical trials. Verubecestat, for example, failed in Phase 3 trials due to adverse effects like cognitive decline and synaptic dysfunction, attributed to BACE1's involvement in cleaving multiple substrates essential for synaptic function and neurodevelopment. This highlighted the challenges of broadly inhibiting BACE1 without affecting other critical physiological processes. Another BACE1 inhibitor, Lanabecestat, was halted in clinical trials despite effectively reducing A β levels. The lack of cognitive improvement indicated that A β reduction alone was insufficient to halt Alzheimer's disease progression. These findings suggest that inhibiting BACE1, while theoretically reducing A β production, disrupts other pathways vital to brain function, limiting the clinical viability of this approach.

γ -secretase inhibitors, such as Semagacestat and Avagacestat, also encountered major obstacles. Semagacestat, a prominent gamma-secretase inhibitor, initially showed promise due to its ability to lower A β levels by targeting gamma-secretase activity. However, Phase 3 trials revealed that the drug not only failed to improve cognitive outcomes but also worsened them, in addition to increasing the risk of skin cancer. The primary issue was that γ -secretase is not specific to APP; it also cleaves other critical substrates, like Notch, involved in cell differentiation and immune function. Inhibiting γ -secretase, therefore, had widespread unintended consequences. Avagacestat, designed to selectively inhibit γ -secretase with minimal impact on Notch, aimed to minimize these side effects. However, it too failed in clinical trials due to gastrointestinal complications and cognitive decline. These outcomes

demonstrate the difficulty of developing selective inhibitors for γ -secretase, given its involvement in multiple cellular pathways beyond APP processing (Figure B).

Research has thus shifted towards understanding not only the structural components of the γ -secretase complex but also the molecular mechanisms by which various modulators regulate its activity. This shift is crucial because, besides the essential components like Nicastrin (NCT), Presenilin (PS), APH1, and PEN2, several modulators interact with these components, influencing γ -secretase's activity and substrate specificity. Identifying and understanding these modulators are essential to developing strategies for selective regulation of γ -secretase without affecting its other physiological roles. As a result, research has focused on studying these modulators and their roles in regulating γ -secretase function to fine-tune therapeutic approaches.

Reported regulators of γ -secretase activity

Recent studies have identified various modulators beyond the core components of γ -secretase that play critical roles in its regulation: IFITM3, known to be upregulated in response to aging and cytokines, such as interferon-gamma ($\text{IFN}\gamma$), interacts with presenilin, influencing γ -secretase activity in neurons, enhancing $\text{A}\beta$ production in Alzheimer's patients, particularly in aged tissues (Ji-Yeun Hur et al. 2020). TMP21, a cargo receptor, binds presenilin and inhibits γ -secretase activity, reducing $\text{A}\beta$ production. β -arrestin2, a GPCR protein, modulates the localization of the γ -secretase complex, relocating it to lipid rafts or endosomes, altering its cleavage activity (Amanth Thathiah et al. 2013). CD147, a transmembrane glycoprotein, binds to γ -secretase components and modifies its localization, enhancing its affinity for APP and thereby increasing $\text{A}\beta$ production (Chen et al 2006). Another example is GSAP (Gamma-

Secretase Activating Protein), which has been shown to specifically increase γ -secretase activity toward APP without affecting Notch cleavage, making it a target of interest for modulating A β production selectively (Figure C).

3-dimensional structure of the γ -secretase complex

Research continues to focus on the structural and molecular mechanisms of the γ -secretase complex, with recent advances in cryo-EM and AI-driven bioinformatics shedding light on its 3D structure. One notable study using cryo-electron microscopy analyzed the conformational states of the γ -secretase complex, particularly focusing on the arrangement of its core components like Presenilin and Nicastrin, under various conditions. This study provided insights into how gamma-secretase adjusts its conformation to accommodate different substrates and modulators, highlighting the enzyme's structural flexibility. These structural models have led to the development of computational simulations to predict how specific inhibitors or activators might interact with the complex, offering a promising direction for the design of more selective therapeutic agents that minimize off-target effects (Peilong Lu et al. 2014).

Issues on the existing research

As the potential for regulating γ -secretase activity was recognized, initial efforts focused on inhibiting its ability to cleave APP in order to reduce amyloid beta (A β) production. However, these attempts faced significant challenges, including severe side effects and clinical failures due to the enzyme's complexity. For instance, Semagacestat, one of the most well-known γ -

secretase inhibitors, not only failed to improve cognitive outcomes but was also linked to the acceleration of cognitive decline and an increased risk of skin cancer in clinical trials. This outcome was attributed to its broad inhibition of γ -secretase, which disrupted critical pathways beyond A β production, such as Notch signaling, leading to unintended effects on cell differentiation and immune responses. Another example, Avagacestat, was designed to minimize Notch-related side effects, but it too caused adverse reactions, including gastrointestinal issues and cognitive impairment, leading to the discontinuation of its development. These cases demonstrate the difficulty in achieving selective inhibition of γ -secretase activity without affecting its essential roles in other signaling pathways (Bruno P et al. 2011).

Complexity and diversity of the γ -secretase complex

The γ -secretase complex's diversity is further highlighted by the existence of homologous proteins and isoforms. For example, the complex can be formed with either Presenilin 1 (PS1) or Presenilin 2 (PS2), which are homologs encoded on different chromosomes. Both PS1 and PS2 are capable of forming functional γ -secretase complexes, but they may exhibit differences in activity and tissue distribution. Additionally, APH1, another essential component, exists as APH1a and APH1b. Within APH1a, there are isoforms such as the long and short forms, each of which can participate in forming the complex. These variations in essential components contribute to the formation of distinct γ -secretase complexes, increasing the complexity of its structure and function (Natalya Gertsik et al. 2015; Sebastien S et al. 2004).

Notch signaling and its interaction with γ -secretase

Notch signaling is a critical pathway regulated by γ -secretase. The Notch receptor, after ligand binding, undergoes two sequential cleavages; the final one is performed by γ -secretase, releasing the Notch intracellular domain (NICD). This NICD moves to the nucleus and regulates gene expression, influencing processes like cell differentiation, proliferation, and apoptosis, particularly through target genes such as HES and HEY. Inhibition of gamma-secretase disrupts this essential pathway, as seen in clinical trials where γ -secretase inhibitors caused immune dysregulation and abnormal skin growths due to compromised Notch signaling. These examples illustrate the dual role of γ -secretase in Alzheimer's disease and other cellular functions, making it challenging to target the enzyme specifically for A β reduction without impacting other essential pathways.

The presence of such diversity highlights why simple, non-specific inhibitors often fail in clinical settings. The γ -secretase complex's ability to adjust its composition and function based on tissue-specific needs and its interaction with various regulatory proteins makes it difficult to achieve selective inhibition of A β production without affecting other critical pathways, such as those involving Notch.

Necessity and importance of the research on γ -secretase

γ -secretase is involved in the final stage of APP cleavage, which directly influences the amount of amyloid beta produced. Additionally, when APP is cleaved, it generates amyloid beta fragments of varying lengths; among these, amyloid beta 42 (A β 42) is known to be more cytotoxic and prone to aggregation compared to the more common amyloid beta 40 (A β 40).

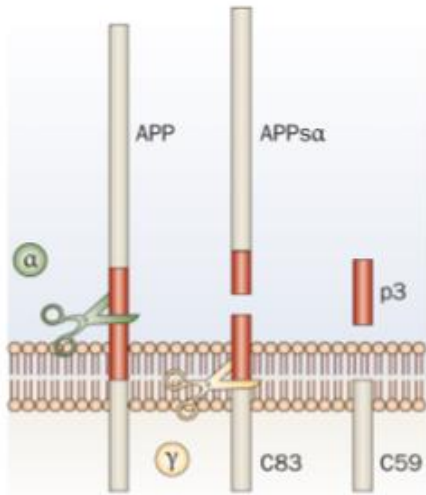
Since these various lengths of amyloid beta are all products of γ -secretase cleavage, it is a crucial enzyme in Alzheimer's disease that must be studied intensively.

γ -secretase forms complexes based on its essential protein components, and these complexes assemble according to the intracellular membrane environment. The fact that γ -secretase is a membrane protein complex, combined with the involvement of regulatory proteins that interact depending on cellular conditions, adds complexity to its regulation. This complexity has made it challenging to fully understand the regulatory mechanisms of γ -secretase. The diversity in substrate specificity, beyond the variation in protein component combinations, further requires a broad perspective and approach in research. This is why there is still an incomplete understanding of its properties and regulatory mechanisms. Comprehensive research to elucidate γ -secretase's function is necessary, as understanding this enzyme will not only shed light on the molecular mechanisms underlying Alzheimer's disease progression driven by amyloid beta but also help explore the physiological consequences related to the various substrates and components involved in its complex.

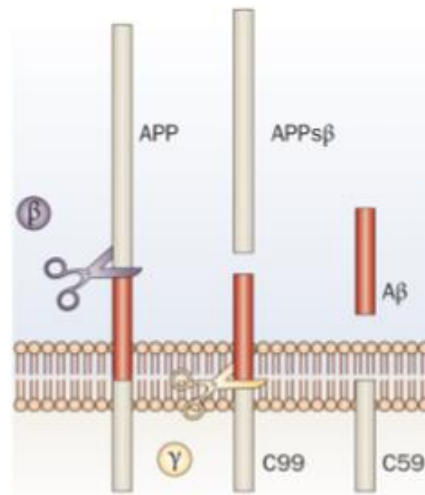
Figure A. Schematic of the APP Cleavage

APP can be processed by ectodomain shedding enzyme, Beta-secretase (BACE1) or Alpha-secretase. When Beta-secretase (BACE1) cleaves APP, C99 is generated. Gamma-secretase cleaves intra-transmembrane region of C99 substrate to release amyloid beta ($A\beta$) species, and APP intracellular domain (AICD) (Bart De Strooper et al. 2010 Nature reviews neurology).

a Nonamyloidogenic pathway



b Amyloidogenic pathway



c Cleavage of APP by secretases

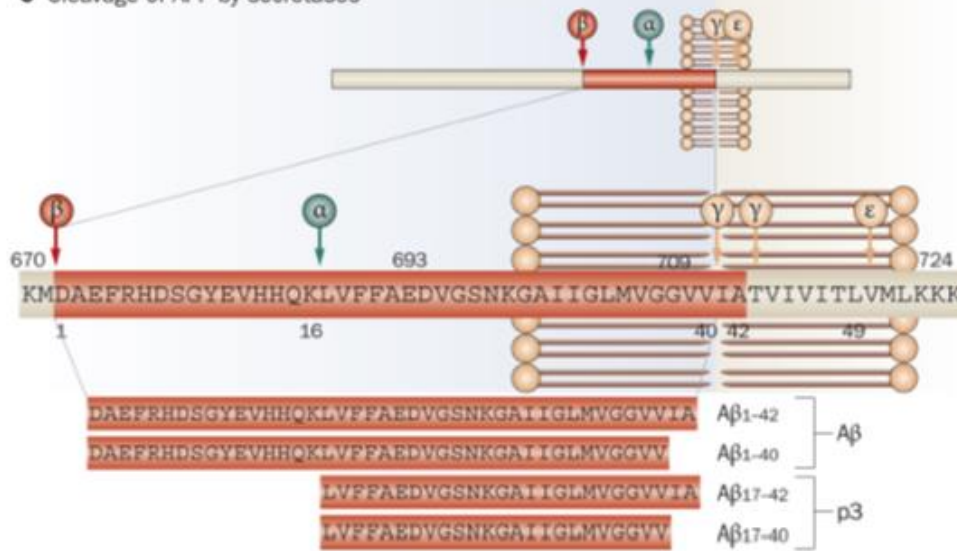


Figure B. A list of γ -secretase inhibitor.

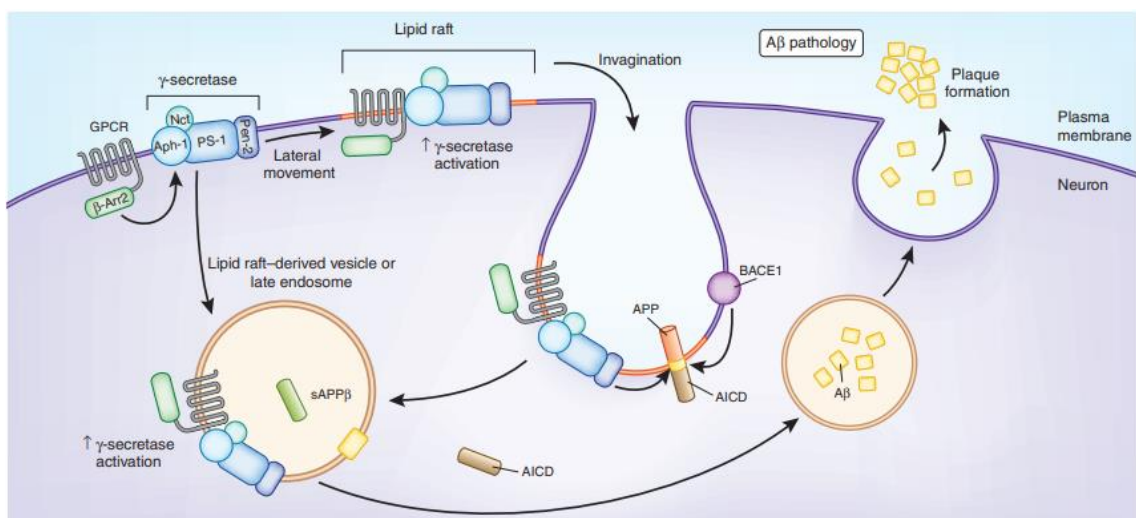
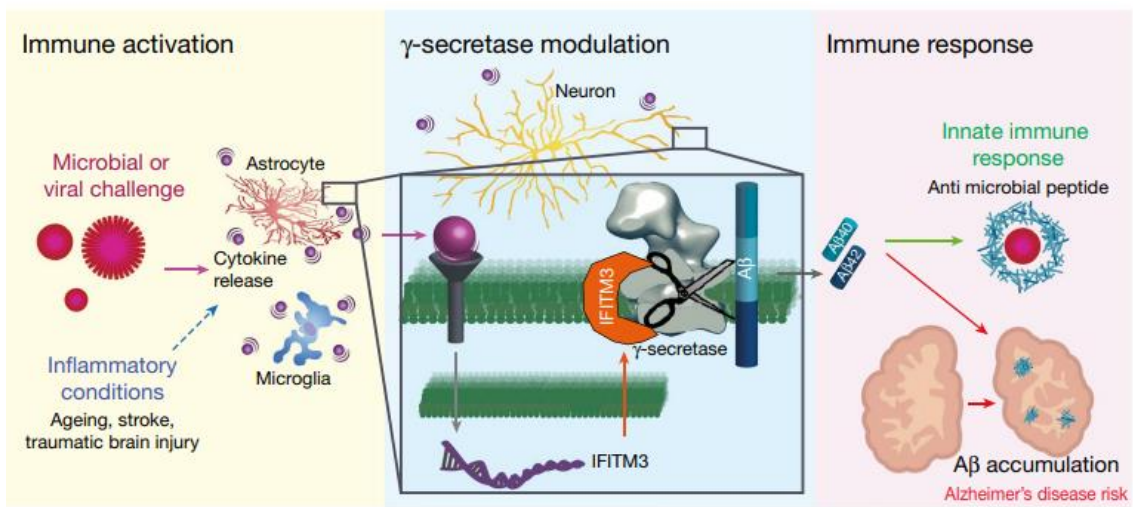
γ -secretase inhibitors which are under development for therapeutics of AD (Bruno P. Imbimbo and Giuseppe A.M. Giardina. 2011 Current Topics in Medicinal Chemistry).

Compound Status	Pros	Cons	Development	Company
Semagacestat (LY-450139)	Decreases production of newly synthesized A β in the CSF of healthy humans	Worsens dose-dependently cognitive and functional decay of AD patients. Increases skin cancer in AD patients. Is neurotoxic (reduced dendritic spine density) in mice. Lack of data on behavioral effects in animal models of AD.	Discontinued	Eli-Lilly
PF-3084014	Notch sparing. Good brain penetration. Long-lasting effects on A β levels in animals. No rebound effect on plasma A β in animals	Lack of data on brain plaque deposition in transgenic mice Lack of data on behavioral effects in animal models of AD. Unfavourable PK/PD profile. In humans	Discontinued for AD	Pfizer
MK-0752	Decreases A β ₁₋₄₀ levels in CSF of healthy volunteers	Inhibits Notch cleavage. Significant gastro-intestinal toxicity in humans	Discontinued for AD	Merck
BMS-708163	Notch sparing. Decreases A β levels in CSF of healthy volunteers	Lack of data on brain plaque deposition in transgenic mice. Lack of data on behavioral effects in animal models of AD Poor tolerability in AD patients	Phase 2	Bristol Myers Squibb
Begacestat (GSI-953)	Notch sparing. Good brain penetration Improves memory in a transgenic mouse model of AD	Lack of data on brain plaque deposition in transgenic mice. Does not decrease A β levels in CSF of AD patients. Causes rebounds on plasma A β ₄₀ levels in man	Phase 2	Wyeth
ELND-006	Notch sparing. Good brain penetration Decrease brain A β burden in transgenic mice	Produces late rebounds in plasma A β in animals. Lack of data on behavioral effects in animal models of AD.	Phase 1	Elan

Figure C. γ -secretase regulators

(Upper) Schematic diagram of Gamma-secretase regulator, IFITM3 (Ji-Yeun Hur et al. 2020 Nature).

(Lower) Schematic diagram of Gamma-secretase regulator, β -arrestin2 (Michael S Wolfe. 2013 Nature medicine, Amantha Thathiah et al. 2013 Nature medicine)



CHAPTER I. PKM2 modulates γ -secretase activity through transcriptional regulation of APH1a

Introduction

Pyruvate kinase M2 (PKM2), a versatile isoform within the pyruvate kinase family, plays a critical role in cellular metabolism by catalyzing the conversion of phosphoenolpyruvate (PEP) to pyruvate in the final step of glycolysis (Harada et al., 1978; Noguchi et al., 1986; Ze Zhang et al., 2019).

This pyruvate kinase family consists of four isoforms encoded by two genes: PKM and PKLR. The PKLR gene produces the L-type (PKL) and R-type (PKR) isoforms, which are mainly expressed in the liver and red blood cells, respectively. These homologs provide essential metabolic stability in specialized tissues, adapting to meet tissue-specific energy and biosynthetic demands (Yamada and Noguchi, 1999; Noguchi et al., 1987).

The PKM gene, in contrast, undergoes alternative splicing to generate two distinct isoforms: PKM1 and PKM2. PKM1 includes exon 9, forming a stable tetrameric structure with a high

affinity for PEP, which supports ATP production, crucial for tissues with high energy demands, such as muscle and brain. PKM2, on the other hand, includes exon 10, which grants it structural flexibility to alternate between tetrameric, dimeric, and monomeric forms. This flexibility allows PKM2 to dynamically shift its activity according to cellular conditions, balancing ATP generation with the production of glycolytic intermediates necessary for biosynthetic pathways. The dimeric form of PKM2, which has a lower affinity for PEP, is predominant in proliferative cells and enables these cells to reroute glycolytic intermediates towards anabolic processes—a trait that is particularly beneficial in rapidly dividing cells such as cancer cells (Bluemlein et al., 2011; Luo and Semenza, 2012; Mazurek, 2011).

Beyond its classical metabolic function, PKM2 has gained attention for its emerging roles in cellular signaling and gene regulation. Recent studies demonstrate that PKM2 can translocate to the nucleus, where it acts as a transcriptional co-activator. In this capacity, PKM2 interacts with transcription factors such as hypoxia-inducible factor 1-alpha (HIF-1 α), STAT3, and β -catenin, modulating the expression of genes involved in cell proliferation, survival, and adaptive responses to stress. Notably, PKM2's nuclear localization is regulated by post-translational modifications, such as phosphorylation at Tyr105, which induces dimer formation and facilitates its entry into the nucleus. This role positions PKM2 as a key mediator in cellular responses to stress, linking metabolic signals with transcriptional control—a mechanism observed in oncogenesis and under hypoxic conditions (Gao et al., 2012; Luo et al., 2011; Yang et al., 2012).

In the context of Alzheimer's disease (AD), metabolic dysfunction and oxidative stress are recognized contributors to disease progression. Hypoxia, a condition of reduced oxygen availability, has been identified as a significant AD risk factor, as it induces oxidative and

endoplasmic reticulum (ER) stress, leading to amyloid beta (A β) accumulation and neuronal degeneration. Hypoxic conditions have been shown to increase PKM2 expression, promoting its nuclear translocation, where it cooperates with HIF-1 α and other transcription factors to activate genes involved in cellular adaptation to low oxygen levels. This interaction highlights PKM2's role in the cellular response to hypoxia, where it could act as a molecular bridge between metabolic stress and A β production (Sun et al., 2006; Wang et al., 2006; Zetterberg et al., 2011).

These insights suggest that PKM2 may play a multifaceted role in AD, not only by influencing glycolysis but also by modulating gene expression in response to cellular stressors common in the AD brain. This ability to regulate metabolic and transcriptional pathways positions PKM2 as a potential metabolic regulator of γ -secretase activity, which is directly implicated in A β production. Given its dual functions, PKM2 may represent a critical point of convergence between metabolic dysregulation and neurodegenerative processes, underscoring its potential as a therapeutic target in AD (Mazurek et al., 2005; Soucek et al., 2003).

Results

PKM2 expression is elevated in the brains of AD patients and AD mouse models.

To investigate the pathological significance of PKM2 in Alzheimer's disease (AD), I analyzed PKM2 expression levels in the brains of AD patients compared with control individuals. PKM2 expression was significantly elevated in AD brains, showing a around 2.5-fold increase compared to controls (Figure I-1. A and B). In contrast, the expression levels of PKM1, the other splicing variant of PKM, remained unchanged (Figure I-1. A and B). Additionally, I observed a positive correlation between PKM2 levels and two key pathological markers of AD: plaque burden and phospho-tau (p-tau) levels, with correlation coefficients of $R^2 = 0.6494$, $p = 0.0162$ for plaque burden and $R^2 = 0.6614$, $p = 0.0042$ for p-tau (Figure I-1 C and D). However, PKM2 levels did not show significant correlations with markers of synaptic loss (SYP, Figure I-1 E) or gliosis (GFAP, Figure I-1 F). Furthermore, the expression of gamma-secretase components, including NCT, PS1-NTF, and APH1a, was also increased in AD brains, suggesting a potential interaction between PKM2 and gamma-secretase in the context of AD pathology (Figure I-1 G).

Next, I assessed PKM2 expression in mouse models of AD. In 5xFAD mice, which carry five familial AD mutations (APPSwedish, APPFlorida, APPLondon, PSEN1M146L, and PSEN1L286V), PKM2 expression was significantly increased at 8 months of age, showing approximately a 2.5-fold elevation compared to wild-type (WT) controls (Figure I-2 H and I). However, there was no significant difference in PKM2 expression at 2 months, suggesting age-dependent upregulation in this AD model. These results support that PKM2 expression is

elevated in both human AD patients and in AD mouse models, highlighting its potential role in AD pathogenesis.

PKM2 modulates γ -secretase activity without affecting other secretase activities.

To examine the role of PKM2 in γ -secretase regulation, I first overexpressed PKM2 and measured its effect on secretase activities. PKM2 overexpression resulted in a significant increase in gamma-secretase activity, approximately doubling compared to control (Ctrl) levels (Figure I-2. A). In contrast, beta-secretase and alpha-secretase activities were not significantly affected by PKM2 overexpression, showing no notable changes compared to control levels (Figure I-2. B and C).

In parallel, I utilized shRNA constructs to selectively knock down PKM2 expression. PKM2 knockdown reduced γ -secretase activity to around 40% of control (shCtrl) levels (Figure I-3. D). As with overexpression, beta-secretase and alpha-secretase activities remained unaffected by PKM2 knockdown, indicating no statistically significant changes (Figure I-3. E and F). Additionally, knockdown of PKM1, the other splicing isoform of PKM, did not result in any change in γ -secretase activity (data not shown). These findings collectively suggest that PKM2 specifically modulates gamma-secretase activity, which may play a role in the amyloidogenic processing associated with Alzheimer's disease, without influencing other secretase pathways.

PKM2 modulates the assembly of the γ -secretase complex.

To elucidate the biochemical role of PKM2 in gamma-secretase regulation, I utilized blue-native polyacrylamide gel electrophoresis (BN-PAGE) to examine the 440-kDa native gamma-

secretase complex, which includes PS1, NCT, APH-1a, and PEN2. PKM2 overexpression resulted in a moderate increase in the levels of the mature gamma-secretase complex, while PKM2 knockdown via shRNA led to a marked decrease in the complex levels (Figure I-4 A and B). Notably, these changes in the mature gamma-secretase complex appear to be driven by alterations in the APH-1a-NCT subcomplex, suggesting that PKM2 influences gamma-secretase assembly beginning at the APH-1a-NCT level.

To investigate the specific role of PKM2 in subcomplex formation, I utilized a PS1/PS2 double knockout (dKO) MEF cell line, which is unable to form the mature gamma-secretase complex. Analysis of subcomplexes in this model revealed that PKM2 modulates the APH-1a-NCT subcomplex independently of mature complex formation. Additionally, when protein synthesis was inhibited with cycloheximide (CHX) to assess stability, the data indicated that PKM2's effect on the gamma-secretase subcomplex was not due to changes in protein stability but rather through the regulation of subcomplex levels themselves (Figure I-5. A and B).

Additionally, I analyzed the expression levels of individual γ -secretase components in denatured conditions using western blotting. The results showed that PKM2 knockdown led to a general reduction in the protein expression of these enzyme components (Figure I-6. A and B), while PKM2 overexpression increased their levels (Figure I-6. C and D). These findings suggest that PKM2 broadly stabilizes the γ -secretase subunits, supporting its role in maintaining the structural integrity and activity of the γ -secretase complex.

PKM2 modulates γ -secretase activity affecting both APP and Notch processing.

To investigate whether PKM2 regulates γ -secretase in an APP-selective manner, I examined

Notch processing by assessing the levels of the Notch intracellular domain (NICD) via western blotting and measuring the expression of NICD-downstream genes, including HES1, HEY1, and HEY2, through quantitative PCR (qPCR). The results demonstrated that both PKM2 overexpression and knockdown affected Notch processing. Specifically, PKM2 overexpression increased NICD levels and elevated HES1 mRNA expression by approximately two-fold, with HEY1 and HEY2 showing a similar but non-significant trend (Figure I-7. A and B). Conversely, PKM2 knockdown reduced NICD levels and significantly decreased the expression of HES1, HEY1, and HEY2 (Figure I-7. C and D). These findings suggest that PKM2 does not regulate γ -secretase in an APP-specific manner; rather, it broadly influences γ -secretase activity, impacting both A β generation and Notch processing.

Dimeric PKM2 modulates γ -secretase activity via transcription regulation.

To better understand the molecular mechanism by which PKM2 regulates the γ -secretase complex, I generated several PKM2 mutants with altered glycolytic functions and examined their effects on γ -secretase activity. Results from γ -secretase activity assays revealed that the dominant-active (DA) PKM2 Y105F mutant, which prefers the tetrameric form and is restricted from nuclear entry, showed no stimulatory effect on γ -secretase activity. In contrast, both the kinase-dead (KD) PKM2 K367M and the dominant-negative (DN) PKM2 R399E mutants exhibited similar stimulatory effects on γ -secretase activity as wild-type (WT) PKM2 (Figure I-8. A). This finding aligns with recent reports suggesting that PKM2 dimers, rather than tetramers, are involved in transcriptional regulation.

Further supporting this transcriptional role, the Y105F mutant, which cannot translocate into the nucleus, failed to enhance γ -secretase activity and showed reduced nuclear localization

compared to WT PKM2, as demonstrated by western blot analysis (Figure I-8. B). Additionally, examining the metabolic products of PKM2 activity, I found that cellular pyruvate levels decreased significantly upon PKM2 overexpression to approximately 60% of control levels (Figure I-9. A). However, adding exogenous pyruvate to the culture medium did not affect γ -secretase activity, indicating that pyruvate is not directly involved in this regulation (Figure I-9. B). Furthermore, cellular ATP levels remained unchanged by either PKM2 knockdown or overexpression, suggesting that the γ -secretase regulation by PKM2 is independent of its glycolytic function (Figure I-9. C).

Taken together, these results suggest that the role of PKM2 in γ -secretase regulation is independent of its metabolic activity and likely involves the transcriptional modulation of APH-1a, a component of the APH1-NCT sub complex, via nuclear-localized dimeric PKM2.

PKM2 specifically modulates mRNA level of APH1a.

Given that PKM2 functions as a transcriptional coactivator, I examined the mRNA levels of various gamma-secretase components and APP to determine if PKM2 influences their transcription. Quantitative PCR (qPCR) analysis showed that overexpression of PKM2 significantly increased APH-1a mRNA levels, while the mRNA levels of other γ -secretase components, such as PS1, NCT, PEN2, and APP, remained unaffected (Figure I-10. A). Conversely, silencing PKM2 expression led to a marked reduction in APH-1a mRNA levels, with no effect on the transcription of the other tested genes (Figure I-10. B).

To further confirm the specific role of PKM2 in APH-1a transcription, I performed a rescue experiment using shRNA-resistant PKM2 in PKM2 knockdown cells. The qPCR results showed that expression of shRNA-resistant PKM2 WT effectively restored APH-1a mRNA

levels in PKM2 knockdown cells, whereas the Y105F mutant, which cannot translocate to the nucleus, failed to rescue APH-1a transcription (Figure I-10. C and D). These findings suggest that the transcriptional regulatory role of PKM2 on APH-1a is specifically mediated by its nuclear dimeric form, underscoring its significance in γ -secretase modulation.

PKM2 modulates APH-1a transcription via HDAC3 inhibition

PKM2 has been reported to induce phosphorylation at Threonine 11 on histone H3 (H3 p-T11), a modification that can influence chromatin structure and gene expression. Given this background, I investigated whether PKM2 modulates APH-1a transcription through histone modification. Stable PKM2 knockdown cells were treated with RGFP-966, a selective HDAC3 inhibitor. Inhibition of HDAC3 partially restored APH-1a expression levels in PKM2 knockdown cells, suggesting that PKM2 modulates APH-1a transcription by weakening HDAC3 activity to maintain basal APH-1a levels (Figure I-11. A and B).

To further understand PKM2's influence on APH-1a transcription, I performed a cross-linked chromatin immunoprecipitation (X-ChIP) assay followed by qPCR to examine PKM2's association with the APH-1a promoter. The results indicated an enrichment of PKM2 at the APH-1a promoter region, implying that PKM2 may act as a co-activator in APH-1a transcriptional regulation (Figure I-11. C). Since APH-1 is a scaffold subunit within the γ -secretase complex, these findings highlight PKM2's role in γ -secretase modulation through transcriptional control of APH-1a, involving chromatin modification mechanisms such as HDAC3 inhibition and PKM2 promoter association.

PKM2 mediates γ -secretase activation in hypoxic neurons.

Hypoxia is recognized as a critical risk factor for Alzheimer's disease (AD), and PKM2 expression has been shown to be transcriptionally regulated by HIF1 α . To explore PKM2's role in hypoxia-mediated γ -secretase activation in AD, I first assessed PKM2 expression in primary neurons and astrocytes isolated from mouse brains. Consistent with prior reports, PKM2 was predominantly expressed in astrocytes, whereas PKM1 was the dominant isoform in neurons (Figure I-12. A). Upon exposure to hypoxic conditions, PKM2 expression significantly increased in neurons, but not in astrocytes (Figure I-12. B). This difference likely reflects the inherent resistance of astrocytes to hypoxic stress, as evidenced by the limited induction of HIF1 α in these cells during our experiments. These results suggest that PKM2 may operate under physiologically hypoxic conditions specifically within neurons.

To further investigate γ -secretase activity under hypoxia, I analyzed γ -secretase components and APP processing in hypoxic neurons. Western blot analysis revealed substantial upregulation of γ -secretase components concurrent with PKM2 expression in hypoxic primary neurons (Figures I-13. A and B). Notably, neither BACE1 expression nor levels of soluble APP alpha (sAPP α) were affected by hypoxia, indicating a selective influence on γ -secretase.

To confirm PKM2's role in mediating γ -secretase activation under hypoxic-like conditions, I treated neurons with CoCl₂, a hypoxia-mimicking agent that induces HIF1 α expression. Western blot analysis indicated that CoCl₂ treatment significantly increased γ -secretase activity, as evidenced by elevated levels of APP C-terminal fragments (APP-CTF) (Figure I-14. A). However, this stimulatory effect on γ -secretase activity was abolished in PKM2 knockdown neurons, confirming that PKM2 is essential for the observed activation. Additionally, γ -secretase activity assays corroborated these findings, showing an increase in activity under

CoCl₂ treatment, though the enhancement was less than twofold and returned to near-control levels upon PKM2 knockdown (Figure I-14. B). These results collectively underscore PKM2's requirement for gamma-secretase activation in hypoxic conditions, supporting its potential role in AD pathology linked to hypoxic stress.

Neuronal expression of PKM2 exacerbates A β production and memory decline in 3xTg AD mice.

To investigate the physiological role of PKM2 in Alzheimer's disease progression, I used transgenic PKM2 mice (PKM2 Tg) generated with the CaMKII α promoter to drive forebrain-specific expression. Western blot analysis of different brain regions revealed that ectopic PKM2 expression was primarily localized to the cortex, hippocampus, and striatum, with weaker expression in the olfactory bulb (Data not shown). The expression levels of the PKM2 transgene in the cortex and hippocampus were comparable to endogenous PKM2 levels, suggesting minimal risk of overexpression artifacts.

To assess PKM2's effects on A β production and memory impairment, I crossed PKM2 Tg mice with the 3xTg AD mouse model, which expresses mutant APP^{swe}, PS1M146L, and TauP301L. Western blot analysis of brain lysates from 3xTg/WT and 3xTg/PKM2 mice demonstrated that γ -secretase components, particularly A β 11a, were elevated in the 3xTg/PKM2 mice, alongside increased PKM2 expression (Figures I-15. A and B). Furthermore, plaque burden, as indicated by MOAB-2 staining, showed an increase in the cortex of 3xTg/PKM2 mice (Figure I-17. A). Quantification of A β ₁₋₄₀ and A β ₁₋₄₂ in both cortical and hippocampal tissues revealed elevated levels in 3xTg/PKM2 mice, while the A β ₄₂/A β ₄₀ ratio remained unchanged (Figure I-16. A). These results suggest that neuronal overexpression of

PKM2 in AD model mice exacerbates amyloid pathology and may contribute to cognitive decline.

Additionally, immunostaining for GFAP, a marker of activated glial cells, showed increased immune reactivity in the brains of 3xTg/PKM2 mice, while the expression of the synaptic protein SYP remained unchanged compared to controls (Figures I-18. A and B). This suggests that ectopic expression of PKM2 may contribute to increased glial activation in 3xTg AD mice without impacting synaptic protein levels.

To further confirm the role of PKM2 in regulating γ -secretase activity and plaque pathology in the AD mouse model, I performed stereotaxic injection to deliver PKM2 knockdown lentivirus into the hippocampus of 3xTg mice. The results demonstrated that knockdown of PKM2 significantly reduced the expression of γ -secretase components (Figure I-19. A and B) and decreased amyloid plaque immunoreactivity (4G8) in the hippocampus of 3xTg/shPKM2 mice (Figures I-20. A and B). However, PKM2 knockdown did not affect glial cell activation or synaptic protein (SYP) levels (Data not shown). These findings indicate that transgenic expression of PKM2 in the forebrain neurons of 3xTg mice enhances γ -secretase activity, exacerbating amyloid plaque accumulation and potentially contributing to AD pathology.

To assess the cognitive impact of PKM2 overexpression in 3xTg AD mice, I conducted Y-maze, novel object recognition, and passive avoidance tests. In the Y-maze test, 3xTg/PKM2 mice exhibited a marked impairment in spatial working memory, as indicated by significantly reduced spontaneous alternation compared to control groups (Figure I-21. A). In the novel object recognition test, 3xTg/PKM2 mice spent less time exploring a novel object, indicating a decline in recognition memory (Figure I-21. B). Additionally, in the passive avoidance test, 3xTg/PKM2 mice displayed deficits in memory retention, with a significantly shorter escape

latency (65 s) compared to the 117 s observed in control mice (Figure I-21. C).

To further explore the effects of PKM2 knockdown on cognition, I injected shPKM2 lentivirus into the hippocampus of 3xTg mice and conducted similar behavioral tests. In the Y-maze test, 3xTg/shPKM2 mice showed a significant increase in spontaneous alternation, indicating improved spatial working memory compared to control 3xTg mice (Figure I-22. A). In the novel object recognition test, 3xTg/shPKM2 mice demonstrated enhanced recognition memory, spending more time exploring the novel object than control mice (Figure I-22. B). These findings suggest that neuronal overexpression of PKM2 exacerbates cognitive decline in 3xTg AD mice, while PKM2 knockdown can mitigate memory impairments, highlighting the potential pathogenic role of PKM2 in Alzheimer's disease progression.

Figure I-1. PKM2 expression is elevated in the brains of AD patients.

(A and B) Expression of PKM2 and PKM1 assessed by western blotting in brain samples from patients with Alzheimer's disease (AD) and non-AD (A). Bars represent the mean \pm SEM (n = 9 for Normal; n = 13 for AD). **p < 0.01 (Student's t test) (B).

(C–F) Linear regression analysis relating levels of PKM2 expression to AD pathological markers plaque burden (C), phospho-tau (p-Tau, D), synapse (SYP, E), and gliosis (GFAP, F) in (blot A).

(G) Quantification of γ -secretase components in (A). Bars represent the mean \pm SEM (n = 5 for Normal; n = 5 for AD). *p < 0.05, **p < 0.01 (Student's t test).

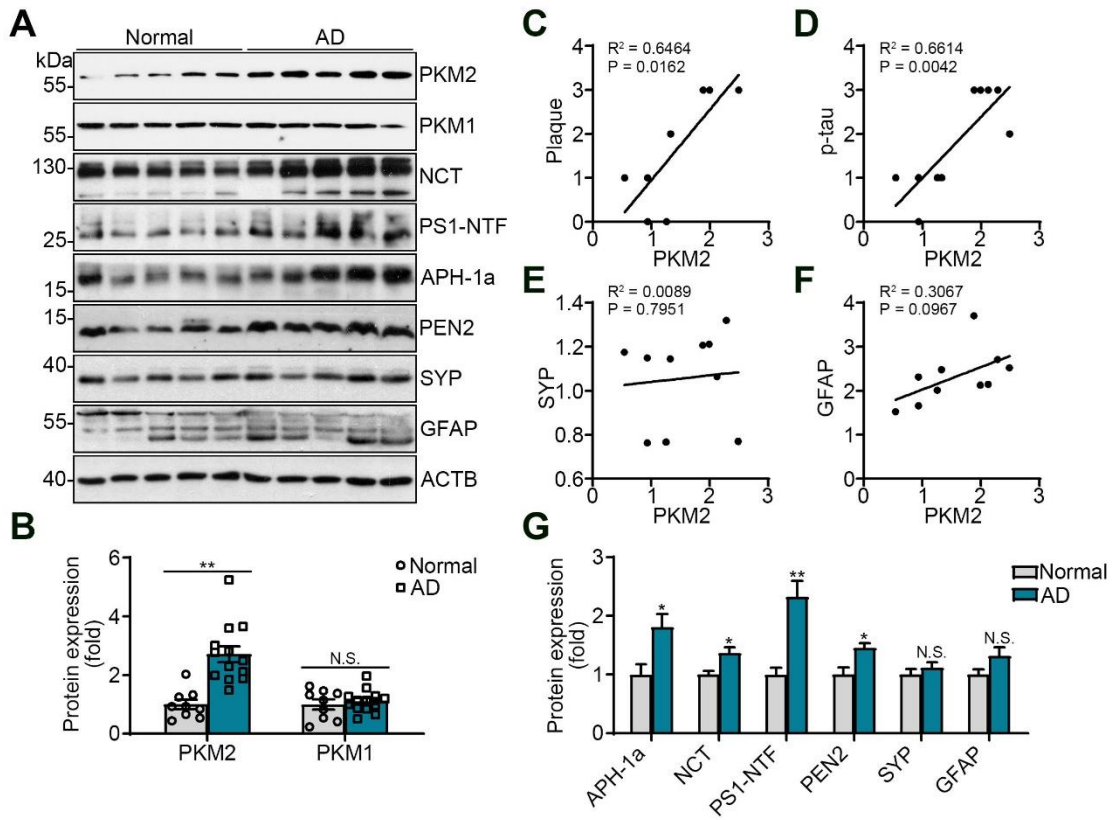


Figure I-2. PKM2 expression is elevated in the brains of AD mouse model.

(H and I) Expression of PKM2 assessed by western blotting in cortical extracts of wild-type (WT) and 5xFAD mice. Bars represent the mean \pm SEM (n = 3 for WT; n = 3 for 5xFAD). **p < 0.01 (Student's t test).

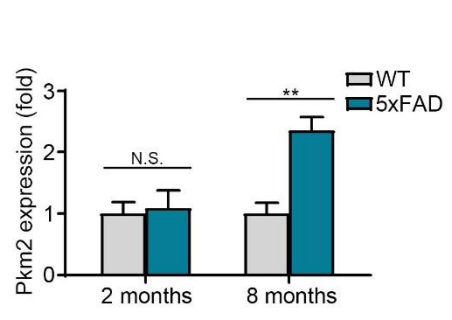
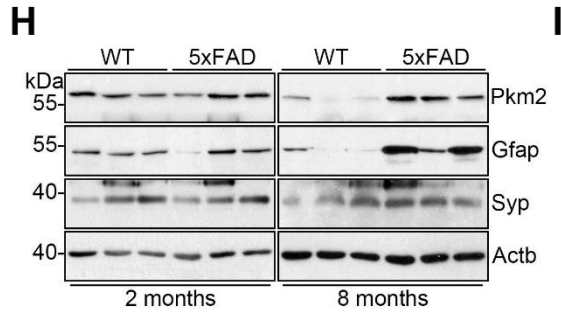


Figure I-3. PKM2 modulates gamma-secretase activity without affecting other secretase activities.

(A) γ -secretase activity determined based on luciferase reporter activity in HEK293T cells overexpressing PKM2. Bars represent the mean \pm SD (n = 3). **p < 0.01 (Student's t test).

(B) The β -secretase activity determined by alkaline phosphatase reporter activity in HEK293T cells overexpressing PKM2. Bars represent the mean \pm SD (n = 3). N.S., not significant (Student's t test).

(C) The α -secretase activity determined by quantification of cleaved sAPP α in CHO-7PA2 cells culture medium after overexpression of PKM2. Bars represent the mean \pm SD (n = 3). N.S., not significant (Student's t test).

(D) The γ -secretase activity determined by luciferase reporter activity in HEK293T cells silencing PKM2 expression. Bars represent the mean \pm SD (n = 3). **p < 0.01 (Student's t test).

(E) The β -secretase activity determined by alkaline phosphatase reporter activity in HEK293T cells silencing PKM2 expression. Bars represent the mean \pm SD (n = 3). N.S., not significant (Student's t test).

(F) The α -secretase activity determined by quantification of cleaved sAPP α in CHO-7PA2 cells culture medium after silencing PKM2 expression. Bars represent the mean \pm SD (n = 3). N.S. (Student's t test).

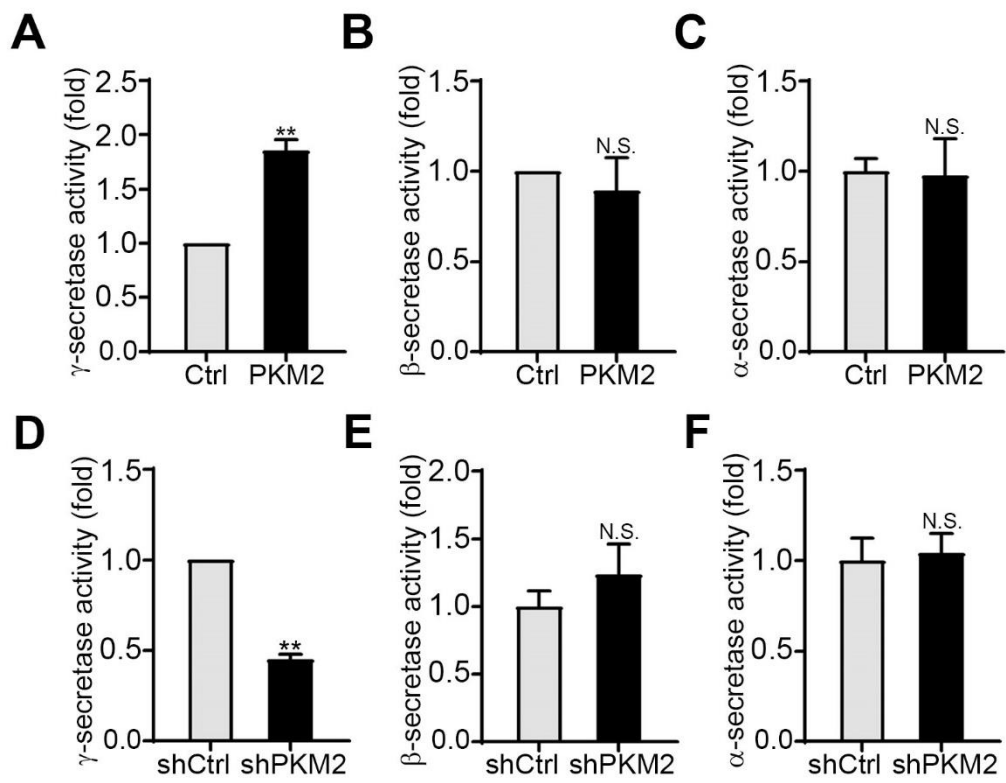
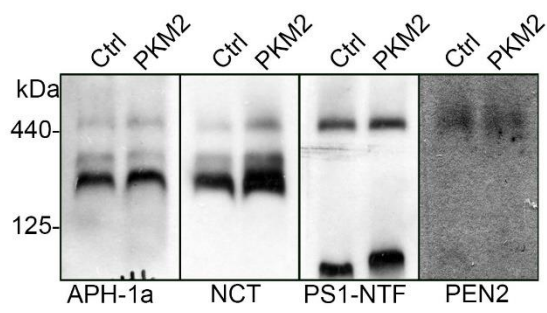


Figure I-4. PKM2 modulates γ -secretase complex level via APH1a-NCT sub-complex.

(A) HEK293T cells were transfected with either pCtrl or pPKM2 for 24 hours. Membrane fractions of transfected HEK293T cells were solubilized in 1% DDM (n-Dodecyl-beta-D-Maltopyranoside, D310) lysis buffer, separated by BN-PAGE, and analyzed by western blotting.

(B) Membrane fractions of HEK293T PKM2 KD cells were solubilized in 1% DDM (n-Dodecyl-beta-D-Maltopyranoside, D310) lysis buffer, separated by BN-PAGE, and analyzed by western blotting.

A



B

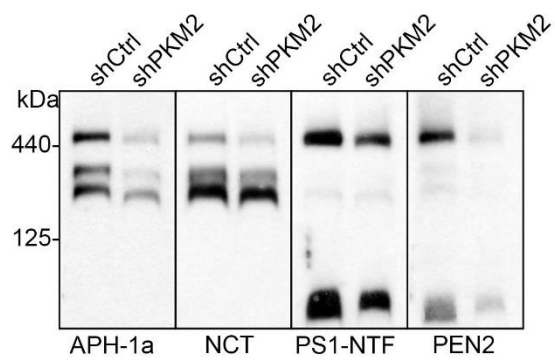


Figure I-5. PKM2 modulates APH1a-NCT sub-complex.

(A) Expression of γ -secretase components assessed by western blotting in HEK293T PKM2 KD cells treated with cycloheximide (CHX) for the indicated times.

(B) Levels of native APH1a-NCT subcomplex assessed using BN gel electrophoresis followed by western blotting after silencing PKM2 in PS1/2 dKO MEF cells treated with CHX for the indicated times.

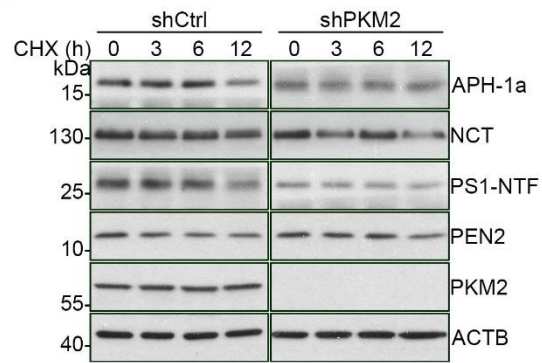
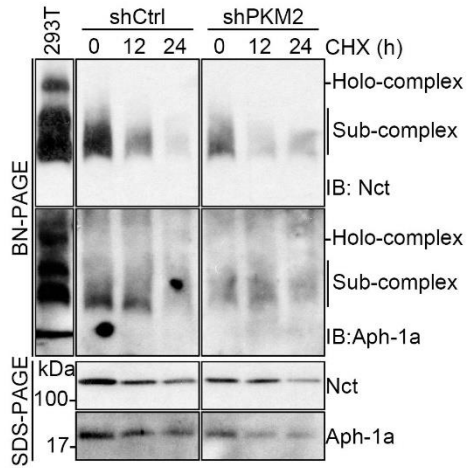
A**B**

Figure I-6. PKM2 regulates individual γ -secretase component levels, especially APH1a.

(A and B) Expression of γ -secretase components assessed by western blotting in HEK293T cells overexpressing PKM2 (A). Bars represent the mean \pm SD (n = 3). *p < 0.05, **p < 0.01 (Student's t test) (B).

(C and D) Expression of γ -secretase components assessed by western blotting in HEK293T cells after silencing PKM2 (C). Bars represent the mean \pm SD (n = 3). *p < 0.05, **p < 0.01 (Student's t test) (D).

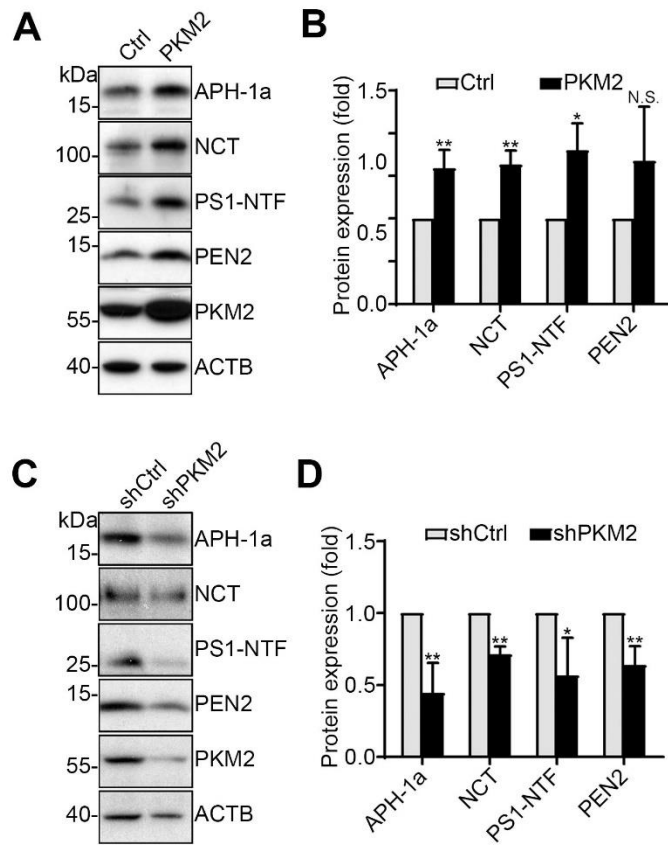


Figure I-7. PKM2 modulates γ -secretase activity affecting Notch processing.

(A) NICD levels assessed by western blotting in HEK293T cells co-expressing Notch Δ E-GFP and PKM2 with or without the treatment with Compound E (Comp. E).

(B) Expression of Notch target genes assessed by qPCR in HEK293T cells overexpressing PKM2. Bars represent the mean \pm SD (n = 3). **P < 0.01 (Student's t test).

(C) Expression of NICD assessed by western blotting in HEK293T cells expressing NotchDE-GFP after PKM2 knockdown with or without Compound E (Comp. E).

(D) Expression of Notch target genes assessed by quantitative PCR (qPCR) in HEK293T cells silencing PKM2 expression. Bars represent the mean \pm SD (n = 3). *p < 0.05 (Student's t test).

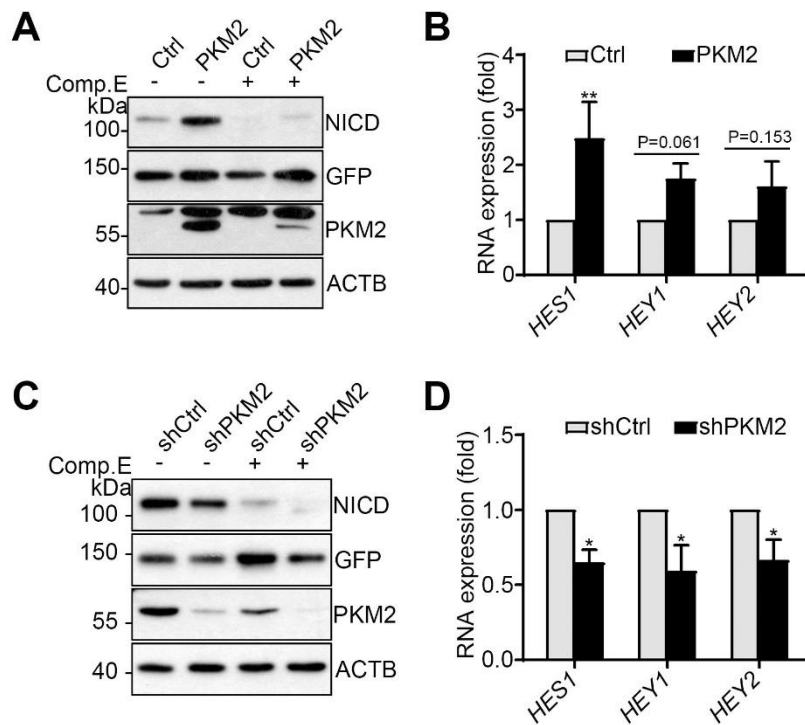


Figure I-8. Dimeric PKM2 regulates γ -secretase activity.

(A) The γ -secretase activity determined by luciferase reporter activity in HEK293T cells overexpressing PKM2 WT and mutants (Y105F, dominant active; K367M, kinase dead; R399E, dominant-negative). Bars represent the mean \pm SD (n = 3). **p < 0.01 (one-way ANOVA with post hoc Tukey's multiple comparisons test).

(B) HEK293T cells were transfected with PKM2 WT and Y105F for 24 hours and cytosol-nucleus fractions of cell extracts were analyzed by western blotting.

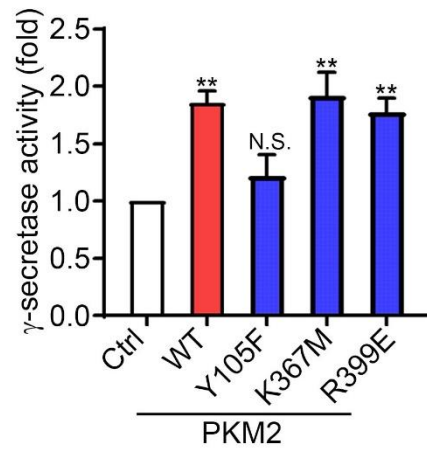
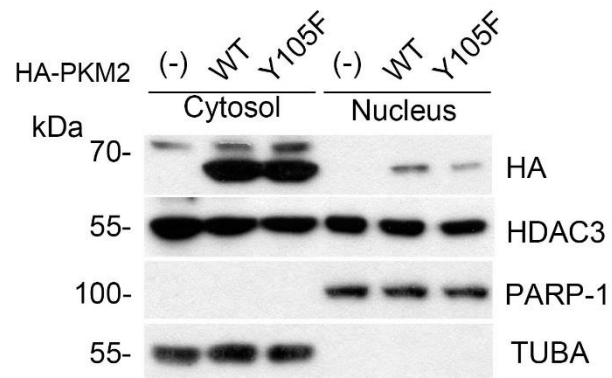
A**B**

Figure I-9. Pyruvate level in culture medium and cellular ATP level do not affect to γ -Secretase activity.

(A) Relative levels of cellular pyruvate were assessed with a pyruvate assay kit in HEK293T cells overexpressing PKM2. Bars represent the mean \pm SD (n = 3). **P < 0.01 (Student's t test).

(B) The γ -Secretase activity was determined by luciferase reporter activity with or without pyruvate in culture medium of HEK293T cells. Bars represent the mean \pm SD (n = 3). N.S. (Student's t test).

(C) Relative levels of cellular ATP were assessed using a cell viability assay kit in HEK293T cells overexpressing PKM2. Bars represent the mean \pm SD (n = 3). N.S. (Student's t-test).

(D) Relative levels of cellular ATP were assessed using a cell viability assay kit in HEK293T PKM2 KD cells. Bars represent the mean \pm SD (n = 3). N.S. (Student's t-test).

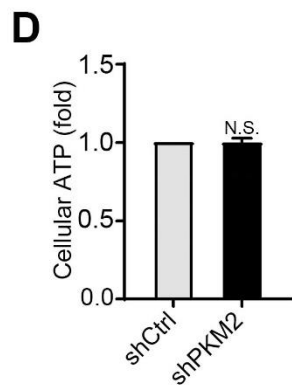
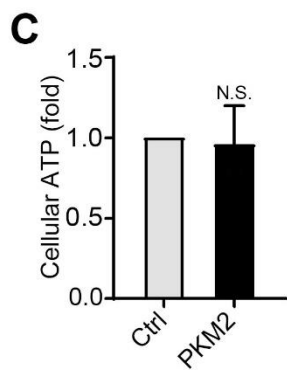
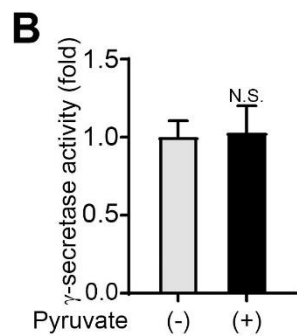
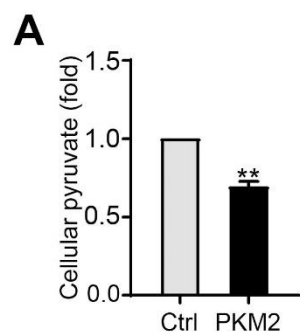


Figure I-10. PKM2 specifically modulates level of APH1a mRNA.

(A and B) Expression of γ -secretase components was assessed by qPCR in HEK293T cells overexpressing (A) or silencing (B) PKM2. Bars represent the mean \pm SD (n = 3). **P < 0.01 (Student's t test).

(C) Expression of APH-1a was assessed by qPCR after overexpression PKM2 shRNA-resistant WT (rWT) or Y105F (rY105F) mutant in HEK293T PKM2 KD cells. Bars represent the mean \pm SD (n = 3). **p < 0.01 (one-way ANOVA with post hoc Tukey's multiple comparisons test).

(D) Expression of PKM2 rWT and Y105F mutant (rY105F) was assessed by western blotting in HEK293T PKM2 KD cells.

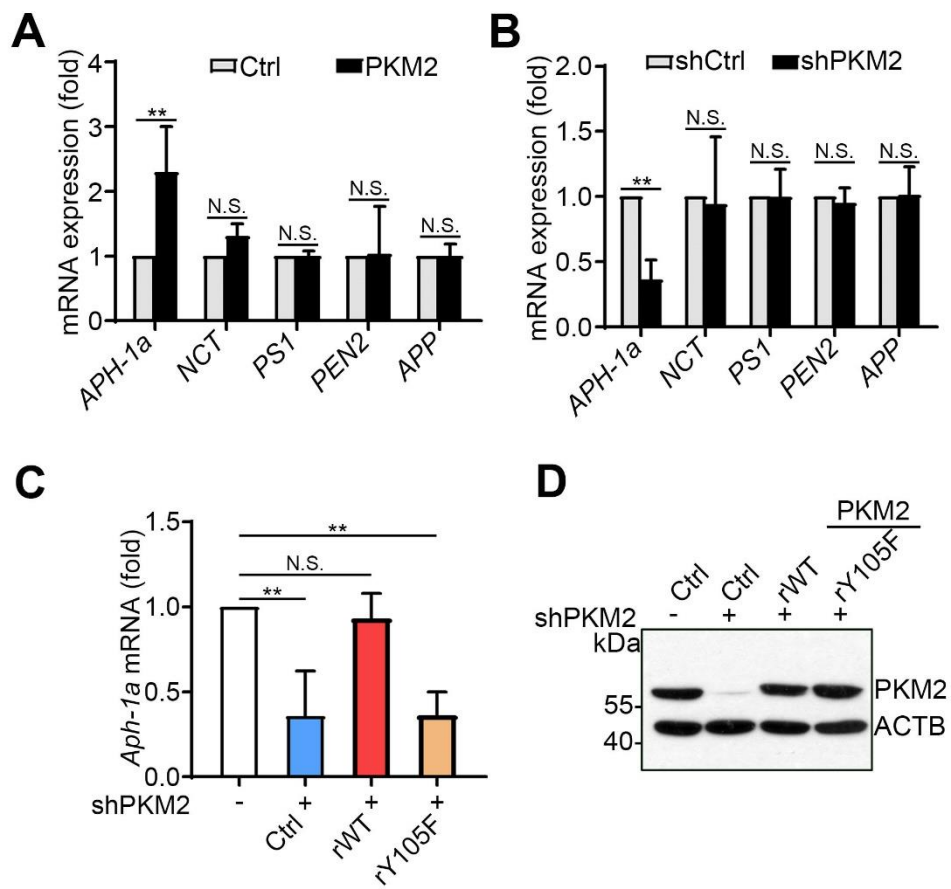


Figure I-11. PKM2 modulates APH-1a transcription via HDAC3 inhibition.

(A) Expression of APH-1a was assessed by western blotting in HEK293T cells treated with 10 μ M RGFP-966 for 24 hours after silencing PKM2.

(B) Relative level of APH1a expression level in panel A. Bars represent the mean \pm SD (n = 3).

*p < 0.05 (two-way ANOVA with post hoc Tukey's multiple comparisons test).

(C) Expression of APH-1a transcript was assessed by X-ChIP followed by qPCR in HEK293T cells after overexpression of PKM2. Bars represent the mean \pm SD (n = 3). **p < 0.01 (Student's t test).

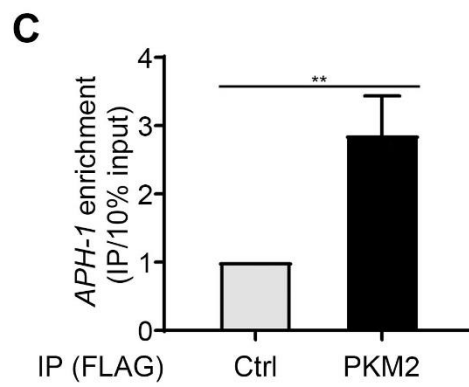
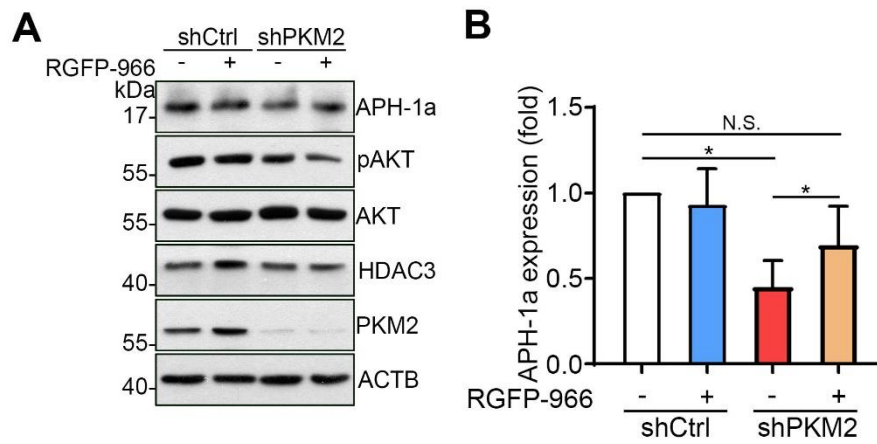
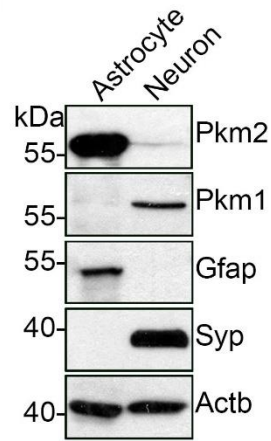


Figure I-12. PKM2 mediates γ -secretase activation in hypoxic primary neurons.

(A) Expression of PKM2 was assessed by western blotting in primary cultured astrocytes and neurons.

(B) Expression of A β 1a and PKM2 assessed by western blotting in astrocytes and neurons under hypoxic conditions (1% O₂).

A



B

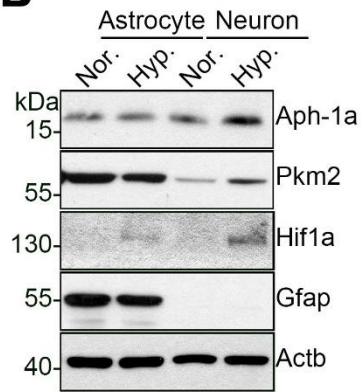


Figure I-13. PKM2 regulates γ -secretase component level in hypoxic primary neurons.

(A) Expression of PKM2 and γ -secretase components was assessed by western blotting in primary cortical neurons under hypoxic conditions (1% O₂) for 24 hours.

(B) Primary cortical neurons were infected with shPKM2 lentiviral particles for 48 hours, then exposed to hypoxic conditions (1% O₂) for 24 hours, and γ -secretase components were subsequently assessed by western blotting.

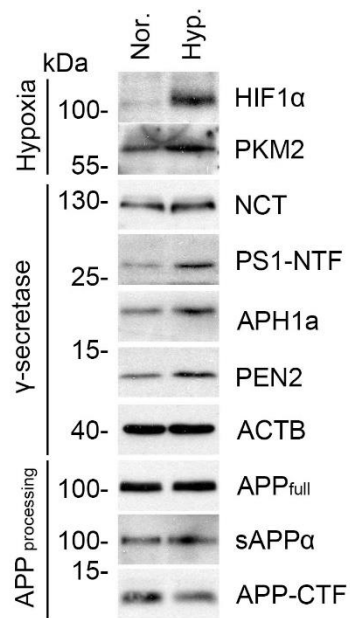
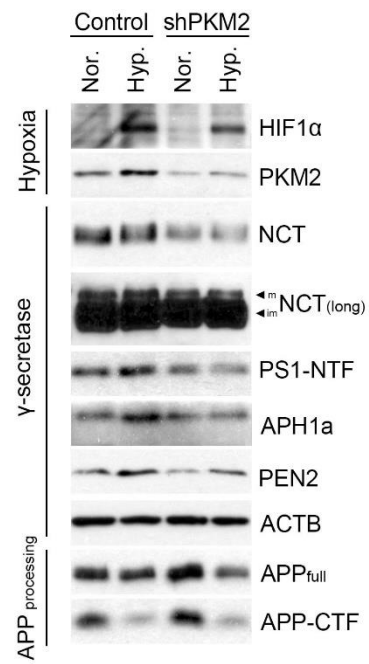
A**B**

Figure I-14. PKM2 regulates gamma-secretase component level under hypoxic stress.

(A) HEK293T/APP695 cell lines were infected with shPKM2 lentiviral particles. After 48 hours of infection, cells were treated with 500 μ M CoCl₂ for 6 hours in serum-free medium. The crude membrane fraction of the cell lysate was used for an in vitro AICD assay.

(B) The γ -secretase activity was determined by luciferase reporter activity in cells after silencing PKM2 expression with or without CoCl₂ treatment. Bars represent the mean \pm SD (n = 3). **p < 0.01 (two-way ANOVA with post hoc Tukey's multiple comparisons test).

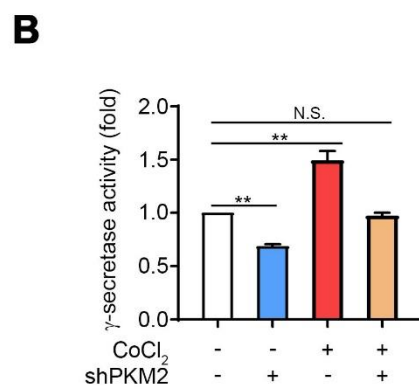
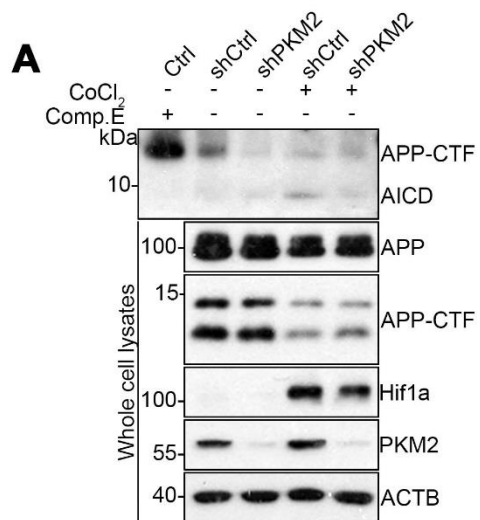


Figure I-15. Neuronal expression of PKM2 elevates A β 1a protein expression in 3xTg AD mice.

(A) Expression of PKM2 and γ -secretase components was assessed by western blotting in cortical extracts from 3xTg/WT and 3xTg/PKM2 transgenic (Tg) mice.

(B) Relative level of protein expression level in panel A. Bars represent the mean \pm SEM (n = 3). **p < 0.01 (Student's t test).

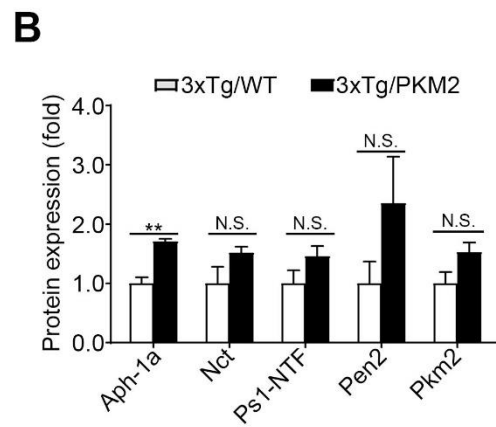
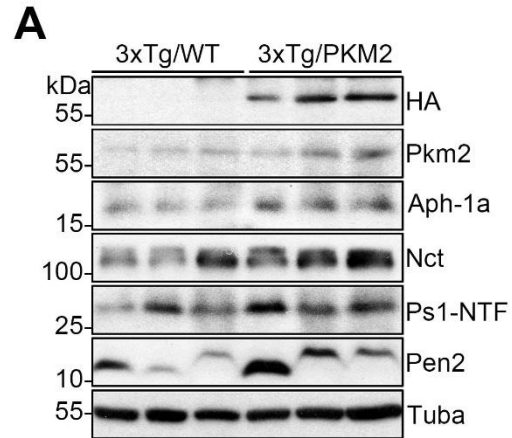


Figure I-16. Neuronal expression of PKM2 aggravates A β generation in 3xTg AD mice

Relative levels of A β 40 and A β 42 were assessed by ELISA in cortical/hippocampal extracts of 3xTg/WT and 3xTg/PKM2 Tg mice. Bars represent the mean \pm SEM (n = 3). *p < 0.05 (Student's t test).

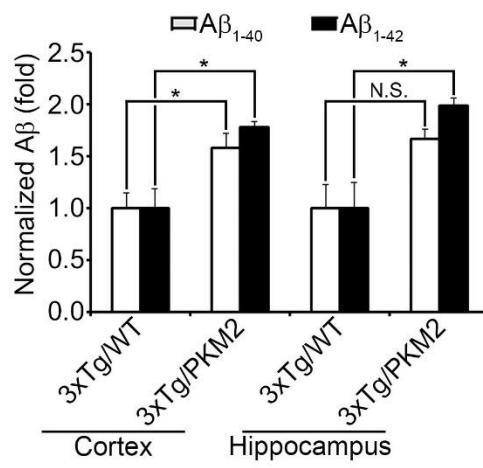


Figure I-17. Neuronal expression of PKM2 accelerates A β burden and gliosis in 3xTg AD mice.

(A and B) Immunohistochemical detection of amyloid burden (anti-MOAB-2) (A) and glial cells (anti-GFAP) (B) in frozen cortical sections of 9-month-old 3xTg/WT and 3xTg/PKM2 mouse brains.

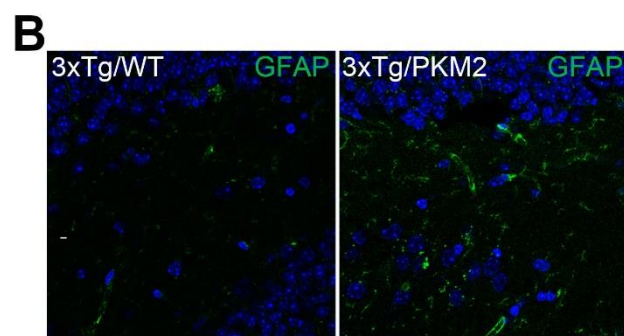
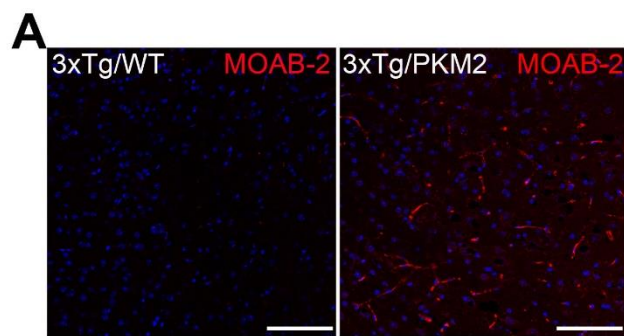


Figure I-18. Neuronal expression of PKM2 accelerates gliosis in 3xTg AD mice

(A) Expression of GFAP and SYP was assessed by western blotting in cortical extracts from 3xTg/WT and 3xTg/PKM2 mouse brains.

(B) Relative protein expression level of GFAP and SYP from panel A. Bars represent the mean \pm SEM (n = 3). **P < 0.01 (Student's t test).

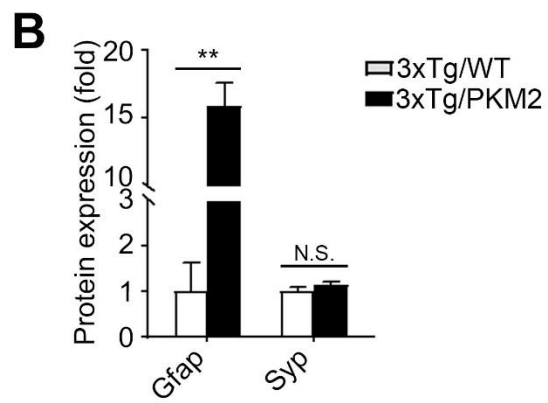
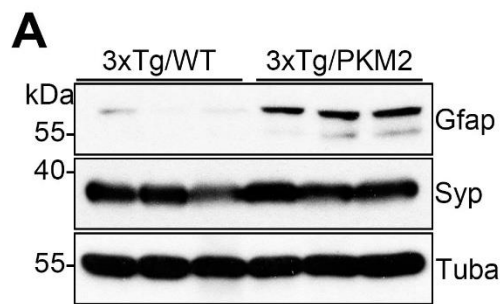


Figure I-19. Hippocampal knockdown of PKM2 dampens expression of γ -secretase components

(A) Expression of PKM2 and γ -secretase components was assessed by western blotting in hippocampal extracts of 3xTg mice stereotaxically injected with lentivirus silencing Pkm2.

(B) Relative protein expression levels from panel A. Bars represent the mean \pm SEM (n = 4).

*P < 0.05, **P < 0.01 (Student's t-test).

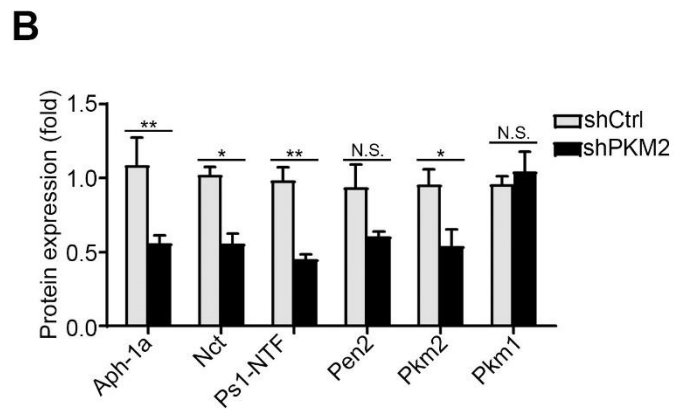
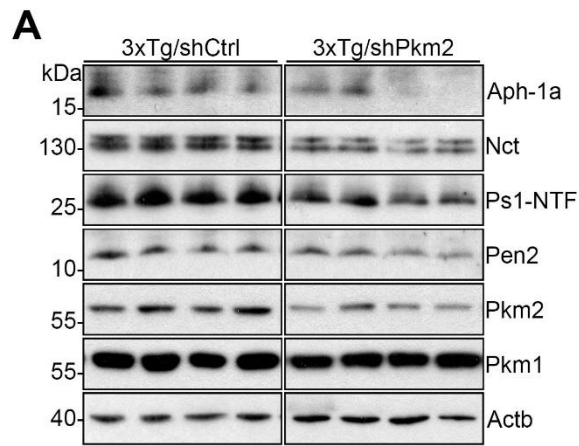


Figure I-20. Hippocampal knockdown of PKM2 reduces amyloid burden in 3xTg AD mice.

(A and B) Immunohistochemical detection of amyloid burden (anti-4G8) (A) and glial cells (anti-GFAP) (B) in frozen hippocampal sections of 3xTg mice stereotaxically injected with lentivirus silencing Pkm2. Scale bars represent 100 μm .

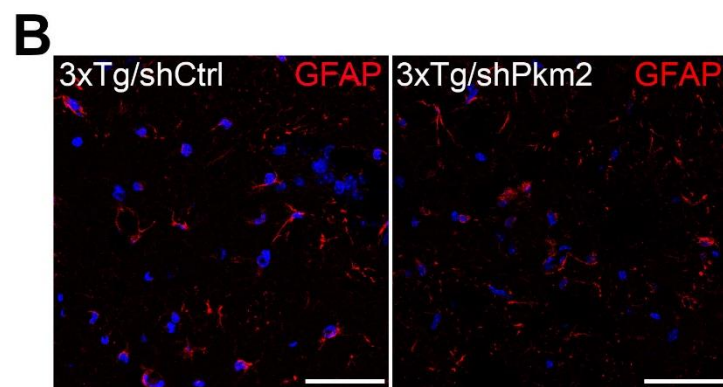
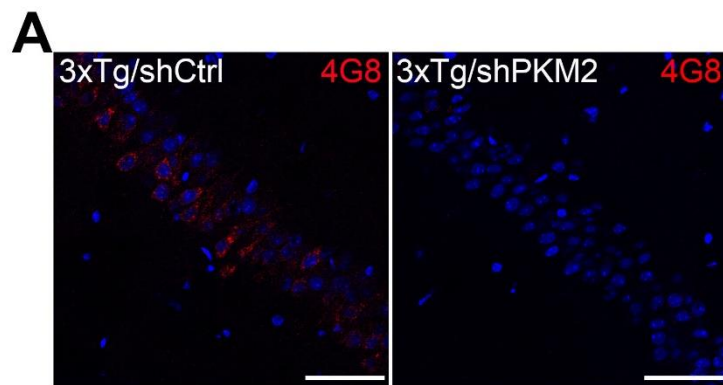


Figure I-21. CaMKII-induced PKM2 expression exacerbates memory decline in 3xTg AD mice.

(A-C) Memory assessed in 8-month-old WT, PKM2 Tg, 3xTg/WT, and 3xTg/PKM2 mice using Y-maze (A), novel object recognition (B), and passive avoidance (C) tests. Bars represent the mean \pm SEM (n = 10 for WT, PKM2 Tg, and 3xTg/WT; n = 13 for 3xTg/PKM2). *p < 0.05, **p < 0.01 (two-way ANOVA with post hoc Tukey's multiple comparisons test).

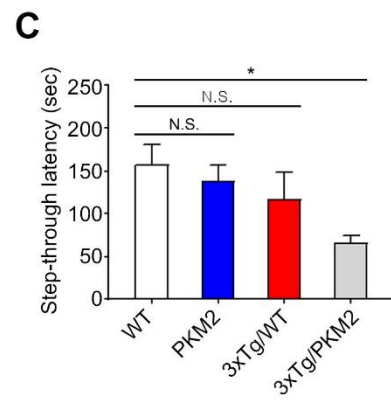
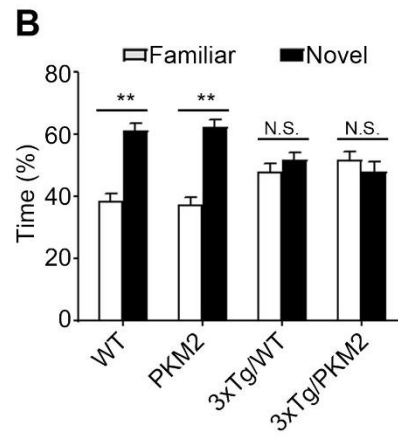
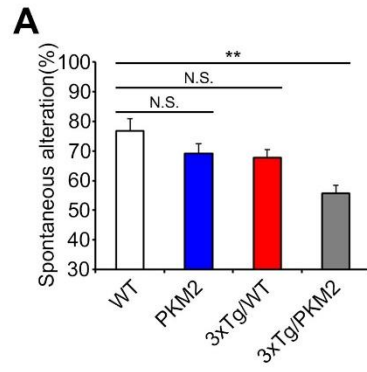


Figure I-22. Hippocampal knockdown of PKM2 rescues memory decline in 3xTg AD mice.

(A-C) Memory was assessed in 3xTg/shControl and 3xTg/shPKM2 mice using the Y-maze (A) and novel object recognition (B). Bars represent the mean \pm SEM (n = 11 for 3xTg/shControl and 3xTg/shPKM2). *p < 0.05, **p < 0.01 (two-way ANOVA with post hoc Tukey's multiple comparisons test).

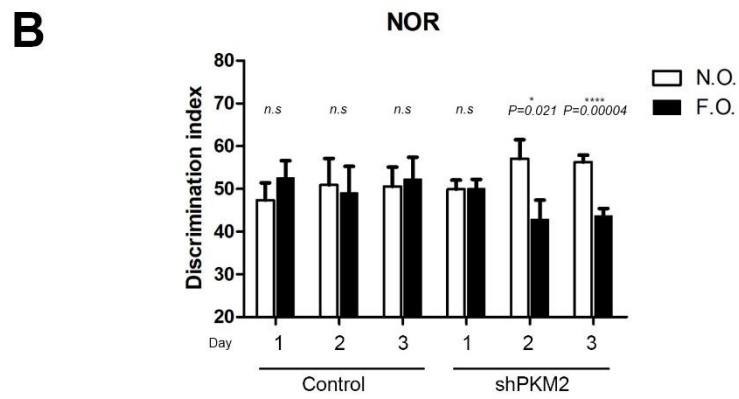
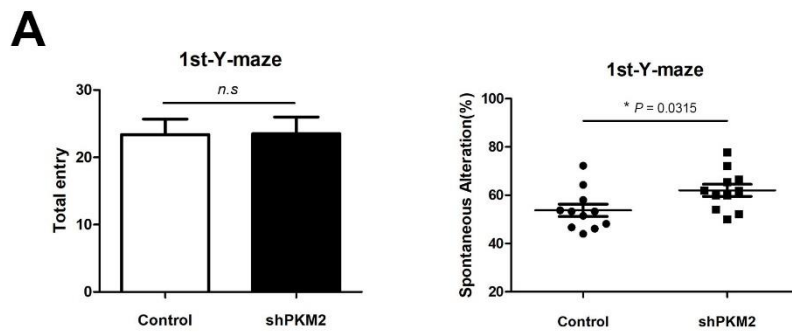
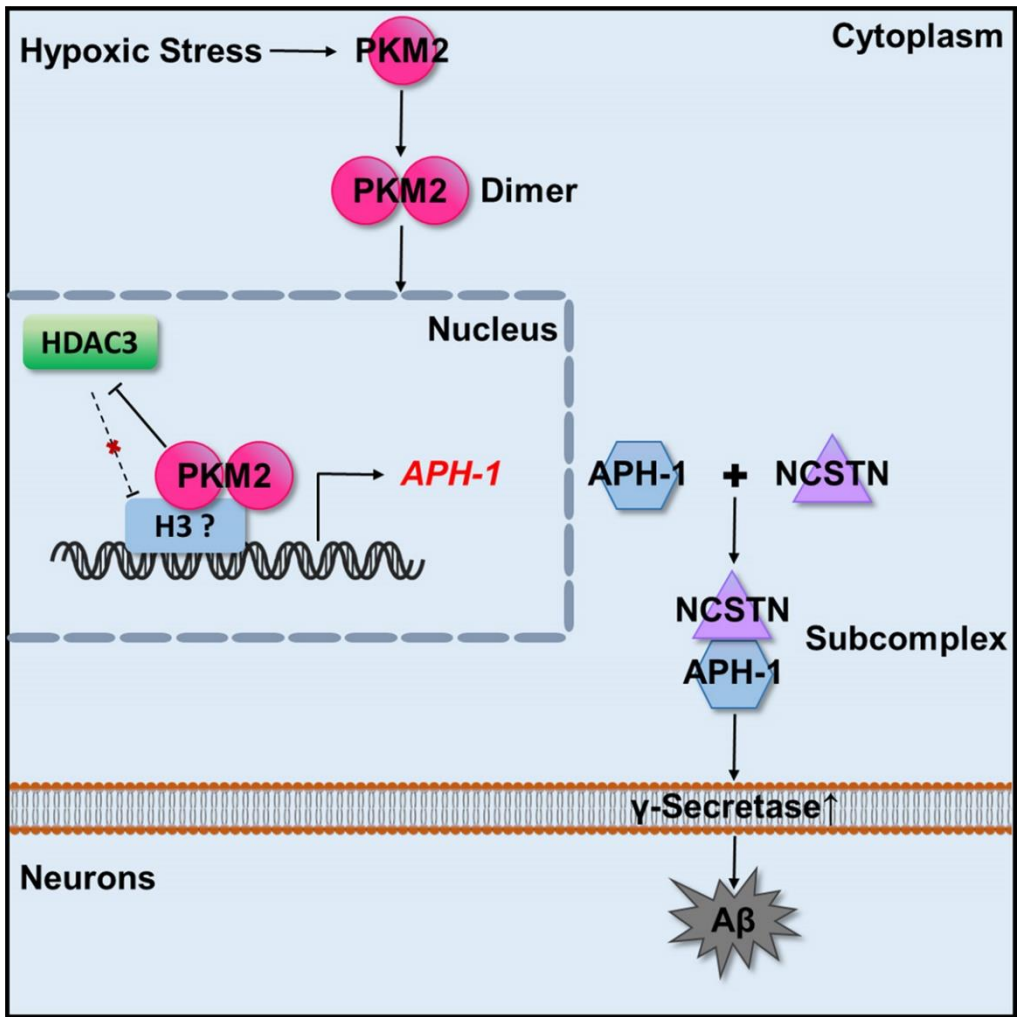


Figure I-23. Schematic diagram of PKM2's molecular mechanism in AD pathogenesis

Under hypoxic stress, PKM2 expression is induced in neurons. Dimeric PKM2 translocates into the nucleus and acts as a transcriptional co-activator of A β 1a. The increase in A β 1a protein promotes the formation of the A β 1a-NCT subcomplex, leading to an increase in the mature γ -secretase complex. This enhanced complex activity results in increased A β production, thereby accelerating AD pathogenesis.



Discussion

In the present study, I demonstrated a novel role of PKM2 in the regulation of γ -secretase activity, potentially contributing to Alzheimer's disease (AD) pathology. PKM2 is well-known for its role in glycolysis and energy metabolism in normal cells, and it also supports tumor growth in various cancers by facilitating the Warburg effect, enabling cancer cells to utilize glucose for rapid proliferation (Luo and Semenza, 2012; Mazurek, 2011). Initially, I hypothesized that the high energy demands of the AD brain could upregulate PKM2 expression to meet this metabolic need. However, my findings suggest that PKM2's role in γ -secretase regulation is independent of its metabolic functions. Cellular treatment with pyruvate or ATP, the metabolic products of PKM2, did not influence γ -secretase activity, indicating that PKM2's regulation of γ -secretase is not mediated by these metabolic products. Additionally, PKM2 overexpression led to a decrease in cellular pyruvate levels, supporting previous observations that PKM2 exhibits relatively low glycolytic activity compared to other pyruvate kinase isoforms (Bluemlein et al., 2011; Noguchi et al., 1987).

Hypoxia is a well-known risk factor for AD and stimulates A β production through γ -secretase activation (Li et al., 2009; Wang et al., 2006). HIF-1 α has been shown to upregulate β -secretase (BACE1) through transcriptional mechanisms and directly enhance γ -secretase activity through protein-protein interactions with γ -secretase components (Sun et al., 2006; Villa et al., 2014). In contrast, my results show that hypoxia selectively induces PKM2 in neurons without altering BACE1 expression, suggesting that PKM2 and HIF-1 α may activate γ -secretase through different mechanisms. Unlike HIF-1 α , which interacts directly with γ -secretase, PKM2 appears to act as a transcriptional co-activator, specifically increasing APH-1a mRNA levels

without direct binding to γ -secretase components. The PKM2 Y105F mutant, which cannot translocate to the nucleus, failed to increase γ -secretase activity, highlighting the role of nuclear PKM2 dimers in γ -secretase regulation. Furthermore, inhibition of HDAC3 in PKM2 knockdown cells partially restored APH-1a expression, indicating that PKM2 may modulate chromatin structure to regulate γ -secretase components.

In my study, 3xTg/PKM2 AD model mice exhibited higher levels of A β species and greater impairment in cognitive and working memory compared to 3xTg/WT mice. Homozygous 3xTg mice, which carry two copies of the APP^{swe}, PS1M146L, and TauP301L mutations, typically show significant memory deficits starting at around 6 months of age. However, the extent of cognitive decline in these homozygous mice would likely obscure the exacerbating effects of PKM2. For this reason, I utilized heterozygous 3xTg mice carrying a single copy of each mutation, allowing me to assess the impact of PKM2 on memory impairment under less severe baseline pathology. Based on my findings, it is reasonable to infer that cognitive deficits in 9-month-old heterozygous 3xTg mice would be less severe than in age-matched homozygous counterparts, providing a more suitable model for detecting PKM2's contribution to AD pathology.

Additionally, I observed that PKM2 expression is upregulated at later stages, coinciding with the onset of amyloid pathology in AD mouse models, such as at 8 months in 5xFAD mice and 17 months in Tg2576 mice. This delayed expression suggests that the development of amyloid pathology, likely driven by overexpression of mutant APP, may trigger increased neuronal PKM2 expression, which in turn accelerates A β production via γ -secretase activation. The correlation between PKM2 upregulation, amyloid plaque formation, and cognitive decline in both human AD brains and AD mouse models further supports the notion that PKM2 acts as a

risk factor in AD, exacerbating A β pathology through γ -secretase activation.

To date, various γ -secretase regulators, such as TMP21, GPR3, and β -arrestin, have been identified, but direct in vivo evidence supporting their role in AD-related amyloid pathology is limited (Chen et al., 2006; Thathiah et al., 2009, 2013). My findings provide significant in vivo evidence that PKM2 directly influences γ -secretase activity and contributes to cognitive impairment in AD. Additionally, the reduction of amyloid pathology observed in 3xTg mice following PKM2 knockdown highlights PKM2 as a promising therapeutic target for AD. Based on our study, I propose that PKM2 acts as a positive regulator of γ -secretase, particularly under hypoxic conditions, making it a potential target for AD treatment.

Limitations of the Study

In this study, I have primarily elucidated the mechanism through which PKM2 regulates γ -secretase activity via transcriptional control of APH-1a. While these findings underscore a role for PKM2 as a transcriptional modulator, the link between APH-1a expression and the assembly of the mature γ -secretase complex remains incomplete. Although my results indicate that PKM2 upregulation increases the APH-1a-NCT subcomplex, it is possible that an additional unidentified factor is required to facilitate the complete assembly and functional activation of γ -secretase. This aligns with previous findings showing that overexpressing individual core components of γ -secretase alone does not affect its enzymatic activity, suggesting a potential cooperative mechanism involving other co-factors or modulatory proteins.

Additionally, given that PKM2 does not directly interact with γ -secretase components, it remains unclear whether the regulation of γ -secretase assembly involves another PKM2-induced transcriptional byproduct or co-regulator that was not identified in this study. This gap suggests that PKM2 may influence γ -secretase indirectly through broader changes in gene expression or cellular processes rather than through direct interactions.

Future studies using high-resolution imaging or proteomics could help uncover potential additional molecules or complexes that mediate PKM2's effect on γ -secretase assembly. Moreover, exploring the functional impact of PKM2 across different cell types and stress conditions, particularly in astrocytes where PKM2 is also expressed, could provide further insights into its broader physiological roles and contribution to AD pathology.

CHAPTER II. NAMPT modulates γ - secretase activity under neuro- inflammatory condition

Introduction

Nicotinamide phosphoribosyltransferase (NAMPT) is an essential enzyme in the NAD⁺ salvage pathway, playing a central role in cellular energy metabolism. As the rate-limiting enzyme, NAMPT converts nicotinamide to nicotinamide mononucleotide (NMN), which subsequently becomes NAD⁺, a cofactor necessary for DNA repair, cellular signaling, and energy production (Weiyi Xu et al., 2020). Beyond its role in NAD metabolism, NAMPT acts as a cytokine-like molecule in inflammatory processes, known as pre-B cell colony-enhancing factor (PBEF) or visfatin, where it mediates immune responses and inflammatory signaling, particularly under conditions of metabolic stress (Massimiliano Gasparrini et al., 2022; Simone Torretta et al., 2020). NAMPT's multifunctional roles, especially in immune modulation and inflammation, underscore its impact on both systemic and neuroinflammatory pathways (Fabrizio Montecucco et al., 2013; Francisco J. Martínez-Morcillo et al., 2021).

NAMPT is involved in a variety of inflammatory diseases, where it often contributes to the progression of disease severity. For example, NAMPT is significantly elevated in conditions

like acute lung injury (Li Qin Zhang et al., 2009) and rheumatoid arthritis, where it amplifies inflammatory signaling pathways and mediates immune cell activity (Simone Torretta et al., 2020). Additionally, in sepsis and cardiovascular disease, NAMPT levels correlate with heightened inflammatory responses, suggesting its key role in inflammatory disease mechanisms (Fabrizio Montecucco et al., 2013). These associations emphasize NAMPT's influence on inflammation-related pathways and its broader impact on disease progression.

In states of metabolic dysregulation, such as obesity, NAMPT levels are elevated and have been observed to contribute to chronic low-grade inflammation (Abdullah A. Alghasham and Youssef A. Barakat, 2008). Notably, NAMPT levels are significantly increased in the serum and plasma of patients with type 2 diabetes (T2D), a representative metabolic disease (Miao-Pei Chen et al., 2006). Visceral fat, a primary site of NAMPT expression, further highlights its involvement in metabolic regulation and inflammation (Eduardo García-Fuentes et al., 2007). These findings suggest that NAMPT may play a pivotal role in linking metabolic dysregulation to systemic inflammation, a hypothesis that has garnered increasing attention in recent research (N P E Kadoglou et al., 2009; Anusha Jayaraman et al., 2015).

Neuroinflammation driven by glial activation and cytokine release is a recognized contributor to AD pathology, and NAMPT's upregulation in response to neuroinflammatory conditions implies its role in neurodegenerative diseases, such as AD (Yang Deng et al., 2022). In AD, where inflammation and amyloid pathology intersect, NAMPT could act as a molecular bridge between systemic inflammation and γ -secretase activation. Given its elevated levels in the cerebrospinal fluid (CSF) of AD patients, NAMPT may significantly contribute to Alzheimer's disease pathology by linking metabolic dysregulation-induced inflammation to neurodegenerative processes. (Bart De Strooper et al., 2010; Anusha Jayaraman et al., 2015).

Result

NAMPT was identified as γ -secretase regulator through a cell-based gain-of-function γ -secretase reporter assay.

I utilized a cell-based gain-of-function γ -secretase reporter assay, leveraging a human secretion DNA pool containing approximately 1,800 different secretory genes. This screening system involves transfection of cultured cells with the DNA pool, enabling gain-of-function analysis by driving γ -secretase activity. The reporter assay relies on a doxycycline-inducible system, where γ -secretase activity cleaves a C99-rtTA construct, thereby activating GFP expression (Figure II-1. A).

The system was validated with both positive and negative controls, demonstrating that increased γ -secretase activity elevates GFP intensity, whereas inhibition of γ -secretase diminishes the signal (Figure II-1. B). Using this approach, NAMPT was identified as a potential γ -secretase regulator. Cells transfected with NAMPT consistently exhibited increased GFP signal intensity compared to control cells, indicating enhanced γ -secretase activity (Figure II-1. C). NAMPT was selected based on its reproducible and sustained elevation of GFP intensity, a mark of its regulatory effect on γ -secretase.

Levels of NAMPT are elevated in brains of 3xTg AD model mice and AD patients.

To determine the pathological relevance of NAMPT in Alzheimer's disease (AD), I analyzed its expression in 3xTg AD model mice and human samples. Western blot analysis revealed

significant upregulation of NAMPT expression in 3xTg mouse brain tissue compared to WT controls, with levels increasing with age (Figure II-2. A and B). This upregulation correlated with the progression of AD pathology and increased γ -secretase components, including NCT and PS1-NTF. In human samples, NAMPT levels in cortical tissue from AD patients were significantly elevated compared to controls (Figure II-3. C). Furthermore, cerebrospinal fluid (CSF) samples from AD patients showed markedly higher NAMPT levels compared to controls (Figure II-3. A and B). This consistent elevation of NAMPT in 3xTg mouse brains, AD patient cortical tissue, and CSF highlights its potential involvement in AD-related γ -secretase regulation. Additionally, correlation analysis in cortical tissue revealed a significant association between NAMPT levels and IFITM3 expression, further implicating NAMPT in pathways relevant to γ -secretase activity (Figure II-3. E)

Given the observed elevation in NAMPT protein levels in 3xTg AD mice brain tissue and AD patient brain tissue, I next investigated whether this increase could be attributed to transcriptional regulation by examining NAMPT mRNA levels in both mouse and human samples. In 3xTg mice, quantitative PCR analysis revealed no significant differences in NAMPT mRNA levels between WT and 3xTg mice at both 6 and 13 months of age (Figure II-4. A and B). These results suggest that the elevated protein levels in the 3xTg AD model are unlikely to result from transcriptional upregulation of NAMPT. To further validate these findings in human samples, I analyzed publicly available RNA-sequencing datasets (GSE36980 and GSE5281), extracting NAMPT mRNA expression values from multiple brain regions, including the hippocampus, temporal cortex, frontal cortex, and entorhinal cortex. Similar to the mouse data, there were no significant differences in NAMPT mRNA levels between AD patients and control groups across these brain regions (Figure II-4. C-F).

These results indicate that the increased NAMPT protein levels observed in 3xTg mouse brain

tissue and AD patient's brain tissue may not arise from changes in mRNA expression. Instead, this discrepancy suggests the involvement of post-transcriptional modifications, enhanced protein stability, or secretion mechanisms. Considering the secretion aspect, the elevated NAMPT levels in the CSF may reflect increased secretion from specific brain regions into the neural circulation system.

NAMPT modulates γ -secretase activity without affecting other secretase activities.

To investigate the specific role of NAMPT in modulating γ -secretase activity, I utilized a luciferase reporter assay as an alternative γ -secretase activity readout. NAMPT, identified through a gain-of-function γ -secretase reporter assay, was hypothesized to influence γ -secretase activity and potentially affect other secretases, such as α - and β -secretases. To test this, I overexpressed and knocked down NAMPT in cultured cells and measured the activities of these secretases.

Luciferase reporter assays demonstrated that NAMPT overexpression significantly increased γ -secretase activity, with a fold-change of approximately 1.5 compared to control cells (Figure II-5. A). In contrast, no significant changes were observed in α -secretase activity, as assessed through sAPP α levels in the culture media (Figure II-5. C). Similarly, β -secretase activity remained unaffected (Figure II-5. B). NAMPT knockdown resulted in a significant reduction in γ -secretase activity to approximately 70% of control levels (Figure II-7. D). However, consistent with the overexpression data, α - and β -secretase activities were not significantly altered by NAMPT knockdown (Figures II-5. E and F). These findings confirm that NAMPT modulates γ -secretase activity in a selective manner, without affecting other secretase pathways.

The regulatory effect of NAMPT on γ -secretase activity was further validated through measurements of secreted A β peptides and APP intracellular domain (AICD) levels. Using an immunoprecipitation (IP) approach, I examined A β peptides in the conditioned medium of cultured cells overexpressing or silencing NAMPT. Additionally, in vitro AICD generation assays were performed to assess NAMPT's impact on γ -secretase activity. Immunoprecipitation of conditioned medium from NAMPT-overexpressing cells revealed a significant increase in secreted A β peptides, including monomers, dimers, and trimer, compared to control cells (Figure II-6. A). Conversely, NAMPT knockdown via shRNA reduced levels of secreted A β , as demonstrated by immunoprecipitation and Western blot analysis (Figure II-6. B).

In in vitro AICD generation assays, NAMPT overexpression enhanced AICD levels, a direct product of γ -secretase-mediated cleavage of APP, compared to control conditions (Figure II-6. C). Consistently, silencing NAMPT decreased AICD levels (Figure II-6. D), confirming that NAMPT positively regulates γ -secretase activity. Furthermore, the levels of APP full-length and C-terminal fragment (APP-CTF), as well as PS1-NTF, remained relatively unchanged in both overexpression and knockdown experiments. These results provide further evidence that NAMPT regulates γ -secretase activity, enhancing the generation of A β peptides and AICD. This regulatory role highlights NAMPT as a potential upstream modulator of γ -secretase in the amyloidogenic pathway.

NAMPT is a Notch-sparing γ -secretase regulator.

To investigate whether NAMPT specifically regulates γ -secretase activity toward APP while sparing other substrates, I analyzed its effect on Notch cleavage. Since γ -secretase processes multiple substrates, including Notch, I measured NICD (Notch Intracellular Domain) levels, a

product of Notch cleavage, to determine if NAMPT influences its processing. In cells overexpressing NAMPT, NICD levels were not significantly different from control cells, as shown by Western blot and quantification (Figure II-7. A and B). Similarly, NAMPT knockdown did not result in any significant changes in NICD levels compared to shControl cells (Figure II-7. C and D). These results suggest that NAMPT does not affect Notch cleavage by γ -secretase. These findings highlight NAMPT as a γ -secretase regulator that selectively enhances APP cleavage without affecting Notch processing, addressing a key limitation in γ -secretase research. By sparing Notch, NAMPT offers a potential pathway to specifically target amyloidogenic processing in Alzheimer's disease without disrupting essential Notch signaling pathways.

Enzymatic activity of NAMPT is not associated with regulation of γ -secretase activity.

To explore the functional mechanism by which NAMPT regulates γ -secretase activity, I focused on its well-known role in NAD biosynthesis. Specifically, I assessed whether NAMPT enzymatic activity or NAD production contributes to γ -secretase regulation. First, I treated cultured cells with FK866, an irreversible inhibitor of NAMPT enzymatic activity, and measured γ -secretase activity using an in vitro AICD generation assay. Western blot analysis showed that FK866 treatment did not alter AICD levels compared to untreated controls, indicating that inhibition of NAMPT enzymatic activity does not affect γ -secretase-mediated APP processing (Figure II-8. A and B). Additionally, I supplemented NAD directly during the in vitro reaction to test if elevated NAD levels resulting from NAMPT overexpression might influence γ -secretase activity. However, the addition of NAD did not alter AICD levels, further supporting the notion that NAMPT's regulatory role on γ -secretase is independent of its NAD

biosynthesis function (Figure II-8. A).

Next, I examined the effect of a dominant-negative NAMPT mutant (H247A) on γ -secretase activity using a luciferase reporter assay. The H247A mutant lacks enzymatic activity but retains structural integrity. Both NAMPT wild-type (WT) and H247A increased γ -secretase activity to comparable levels, as indicated by the luciferase assay results (Figure II-8. C). These findings confirm that NAMPT's regulatory role in γ -secretase activity is independent of its enzymatic activity in NAD biosynthesis.

NAMPT does not alter levels of γ -secretase complex and components.

To investigate whether NAMPT regulates γ -secretase activity by modulating the levels of its complex or components, I analyzed the γ -secretase complex and its components proteins under NAMPT overexpression and knockdown conditions. Blue-native PAGE (BN-PAGE) analysis revealed that overexpression of NAMPT did not lead to any significant change in the 440-kDa γ -secretase complex levels, as indicated by the levels of NCT and PS1-NTF (Figure II-9. A). Similarly, knockdown of NAMPT also showed no reduction in γ -secretase complex levels (Figure II-9. B).

In addition, I examined the individual expression levels of γ -secretase components, including NCT, PS1-NTF, APH1a, and PEN2, in denaturing conditions. Western blot analysis confirmed that neither overexpression (Figure II-9. C) nor knockdown (Figure II-9. D) of NAMPT altered the levels of these components. These results suggest that NAMPT does not regulate γ -secretase activity by influencing the total levels of the γ -secretase complex or its components. Instead, its regulatory mechanism likely involves other pathways or factors beyond simple modulation of γ -secretase abundance.

NAMPT is mainly expressed in glial cells and is upregulated by LPS stimulation.

To explore potential and non-canonical roles of NAMPT in γ -secretase regulation, I investigated its expression patterns in the brain and its responsiveness to inflammatory stimuli. Given that NAMPT has been previously reported to act as a pro-inflammatory cytokine-like factor under certain conditions (Massimiliano Gasparrini et al. 2022; Zhongjie Sun et al. 2013), I analyzed its expression across different brain cell types and its induction upon LPS stimulation. Western blot analysis of primary cultures derived from neurons, microglia, and astrocytes revealed that NAMPT is predominantly expressed in glial cells, including both microglia and astrocytes, with lower levels detected in neurons (Figure II-10. A).

To further investigate regulation of NAMPT expression under inflammatory conditions, I treated the Bv2 microglial cells with increasing concentrations of lipopolysaccharide (LPS). Western blot analysis demonstrated a dose-dependent induction of NAMPT expression, consistent with the upregulation of the pro-inflammatory cytokine IL-1 β (Figure II-10. B). Similar results were observed in primary astrocytes upon LPS treatment, where NAMPT expression was significantly increased (Figure II-10. C). These findings suggest that NAMPT is predominantly expressed in glial cells within the brain and is upregulated in response to inflammatory stimuli, such as LPS. This aligns with its potential role as an inflammatory mediator, which may contribute to its regulation of γ -secretase activity in the context of neuroinflammation observed in Alzheimer's disease.

NAMPT knockdown blocks the induction of AICD levels under LPS stimulation.

To investigate whether NAMPT mediates γ -secretase activation under inflammatory conditions, I analyzed the impact of NAMPT knockdown on AICD generation in response to LPS stimulation. As LPS induces inflammation and upregulates NAMPT expression, this experimental approach aimed to determine if γ -secretase activation under these conditions is NAMPT-dependent. Western blot analysis revealed a marked increase in AICD levels in control cells upon LPS stimulation, consistent with enhanced γ -secretase activity (Figure II-11. A).

On the other hand, in cells where NAMPT was knocked down using shRNA, the LPS-induced increase in AICD levels was effectively blocked, despite similar levels of APP being observed in all conditions. This suggests that NAMPT is necessary for the γ -secretase activation observed under inflammatory conditions. These results highlight NAMPT as a critical mediator of γ -secretase regulation in response to inflammation and suggest that its upregulation in LPS-stimulated environments is functionally linked to γ -secretase activity. This provides further evidence for NAMPT's role as a regulator of γ -secretase, particularly in inflammation-associated processes relevant to Alzheimer's disease.

NAMPT binds to IFITM3, a Presenilin regulator.

IFITM3 was previously identified as a regulator of γ -secretase through its interaction with presenilin (Ji-Yeun Hur et al. 2020), raising the possibility of its involvement in NAMPT-mediated γ -secretase modulation. Furthermore, yeast two-hybrid assays suggested a potential physical interaction between NAMPT and IFITM3 (Li Qin Zhang et al. 2009). To explore this, I investigated whether NAMPT and IFITM3 interact in a cell culture system. To test this, I performed co-immunoprecipitation (Co-IP) experiments. In overexpression models, FLAG-tagged NAMPT and HA-tagged IFITM3 were co-transfected into HEK293T cells. Subsequent

IP assays revealed that NAMPT co-precipitated with IFITM3, demonstrating a physical interaction between them (Figure II-12. A). Additionally, endogenous IP experiments in HEK293T cells confirmed that NAMPT and IFITM3 form a protein complex under physiological conditions (Figure II-12. B). These findings establish a physical interaction between NAMPT and IFITM3, suggesting a possible collaborative role in γ -secretase regulation.

NAMPT and IFITM3 are induced by LPS injection and mediate increase of γ -secretase activity in mice.

To investigate the role of NAMPT and its potential association with IFITM3 under inflammatory conditions, I utilized a systemic inflammation model via intraperitoneal (i.p.) injection of LPS in mice. This approach is known to induce both systemic and neuroinflammation (Liya Qin et al. 2010). Two experimental conditions were applied: mild-dose LPS (250 μ g/kg) administered over seven consecutive days and higher-dose LPS (0.5 and 1 mpk) injected twice over two days to assess dose-dependent effects. Western blot analysis of brain tissues revealed a significant increase in NAMPT expression in both mild-dose and higher-dose LPS injection groups compared to PBS-treated controls (Figures II-13. A and B). Notably, higher doses of LPS also induced IFITM3 expression, which was not assessed in the mild-dose condition. These results suggest a dose-dependent co-regulation of NAMPT and IFITM3 under acute inflammatory conditions.

To evaluate the functional relevance of NAMPT upregulation in γ -secretase activation, I performed an in vitro AICD generation assay using brain extracts. In the mild-dose LPS injection group, γ -secretase activity was significantly enhanced, as evidenced by increased

AICD levels compared to controls (Figures II-13. C and D). This was consistent with the observation of elevated NAMPT expression.

To further validate the co-regulation of NAMPT and IFITM3 under inflammatory conditions, I examined the effect of LPS treatment on their expression in primary astrocytes in vitro. Higher concentrations of LPS significantly induced both NAMPT and IFITM3 expression, supporting the in vivo findings and reinforcing their potential collaborative role (Figure II-13. E). These findings demonstrate that LPS-induced systemic inflammation upregulates NAMPT in both mild and acute conditions, while IFITM3 is specifically induced under higher-dose LPS. The co-induction of NAMPT and IFITM3 highlights their potential interplay in γ -secretase regulation under inflammatory conditions. Furthermore, the functional link between NAMPT upregulation and γ -secretase activation underscores its relevance to Alzheimer's disease pathogenesis.

Recombinant NAMPT induces increase of NAMPT and IFITM3 expression through NF- κ B signaling.

NAMPT has been reported to be secreted under various conditions, acting as an extracellular signaling molecule (Alexander N Garcia et al. 2022; Belinda L Sun et al. 2023). In my experiments, LPS treatment was shown to increase both intracellular NAMPT levels and its secretion into the extracellular space. Based on these findings, I hypothesized that extracellular NAMPT (eNAMPT) might exert functional effects within recipient cells. To test this hypothesis, I purified recombinant NAMPT using a bacterial expression system and treated BV2 microglial cells with increasing concentrations of rNAMPT. Western blot analysis revealed that rNAMPT treatment elevated intracellular levels of both NAMPT and IFITM3 in

a dose-dependent manner (Figure II-14. A and B).

Additionally, since eNAMPT was reported to act as a pro-inflammatory cytokine-like molecule, I examined its role in NF- κ B signaling. In HT22 hippocampal cells, rNAMPT treatment resulted in decrease of I κ B α levels, consistent with the activation of NF- κ B signaling, along with an increase in IFITM3 expression (Figure II-14. C and D). These results were similar to those observed with LPS treatment, suggesting that eNAMPT may function through a shared mechanism. These findings indicate that eNAMPT promotes the upregulation of intracellular NAMPT and IFITM3, potentially through NF- κ B signaling, providing further evidence of its role as an extracellular regulator in neuroinflammatory contexts.

NAMPT knockdown reduces IFITM3-associated γ -secretase complex levels without affecting overall complex abundance.

To explore whether NAMPT influences γ -secretase complex composition through its interaction with IFITM3, I examined levels of the γ -secretase complex by analyzing IFITM3-associated complexes. SDS-PAGE analysis revealed that NAMPT knockdown did not affect the overall protein levels of IFITM3 or other core γ -secretase components, such as NCT, PS1-NTF, APH1a, and PEN2, indicating that NAMPT is not required for maintaining the total abundance of γ -secretase components (Figure II-15. A). On the other hand, BN-PAGE analysis demonstrated a more specific effect: While the overall levels of γ -secretase holo-complexes (as assessed by NCT and PS1-NTF signals) were unchanged, the levels of IFITM3-associated γ -secretase complexes were significantly reduced upon NAMPT knockdown (Figure II-15. B).

These results indicate that NAMPT selectively influences the assembly or stability of IFITM3-containing γ -secretase complexes without affecting the total holo-complex levels.

This selectivity was further validated under LPS-induced inflammatory conditions, where NAMPT knockdown specifically prevented the increase in IFITM3-associated complexes while leaving the levels of other core γ -secretase complexes unaffected (Figure II-15. C). These findings suggest that while NAMPT does not alter the overall abundance of γ -secretase holo-complexes, it specifically regulates IFITM3-containing complexes. This provides a potential mechanism for NAMPT's selective regulation of γ -secretase activity, aligning with its previously observed substrate-specific effects.

Figure II-1. Schematic diagram showing gain-of-function screening and isolation of NAMPT which increases reporter activity of γ -secretase.

(A) Schematic diagram of gain-of-function screening.

(B) Fluorescence intensity observed during cell-based screening.

(C) Fluorescence intensity following NAMPT overexpression during gain-of-function screening in HEK293T cells.

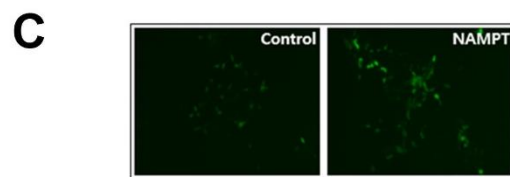
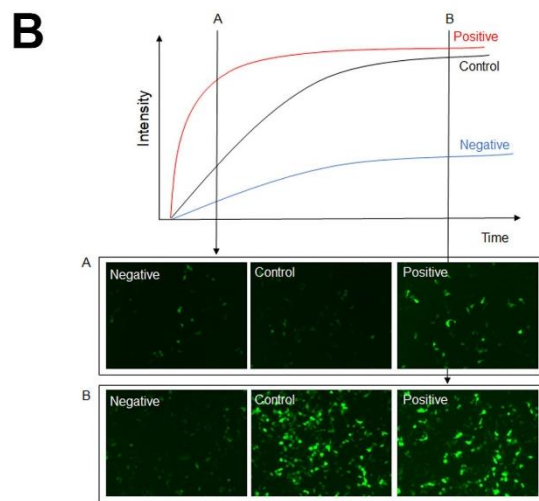
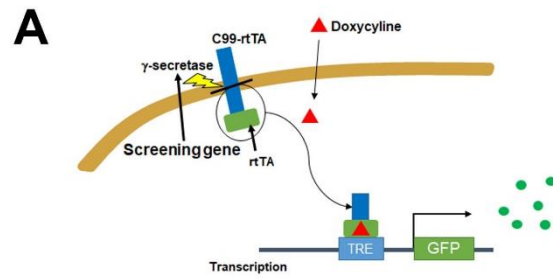


Figure II-2. Levels NAMPT expression and γ -secretase components are elevated in 3xTg mouse brain.

(A and B) Expression of NAMPT and γ -secretase components was assessed by western blotting in cortical extracts from 6-month-old (A) and 13-month-old (B) 3xTg mice.

(C and D) Relative expression levels of NAMPT (C) and γ -secretase components (D) from panels A and B. Bars represent the mean \pm SEM. *P < 0.05, **P < 0.01, ***P < 0.005, ****P < 0.001 (Student's t-test).

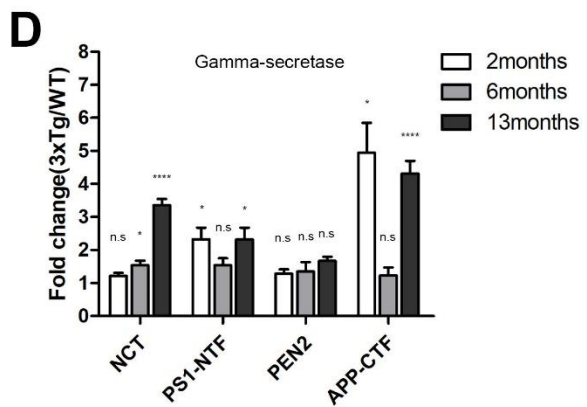
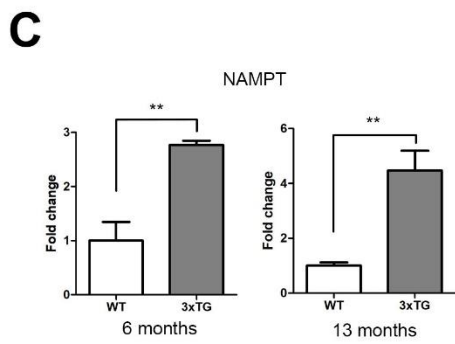
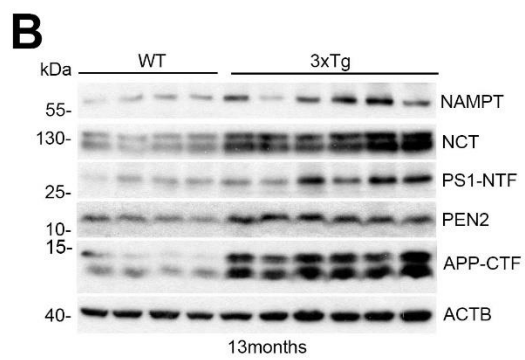
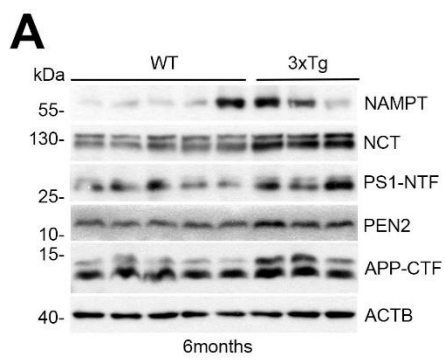


Figure II-3. NAMPT expression level is elevated in the CSF and cortex of AD patients.

(A) CSF samples from patients with AD and non-AD were analyzed by western blotting.

(B) Relative expression levels of NAMPT in CSF samples. Bars represent the mean \pm SEM.

***P < 0.005 (Student's t-test).

(C) Expression of NAMPT and IFITM3 was assessed by western blotting in brain cortex samples from patients with Alzheimer's disease (AD) and non-AD.

(D) Relative expression levels of NAMPT in cortex samples. Bars represent the mean \pm SEM.

*P < 0.05 (Student's t-test). One sample was removed by Grubbs' outlier test.

(E) Linear correlation between expression levels of NAMPT and IFITM3.

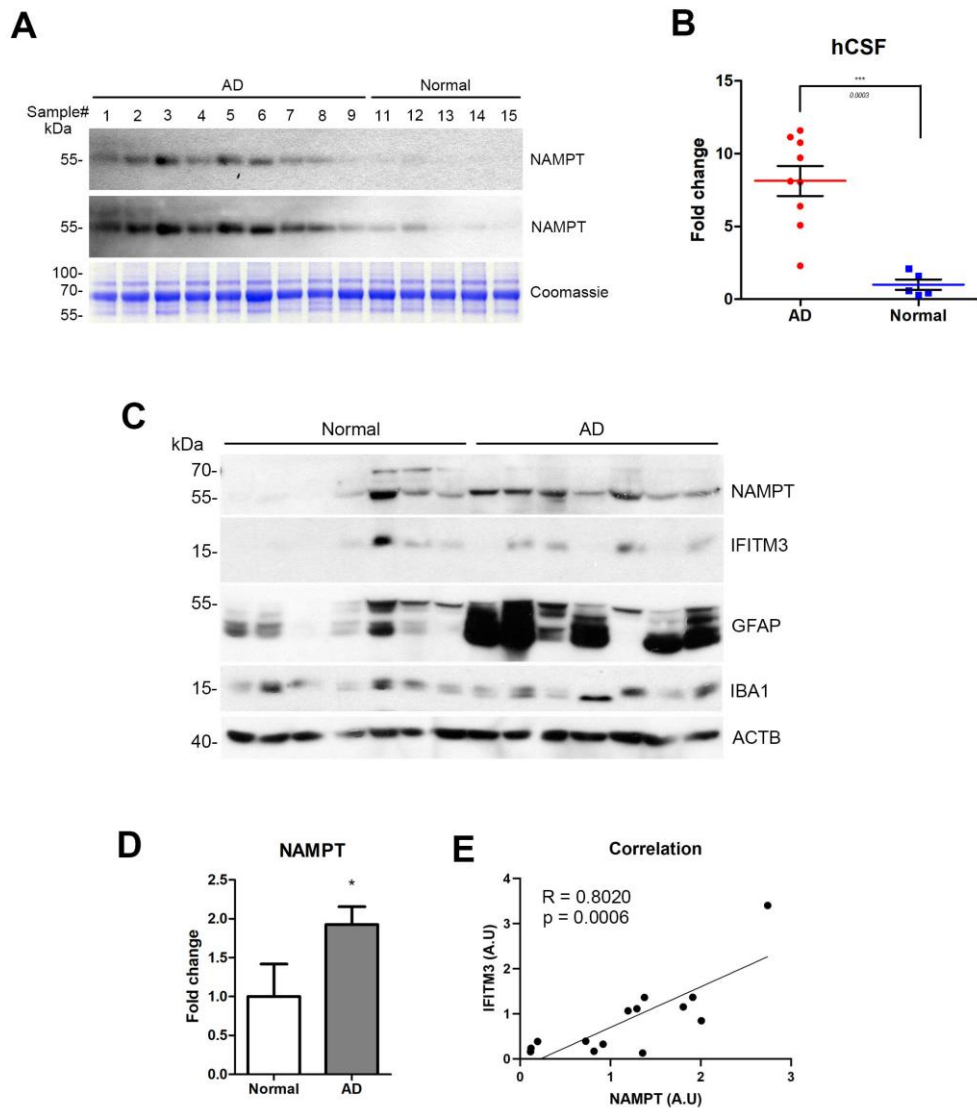


Figure II-4. Levels of NAMPT mRNA expression in 3xTg mice and AD patients.

(A and B) Relative levels of NAMPT mRNA in 6-month-old (A) and 13-month-old (B) 3xTg mice.

(C-F) Relative levels of NAMPT mRNA in the hippocampus (C), temporal cortex (D), frontal cortex (E), and entorhinal cortex (F) of AD patients. Data were extracted from GSE36980 (C-E) and GSE5281 (F).

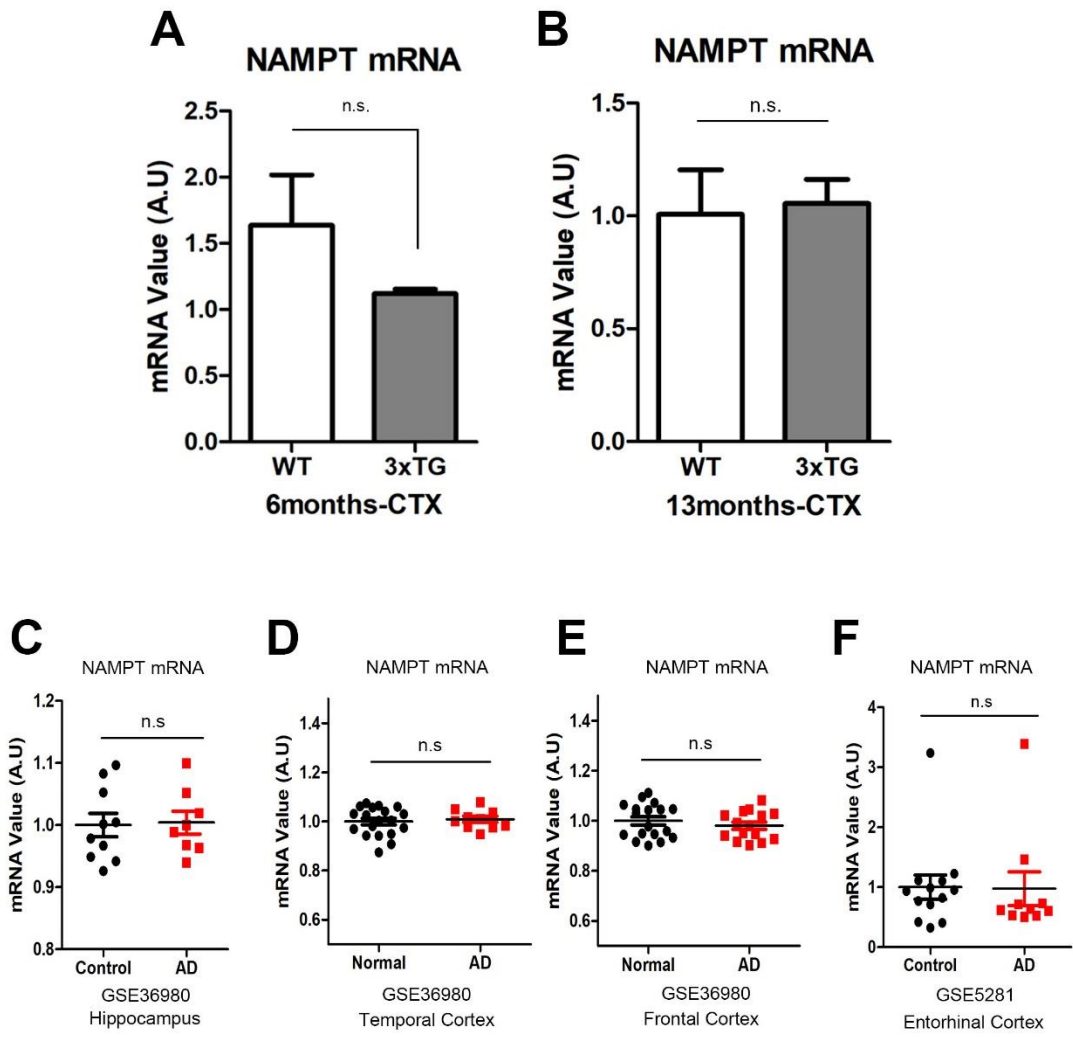


Figure II-5. NAMPT affects γ -secretase activity without affecting other secretases.

(A) The γ -secretase activity determined by luciferase reporter activity in HEK293T cells overexpressing NAMPT. Bars represent the mean \pm SD (n =4). *p <0.05 (Student's t test).

(B) The β -secretase activity determined by alkaline phosphatase reporter activity in HEK293T cells overexpressing NAMPT. Bars represent the mean \pm SD (n = 3). N.S., not significant (Student's t test).

(C) The α -secretase activity determined by quantification of cleaved sAPP α in culture medium of CHO-7PA2 cells overexpressing NAMPT. Bars represent the mean \pm SD (n = 3). N.S. (Student's t test).

(D) The γ -secretase activity determined by luciferase reporter activity in HEK293T cells after silencing NAMPT. Bars represent the mean \pm SD (n =5). *p <0.05 (Student's t test).

(E) The β -secretase activity determined by alkaline phosphatase reporter activity in HEK293T cells after silencing NAMPT. Bars represent the mean \pm SD (n = 3). N.S., not significant (Student's t test).

(F) The α -secretase activity determined by quantification of cleaved sAPP α in culture medium of CHO-7PA2 cells after silencing NAMPT. Bars represent the mean \pm SD (n = 3). N.S. (Student's t test).

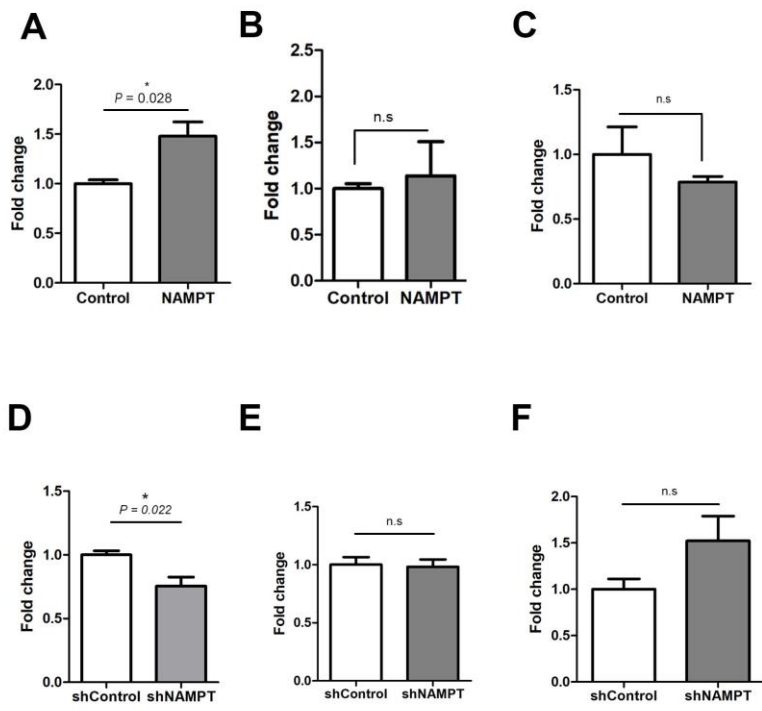


Figure II-6. Expression of NAMPT enhances A β secretion after proteolytic processing of APP into the conditioned medium.

(A and B) Secreted A β levels were analyzed by immunoprecipitation (IP) assay using 6E10 antibody in NAMPT-overexpressing SH-SY5Y/APPs1PS1dE9 cells (A) and NAMPT knockdown SH-SY5Y/APPsw cells (B).

(C and D) AICD levels were determined by in vitro AICD generation assay after overexpressing NAMPT in SH-SY5Y/APPs1PS1dE9 cells (C) and in NAMPT knockdown SH-SY5Y/APPs1PS1dE9 cells (D).

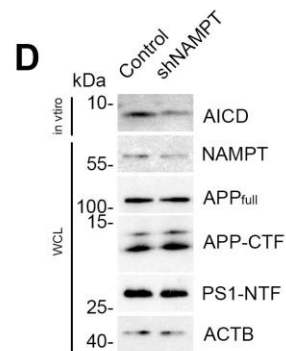
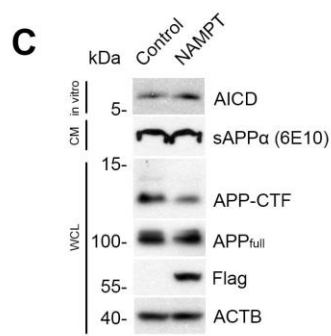
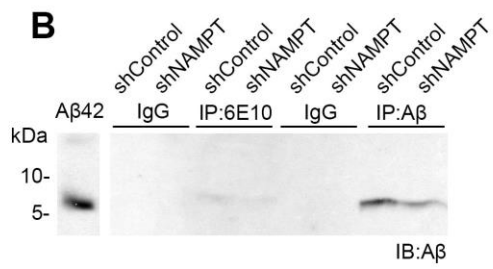
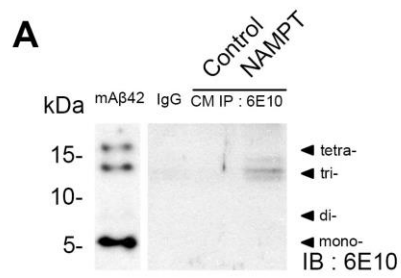


Figure II-7. NAMPT is a notch-sparing γ -secretase regulator.

(A and B) NICD levels were assessed by western blotting in HEK293T cells co-expressing Notch Δ E-GFP and NAMPT (A) and NICD levels were quantified using ImageJ. Bars represent the mean \pm SD (n = 3) (B).

(C and D) NICD levels were assessed by western blotting in HEK293T cells expressing Notch Δ E-GFP after NAMPT knockdown (C) and NICD level were quantified using ImageJ. Bars represent the mean \pm SD (n = 3) (D).

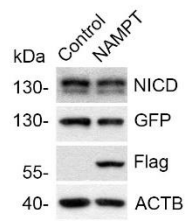
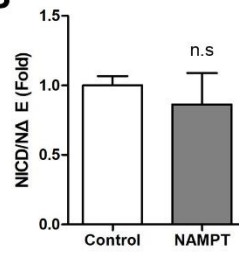
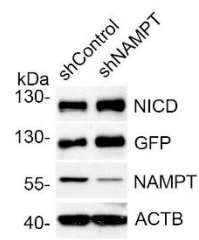
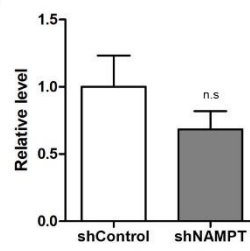
A**B****C****D**

Figure II-8. The enzymatic activity of NAMPT is not associated with its effects on γ -secretase activity.

(A) AICD levels were determined by an in vitro AICD generation assay in HEK293T/APPsw cells. HEK293T/APPsw cells were treated with 10 mM FK866. The crude membrane fraction was incubated with 1 mM NAD for 16 hours in vitro. Generated AICD levels were analyzed by SDS-PAGE.

(B) HEK293T/APPsw cells were treated with 10 mM FK866. AICD levels were quantified using ImageJ. Bars represent the mean \pm SD (n = 3).

(C) The γ -secretase activity was determined by luciferase reporter activity in HEK293T cells after overexpression of NAMPT WT and the H247A dominant mutant. Bars represent the mean \pm SD (n = 5). *p < 0.05, **p < 0.01 (one-way ANOVA with post hoc Tukey's multiple comparisons test).

(D) Cell extracts from panel C were analyzed by SDS-PAGE for NAMPT and H247A mutant expression.

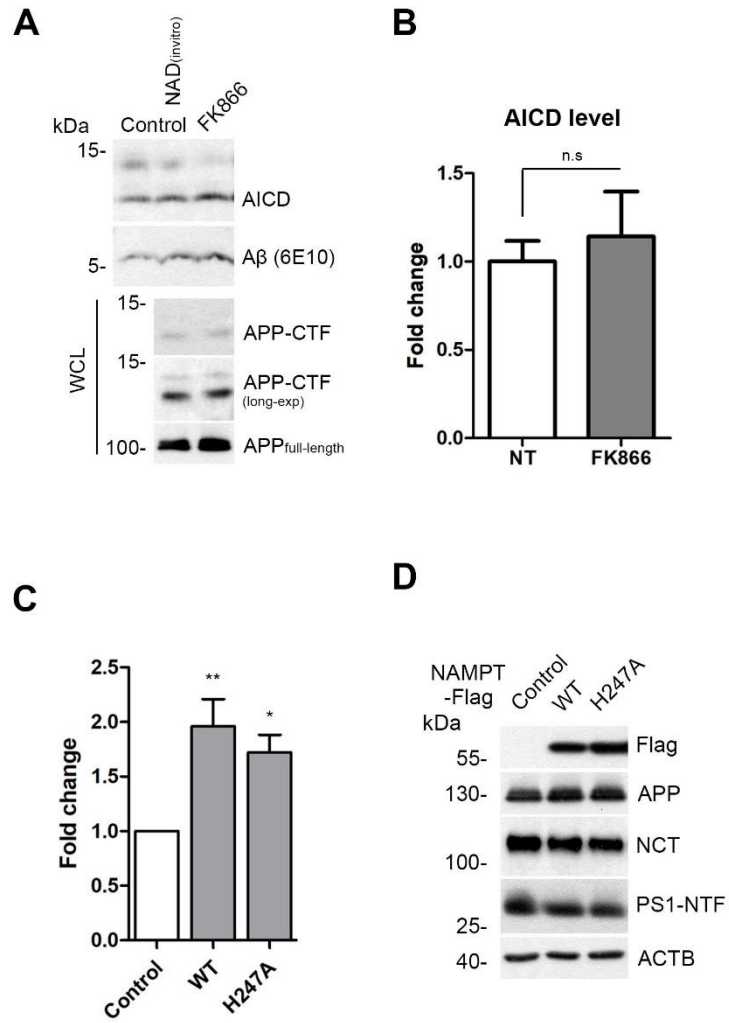


Figure II-9. Expression levels of NAMPT do not affect γ -secretase components and complex expression.

(A and B) Levels of γ -secretase complex assessed with blue-native (BN) gel electrophoresis followed by western blotting in HEK293T cells overexpressing NAMPT (A) or silencing NAMPT (B).

(C and D) Expression of γ -secretase components assessed with SDS-PAGE after overexpression (C) or knockdown of NAMPT (D).

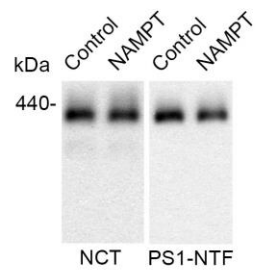
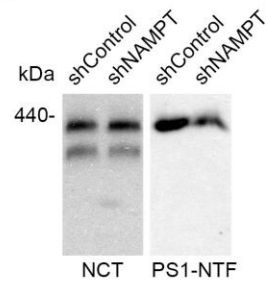
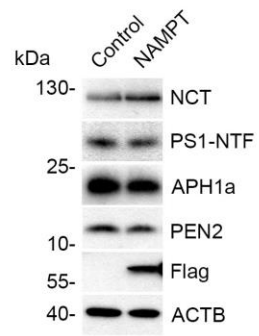
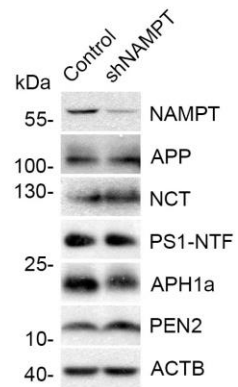
A**B****C****D**

Figure II-10. NAMPT expression in glial cells is upregulated by LPS stimulation.

(A) Cell extracts of primary cortical neurons, microglia and astrocytes were analyzed by western blotting.

(B) BV2 cells were treated with 0 - 1 $\mu\text{g/ml}$ LPS for 24 hours and expression of NAMPT was assessed by western blotting.

(C) Primary astrocytes were treated with 1 $\mu\text{g/ml}$ LPS 24 hours and expression of NAMPT was analyzed by western blotting.

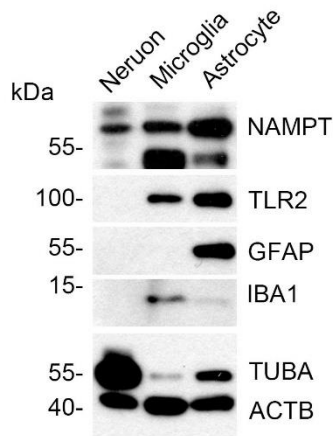
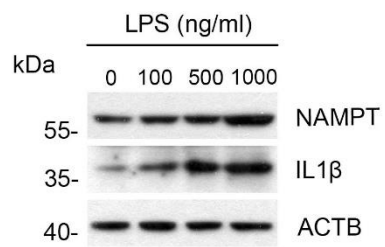
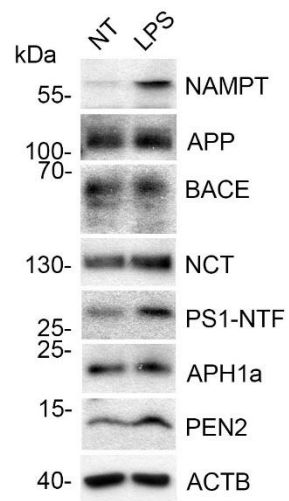
A**B****C**

Figure II-11. NAMPT knockdown blocks the LPS-induced induction of AICD level.

SH-SY5Y/APPs1-PS1dE9 cells were transiently transfected with empty vector and shNAMPT for 24 hours and then treated with 1 μ g/ml LPS for an additional 24 hours. Crude membrane fractions were prepared from cell lysates and subjected to an in vitro AICD assay for 2 hours.

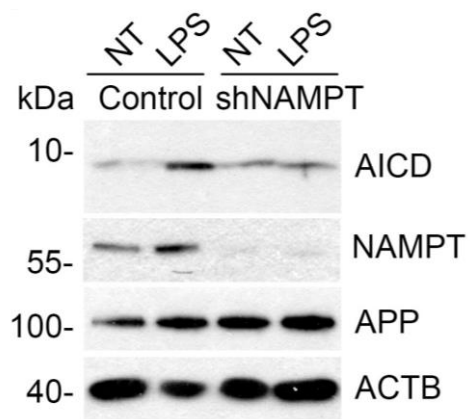


Figure II-12. NAMPT binds to IFITM3, a presenilin regulator.

(A) HEK293T cells were transfected with NAMPT and IFITM3 for 24 hours and then analyzed by immunoprecipitation assays using anti-FLAG and anti-HA antibodies. The immunoprecipitates and whole-cell lysates were analyzed by western blotting.

(B) Crude membrane fractions of HEK293T cells were solubilized in 0.5% DDM buffer and subjected to immunoprecipitation using an anti-IFITM3 antibody.

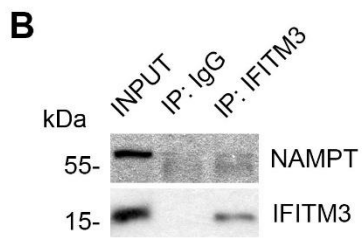
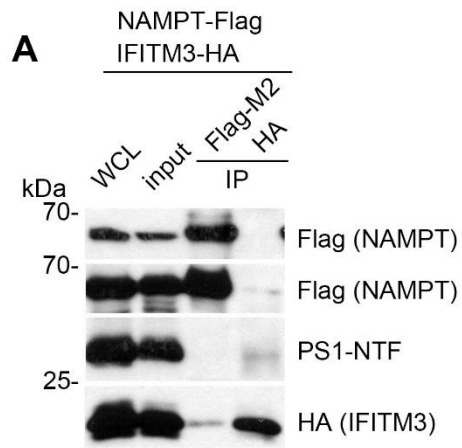


Figure II-13. LPS (i.p.) injection increases NAMPT and IFITM3 levels in the mouse brain and upregulates γ -secretase activity.

(A and B) The 3-months old-C57BL6 WT mice were daily and intraperitoneally injected with 250 $\mu\text{g}/\text{kg}$ LPS for 7 days. Mouse hippocampal tissues were analyzed by western blotting (A). Relative expression levels of NAMPT in panel A were quantified using ImageJ (B).

(C and D) Crude membrane fractions from mouse cortex were prepared and subjected to an AICD generation assay for 2 hours, followed by western blotting (C). AICD levels in panel C were quantified using ImageJ (D).

(E) The 3-months old-C57BL6 WT mice were daily and intraperitoneally injected with 500 $\mu\text{g}/\text{kg}$ and 1,000 $\mu\text{g}/\text{kg}$ LPS for 2 days. Mouse cortex was analyzed by western blotting.

(F) Primary astrocytes were treated with 1 $\mu\text{g}/\text{ml}$ LPS and cell extracts and conditioned medium were analyzed by immunoprecipitation and western blotting.

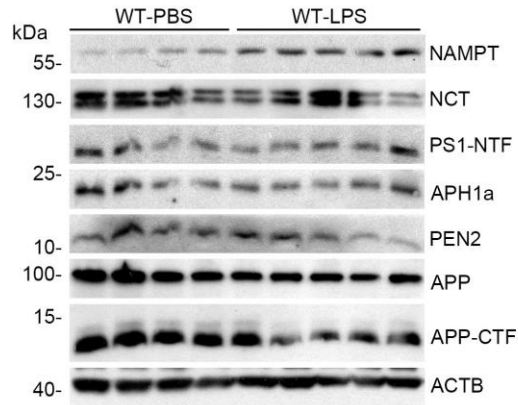
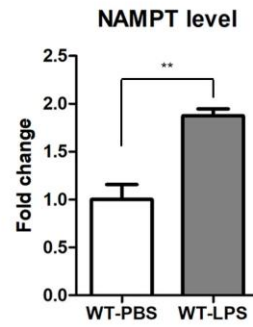
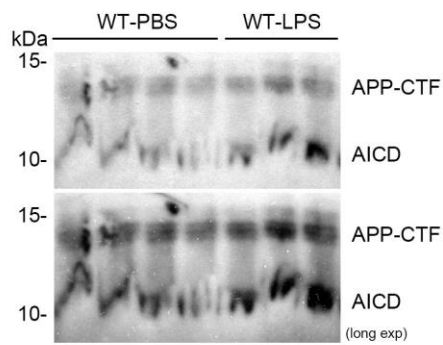
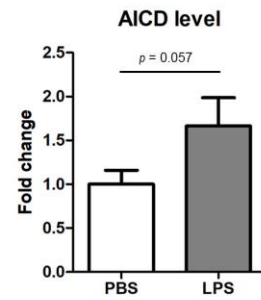
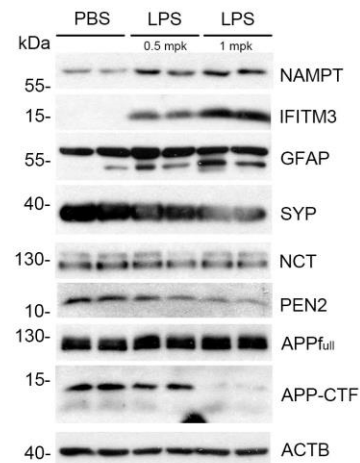
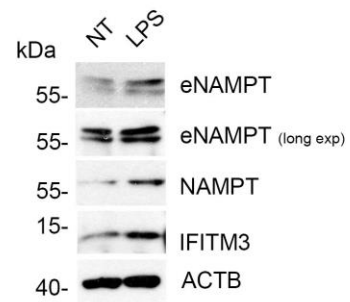
A**B****C****D****E****F**

Figure II-14. Treatment with recombinant NAMPT protein increases levels of NAMPT and IFITM3 through NF-kB signaling.

(A) His-NAMPT (mouse) protein was purified from BL21 Rosetta strain after IPTG treatment.

(B) Bv2 cells were treated with recombinant 500 ng/ml His-NAMPT for 24 hours and cell extracts were analyzed by western blotting.

(C) HT22 cells were incubated with recombinant 500 ng/ml His-NAMPT and 1 μ g/ml LPS for 1 hour and cell extract was analyzed by western blotting.

(D) Relative levels of I κ B α and IFITM3 were measured using ImageJ. Bars represent the mean \pm SD (n = 4). *p < 0.05; **p < 0.01 (one-way ANOVA with post hoc Tukey's multiple comparisons test).

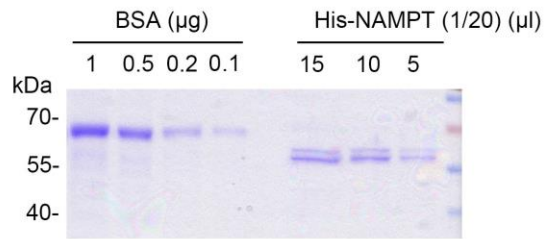
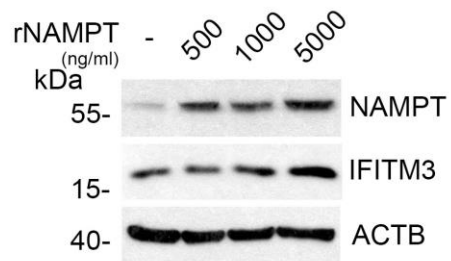
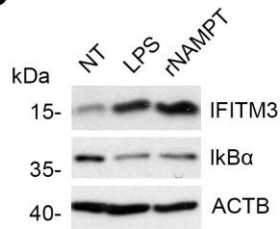
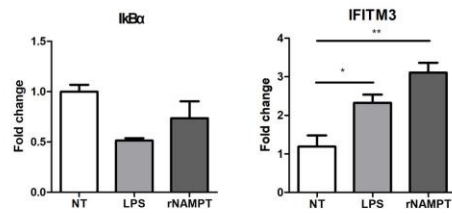
A**B****C****D**

Figure II-15. NAMPT knockdown interferes with the IFITM3-associated γ -secretase complex.

(A) SH-SY5Y/APP^{sw} shNAMPT knockdown cells and control cells were analyzed by western blotting.

(B) Crude membrane fractions of SH-SY5Y/APP^{sw} shNAMPT knockdown and control cells were solubilized with 0.5% DDM detergent for 2 hours and then analyzed by BN-PAGE.

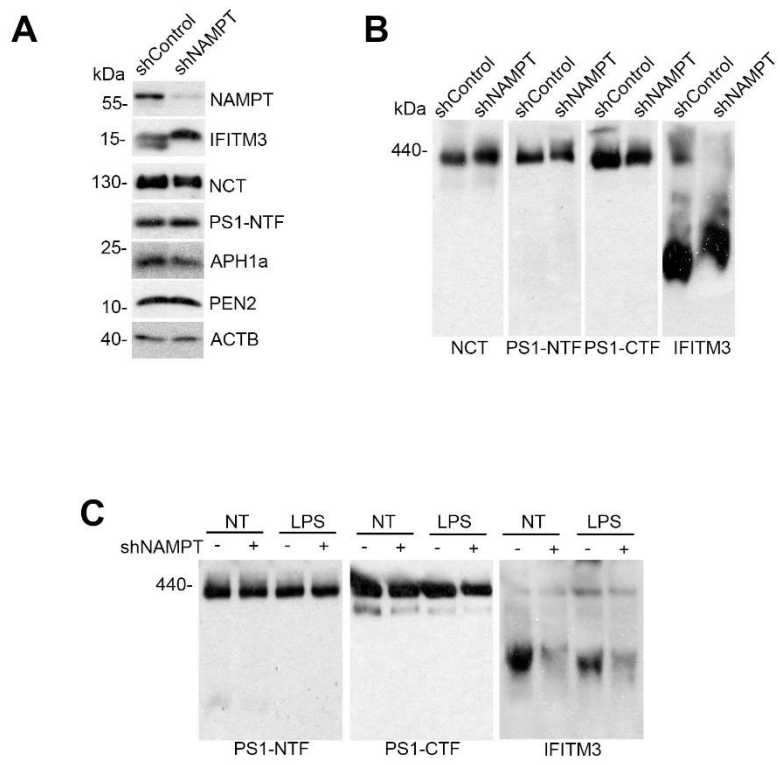
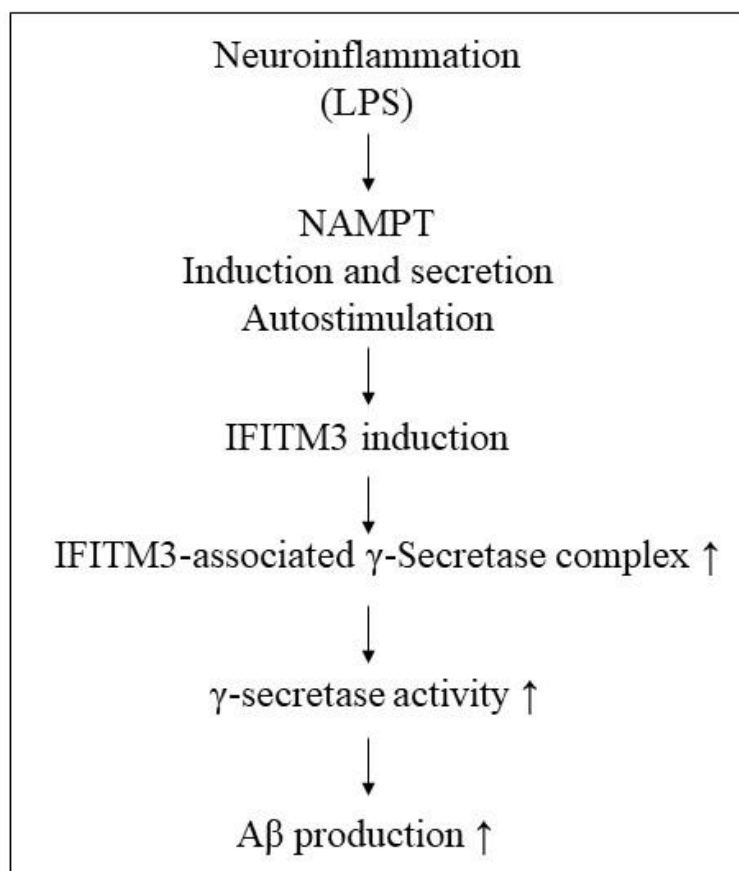


Figure II-16. Schematic diagram of the proposed molecular mechanism of NAMPT in AD pathogenesis.

Under inflammatory conditions, NAMPT expression is upregulated and secreted into the extracellular space. Extracellular NAMPT binds to IFITM3, a known presenilin regulator. Additionally, NAMPT autostimulates IFITM3 expression through NF- κ B signaling. The increase in IFITM3 levels promotes the formation of the IFITM3-associated γ -secretase complex. This regulation of complex composition results in elevated A β production, contributing to AD pathogenesis.



Discussion

NAMPT is a multifunctional protein primarily known for its role in NAD biosynthesis, where it catalyzes the rate-limiting step of nicotinamide conversion to nicotinamide mononucleotide (NMN). Beyond its enzymatic activity, NAMPT has recently gained attention for its extracellular roles in inflammation and immune modulation, acting as a cytokine-like molecule under pathological conditions (Alexander N Garcia et al., 2022; Belinda L Sun et al., 2023). This pro-inflammatory role aligns with the growing recognition of neuroinflammation as a critical contributor to AD pathogenesis, where systemic and localized inflammatory responses exacerbate disease progression. Importantly, recent therapeutic approaches have explored the use of neutralizing antibodies targeting extracellular NAMPT (eNAMPT) to mitigate inflammation in various disease models, highlighting its clinical relevance in inflammatory disorders. These strategies underscore the potential of NAMPT as both a biomarker and a therapeutic target, particularly in diseases characterized by chronic inflammation, such as AD.

Neuroinflammation is increasingly regarded as a pivotal risk factor for AD, with substantial evidence linking pro-inflammatory states to amyloid-beta ($A\beta$) accumulation and tau pathology. Among the key molecular processes in AD, γ -secretase plays a central role in generating $A\beta$ by cleaving the amyloid precursor protein (APP). Despite its importance, the mechanisms by which γ -secretase is regulated under inflammatory conditions remain poorly understood. Addressing this gap, my study identifies NAMPT as a novel γ -secretase regulator with dual roles in APP processing and inflammation.

NAMPT's role in AD was first suggested through a cell-based gain-of-function γ -secretase

reporter assay, which highlighted its capacity to enhance γ -secretase activity. Subsequent validation demonstrated that NAMPT is upregulated in both 3xTg AD mouse models and AD patient CSF and cortex, suggesting its potential relevance in disease pathology. Importantly, NAMPT selectively modulates γ -secretase without affecting α - or β -secretases, a characteristic that circumvents the side effects associated with broad γ -secretase inhibition, such as Notch signaling disruption.

Mechanistically, I reveal that NAMPT interacts with IFITM3, a known presenilin regulator (Ji-Yeun Hur et al., 2020), providing insights into how it may influence γ -secretase activity. NAMPT knockdown reduced IFITM3-associated γ -secretase complex levels, further supporting the hypothesis that NAMPT regulates γ -secretase through its interaction with IFITM3. Additionally, recombinant NAMPT treatment induced intracellular NAMPT and IFITM3 expression via NF- κ B signaling, suggesting that extracellular NAMPT might act as an upstream signal amplifying γ -secretase activity in neuroinflammatory conditions.

NAMPT's link to inflammation was further corroborated by in vivo LPS injection experiments, where NAMPT expression was induced in a dose-dependent manner. Higher LPS doses also upregulated IFITM3, indicating a coordinated inflammatory response involving these molecules. These data suggest that systemic inflammation not only upregulates NAMPT but also creates a permissive environment for its interaction with IFITM3, amplifying γ -secretase activity under pathological conditions.

The discovery that NAMPT enhances γ -secretase activity without disrupting Notch cleavage addresses a major limitation of current γ -secretase-targeted approaches. The selective regulation of APP processing positions NAMPT as a potential therapeutic target for reducing amyloid burden while sparing essential γ -secretase functions. This selectivity is further

supported by findings that NAMPT's enzymatic activity in NAD biosynthesis is dispensable for its γ -secretase regulatory role, emphasizing its non-canonical functions in protein-protein interactions and signaling. Moreover, the use of eNAMPT-neutralizing antibodies in inflammatory disease models further supports the therapeutic potential of targeting extracellular NAMPT to mitigate its role in inflammation and γ -secretase regulation.

Despite these advances, the precise molecular mechanisms by which NAMPT-IFITM3 interactions influence γ -secretase remain unclear. Additionally, the *in vivo* role of extracellular NAMPT, particularly in the neural environment, requires further exploration to understand its impact on amyloid pathology and cognitive outcomes. Future studies should also investigate the long-term effects of NAMPT modulation in AD mouse models, particularly in the context of neuroinflammation.

Limitations of the Study

This study highlights the role of NAMPT as a γ -secretase regulator and its potential relevance in Alzheimer's disease (AD) pathology. However, there are notable limitations that require further investigation. First, while a physical interaction between NAMPT and IFITM3 was demonstrated, the precise mechanism by which this interaction influences γ -secretase activity remains unclear. Whether this effect is mediated through changes in IFITM3-associated complex dynamics, conformational alterations, or downstream signaling pathways is not fully understood. Additionally, the study showed that extracellular NAMPT induces intracellular NAMPT and IFITM3 levels via NF- κ B signaling, yet it remains uncertain whether this induction directly regulates γ -secretase activity or reflects a broader inflammatory response.

Another limitation lies in the *in vivo* validation of NAMPT's role in AD-specific pathology. While LPS-induced NAMPT upregulation and its association with γ -secretase activity were observed in mouse models, direct evidence linking NAMPT to amyloid deposition or cognitive decline is lacking. Studies employing NAMPT-specific knockdown or overexpression in AD mouse models are needed to confirm its pathological relevance. Furthermore, the observed variability in NAMPT levels across human hippocampal tissue samples raises questions about its robustness as a biomarker for AD. Larger clinical studies are required to assess the consistency and translational potential of NAMPT as a diagnostic or therapeutic target.

The selective regulation of γ -secretase activity by NAMPT is another area requiring further exploration. While NAMPT does not affect Notch processing, the extent to which its function overlaps or is redundant with other inflammatory mediators remains unclear. Additionally, the broader implications of NAMPT's regulatory role in γ -secretase activity in non-inflammatory

contexts of AD have not been addressed. Understanding how microenvironmental factors influence NAMPT's function will provide greater insight into its role in AD progression.

To address these limitations, future studies should focus on the structural and biochemical characterization of the NAMPT-IFITM3 interaction, investigate the role of eNAMPT in vivo, and explore the broader inflammatory and metabolic networks involving NAMPT. Genetic modifications in advanced AD models and expanded clinical cohort studies will be critical in validating NAMPT's potential as a therapeutic target. Resolving these uncertainties will enhance the understanding of NAMPT's role in AD and open new avenues for targeted therapeutic strategies.

Conclusion

This study identifies two novel regulators of γ -secretase, PKM2 and NAMPT, each contributing to amyloid pathology in Alzheimer's disease (AD) through distinct mechanisms tied to metabolic and inflammatory pathways. These findings provide new insights into γ -secretase regulation under different pathological conditions.

PKM2 was revealed to transcriptionally upregulate A β 1-42, a core component of γ -secretase, thereby promoting its assembly and activity. This regulatory role, driven by transcriptional mechanisms rather than PKM2's metabolic functions, is particularly pronounced under hypoxic stress—a known AD risk factor. In vivo studies using 3xTg AD mice further validated PKM2's pathogenic role, showing increased amyloid-beta (A β) production, plaque burden, and cognitive decline with PKM2 overexpression, whereas its knockdown mitigated these effects. These findings position PKM2 as a critical regulator of γ -secretase and a potential therapeutic target for selective modulation of amyloidogenic processing.

NAMPT was shown to selectively enhance γ -secretase-mediated APP cleavage without affecting other substrates such as Notch, addressing a major limitation of broad γ -secretase inhibition. The regulatory role of NAMPT is independent of its enzymatic activity in NAD biosynthesis, emphasizing its non-canonical functions in protein-protein interactions and signaling. Mechanistically, NAMPT interacts with IFITM3, influencing IFITM3-associated γ -secretase complex levels, while extracellular NAMPT induces intracellular IFITM3 via

inflammatory signaling pathways. These findings underscore NAMPT's dual role as both an amyloidogenic regulator and a mediator of neuroinflammation, highlighting its relevance in AD pathogenesis.

Together, this study advances our understanding of γ -secretase regulation, with PKM2 and NAMPT representing distinct molecular mechanisms tied to hypoxic and inflammatory conditions, respectively. Both molecules emerge as promising therapeutic targets for AD, offering the potential to selectively modulate γ -secretase activity while sparing essential functions. Future investigations into their molecular mechanisms and therapeutic applications could pave the way for novel strategies to mitigate AD pathology.

Materials and Methods

Genome-wide functional screen using cDNA

Control vector (pCtrl) or each cDNA gene was co-transfected into cells along with reporter plasmids (pC99-TetOn and pTRE-GFP) encoding GFP following g-secretase-mediated cleavage of C99-TetOn. After 24 h, doxycycline (100 ng/ml) was added to cells for an additional 24 h. Putative cDNA clones, which exhibited green fluorescence under a fluorescence microscope (Olympus) were isolated. After the primary screening, luciferase activity-based g-secretase activity assays were used to quantitatively assess the clonal effect on γ -secretase activity (Han et al., 2014).

SDS-PAGE and western blot

Ice-cold PBS-washed cells were sonicated and solubilized in lysis buffer (100 mM HEPES pH 7.4, 150 mM NaCl, 1 mM EDTA, 1 % Triton X-100 and protease inhibitor cocktail). The amount of protein was measured by Bradford assay (Bio-Rad) and protein samples were denatured by mixing 2x sampling buffer (60 mM Tris pH 6.8, 2% SDS, 20% Glycerol, 10% 2-Mercaptoethanol, and 0.04% Bromophenol blue) followed by boiling for 10 min at 100C. The denatured protein samples were separated by sodium dodecyl sulfate polyacrylamide gel electrophoresis (SDS-PAGE) using SDS-PAGE gels (10 to 15% gels) and transferred to polyvinylidene fluoride membrane (PVDF) using semi-dry transfer device (Bio-Rad). Blots were blocked with 3% (w/v) BSA or 5% Milk in TBS-T buffer (25 mM Tris pH 7.5, 150 mM NaCl, and 0.05% Tween-20) for 30 min and incubated with indicated primary antibodies. The probed blots were detected by horseradish peroxidase-conjugated secondary antibodies for ECL analysis.

ELISAs

A β 40 and A β 42 levels in both culture medium and guanidine-HCl soluble brain tissue lysates were measured using ELISAs following the manufacturer's instructions

In vitro AICD generation assays

The conditioned cells were washed with ice-cold PBS and sonicated in buffer A (50 mM HEPES pH 7.4, 150 mM NaCl, 5 mM 1,10phenanthroline monohydrate, 2mM EDTA, 1 mM PMSF and 1 mM Leupeptin). The nuclear fraction was removed by centrifugation at 1,000 g for 10 min and remaining crude membrane fraction was harvested by further centrifugation at 10,000 g for 15 min. After washing with buffer A, the amount of total protein was quantified by Bradford assay (Bio-Rad). Same amount of protein under resuspended membrane homogenate was incubated for 2 - 16 h at 37 °C with or without γ -secretase inhibitor, Compound E (Comp.E,100mM).

BN-PAGE

Conditioned cells were washed with ice-cold PBS and sonicated in resuspension buffer (50 mM PIPES, pH 7.0, 250 mM sucrose, 1 mM EGTA, and protease inhibitor cocktail). The nuclear fraction was removed by centrifugation at 600 g for 10 minutes, and the microsomal fraction was isolated by further centrifugation of the remaining supernatant at 100,000 g for 60 minutes. Microsomal proteins were solubilized in solubilization buffer (50 mM PIPES, pH 7.0, 250 mM sucrose, 1 mM EGTA, 0.5% dodecylmaltoside, and protease inhibitor cocktail) for 60 minutes on ice. Solubilized proteins were then separated by BN-PAGE gel (8-10%).

γ -secretase activity assay

Luciferase reporter-mediated γ -secretase activity assays were conducted as described

previously (Gwon et al., 2012). Cells were co-transfected with pC99-GVP, pUAS-Luciferase, p β -galactosidase and either pCtrl or plasmids of tested genes. After 24 h, cell extracts were analyzed in luciferase assays following the manufacturer's instructions (Promega). To control for transfection efficiency, the luciferase activity was normalized to β -galactosidase activity.

β -secretase assays

Alkaline phosphatase reporter-mediated b-secretase activity assays were conducted as described below. Cells were co-transfected with pSEAP-APPa-muta and either pCtrl or a plasmid of tested genes for 24 h. pBACE1 was used as a positive control while selective BACE1 inhibitor, LY2886721 (20 mM), was co-treated as a negative control. Harvested medium was heat-inactivated for 1 h at 70 °C to minimize nonspecific enzymatic reaction and then reacted with alkaline phosphatase substrate for 1 hour at room temperature. The yellow reaction product was read at 405 nm.

α -secretase assays

α -Secretase assays were performed as described previously (Hanetal., 2014). Cells were incubated for 6 h in serum-free DMEM. The conditioned medium was harvested with cells, and aliquots containing same amount of protein from both the cells and medium concentrated with Amicon Ultra-15 (30 kDa molecular weight cutoff, Millipore) were subjected to SDS-PAGE and western blotting using an anti-sAPP α antibody (anti-6E10). α -Secretase activity was quantified by measuring the sAPP α signal relative to the APP level.

qPCR

Total RNAs were extracted by Trizol method. For reverse transcription, total RNA (2 mg) was reacted with oligo dT, dNTP, M-MLV reverse transcriptase and M-MLV buffer for 2 h

at 42 °C. The same amount of cDNA templates (100 ng) was reacted with SYBR green master mixture (Applied biosystems, 4367659) and specific qPCR primers (300 nM) by using qPCR machine (Thermo Fisher Scientific, QuantStudio3).

Glutaraldehyde cross-linking

Cell lysates in sodiumphosphate buffer (pH 7.3) containing 0.5% Triton X-100 and protease inhibitors were treated with 0.01% glutaraldehyde for 1 min at 37C. The reaction was terminated by adding 1 M Tris buffer (pH 8.0) to make a final concentration of 50 mM of Tris.

X-ChIP

Cells were cross linked with 5% formaldehyde for 5 min at room temperature. Glycine (final 125 mM) was added to stop the reaction followed by washing with ice-cold PBS (twice). The cell pellet was resuspended with nucleus-cytosol (N-C) fractionation buffer (5 mM HEPES pH7.4, 85 mM KCl, 0.5% NP-40, protease inhibitor cocktail) for 10 min and centrifuged at 500 g for 10 min. The nuclear fraction in RIPA buffer (10 mM Tris-Cl pH 8.0, 140 mM NaCl, 1 mM EDTA, 0.5 mM EGTA, 1% Triton X-100, 0.1% SDC, 0.1% SDS, 1 mM PMSF, 5mM NaF, 1 mM Na₃VO₄) was sonicated to shear DNA to an average fragment size of 500 bp and centrifuged at 13,000 g for 10 min. The harvested samples (10%) were used as input and remaining samples were subjected to immunoprecipitation by adding anti-FLAG antibody. The pulldown samples were washed with low salt buffer (50 mM HEPES pH 7.5, 150 mM NaCl, 0.1% SDC, 1% Triton X-100, 1 mM EDTA) twice followed by washing with high salt buffer (50 mM HEPES pH7.5, 500 mM NaCl, 0.1% SDC, 1% Triton X-100, 1mM EDTA). The samples were further washed with LiCl buffer (10 mM Tris-Cl pH 8.1, 250 mM NaCl, 0.5% NP-40, 0.5% SDC, 1 mM EDTA) and TE

buffer (10 mM Tris-Cl pH 8.1, 1 mM EDTA). To elute the DNA from the samples, elution buffer (0.1 M NaHCO₃, 1% SDS) was added and the samples were incubated on shaker for 15 min. The eluants were harvested following centrifugation at 5,000 g for 2 min and NaCl (final 200 mM) was added and incubated for overnight at 65 °C. The final DNA was purified by phenol-chloroform extraction method followed by qPCR analysis with indicated primers.

Behavior tests

All mouse experiments were performed according to animal protocols approved by the Seoul National University Institutional Animal Care and Use Committee (SNU IACUC). Behavior tests were performed as described previously with minor modification (Carroll et al., 2007; Clinton et al., 2007; Kam et al., 2013; Leger et al., 2013). Briefly, in the Y-maze test, each mouse was placed at the end of one arm of a triangular apparatus (32.5 cm length x 15 cm height) and allowed to explore freely for 7 min. An entry was counted when the mouse placed all four paws into an arm. The percent of spontaneous alterations was calculated as the ratio of the number of successful alterations to the total number of alterations. In the novel object recognition test, each mouse was habituated to two objects in a white plastic chamber (22 cm wide x 27 cm long x 30 cm high) being allowed to explore freely for 7 min (familiarization) before being return to its cage. After 6 h, the mouse was returned to the white chamber but one of the familiar objects was replaced with a novel object. Object recognition was then scored for 7 min. Recognition was scored based on time spent oriented toward the object at 1cm or less, sniffing the object, or touching it with the nose. In the passive avoidance test, an apparatus consisting of a light and a dark compartment (20 x 20 x 20 cm each) separated by a guillotine door was used.

During habituation, each mouse could move freely in the box for 5 min with the door open and was then returned to its cage. After 24 h, the mouse was placed in the light compartment. When all four paws of the mouse were inside the dark side of the box, the door was closed, and an electric foot shock (0.25 mA, 2 s) was delivered via floor grids. The mouse was then returned to its home cage. Then after 1.5 h, the mouse was returned to the light compartment, and the latency before the mouse entered the dark compartment was measured with a 5 min cut-off. All apparatuses and objects were cleaned with 70% ethanol before and after each trial.

Measurement of intracellular concentrations of pyruvate and ATP

Intracellular concentrations of pyruvate and ATP were measured using a Pyruvate Colorimetric/Fluorometric Assay Kit (BioVision, K609-100) and CellTiter Glo 2.0 Cell Viability Assay kit (Promega) following the manufacturer's instruction, respectively.

Immunohistochemistry

Perfused and fixed mouse brain tissues were frozen sectioned and fixed again for 30 min in 4% paraformaldehyde/PBS. Tissue samples were then permeabilized for 30 min in 0.5% Triton X-100 and blocked in 1% BSA/PBS for 1h before applying primary antibodies. The samples were incubated with anti-MOAB-2 (1:500), anti-4G8 (1:500) or anti-GFAP (1:500) for overnight at 4C, after which they were washed with PBS three times (5 min each). The samples were then incubated with FITC- or TRITC-conjugated secondary antibodies (1:500) for 1 h at room temperature. Finally, the samples were washed again as described above, mounted, and observed under a confocal microscope (Zeiss LSM700).

Lentivirus generation

Lenti-X 293T Cell Line was used to generate lentivirus. The cells were co-transfected with

PAX2, VSVG and either empty vector or PKM2 expression vector (CSII-EF-MCS-PKM2-Venus for overexpression; pGIPZ-shPkm2-IRES-tGFP and pGIPZ-shNamp1-IRES-tGFP for knockdown) using pMAX reagent following manufacturer's instruction. 60 h after transfection, harvested medium was filtered (40 mm pore) and incubated in lenti-X concentrator (Takara) for 30 min at 4°C. Finally, viral suspension was centrifuged at 1500 g for 45 min and viral pellet was resuspended with PBS and stored at -70°C.

Stereotaxic injection

Mouse was anesthetized with a mixture of zoletil, rompun and PBS (volume ratio Z15 : R10 : P75). The lentivirus (1.4×10^9 TU/ml ; TU, transduction unit) was stereotaxically injected into hippocampus (5 ml/hemisphere) with the following coordinates (anteroposterior = -2.1 mm from bregma, mediolateral = ± 1.8 mm, dorsoventral = -2.0 mm). After the injection, cannula was maintained for an additional 5 min for a complete absorption of the virus. The mouse brains were harvested for further experiments after 50 days of viral injection.

Primary neuron culture

Primary cortical neurons were prepared from embryonic day 16-17 (E16-17) mouse embryos (C57BL/6) in accordance with institutional animal care and use guidelines. Pregnant mice were sacrificed, and the embryos were quickly removed. Cortical tissue was dissected under sterile conditions in cold phosphate-buffered saline (PBS, pH 7.4). The meninges were carefully removed, and the cortical tissue was minced into small pieces using fine scissors.

The minced tissue was digested in 0.05% Trypsin-EDTA at 37°C for 10 minutes with gentle agitation. After digestion, the reaction was quenched by adding Neurobasal medium

containing 10% fetal bovine serum (FBS). The tissue was gently triturated using a fire-polished Pasteur pipette to obtain a single-cell suspension, which was then passed through a 70 μ m cell strainer to remove debris.

The neurons were plated on tissue culture plates pre-coated with Poly-L-lysine and cultured in Neurobasal medium supplemented with B-27, GlutaMAX, and penicillin-streptomycin. The cultures were maintained in a humidified incubator at 37°C with 5% CO₂, and half of the medium was replaced every 2-3 days with fresh supplemented Neurobasal medium. Neurons were allowed to differentiate for 7-14 days in vitro (DIV) before being used for experiments.

Primary astrocytes culture

Primary astrocytes were isolated from the cortices of postnatal day 0-2 (P0-P2) mouse pups (C57BL/6). The pups were decapitated, and their brains were dissected in cold phosphate-buffered saline (PBS, pH 7.4). The meninges were carefully removed, and the cortical tissue was minced into small pieces using fine scissors.

The minced tissue was digested in 0.05% Trypsin-EDTA at 37°C for 15 minutes with gentle agitation. After digestion, the tissue was triturated in Dulbecco's Modified Eagle Medium (DMEM) supplemented with 10% fetal bovine serum (FBS) and penicillin-streptomycin. The resulting cell suspension was passed through a 70 μ m cell strainer to remove debris. The cells were plated in T75 flasks and cultured in DMEM supplemented with 10% FBS. The cultures were maintained in a humidified incubator at 37°C with 5% CO₂. After 7-10 days, microglia and other non-astrocytic cells were removed by vigorous shaking followed by medium replacement. The astrocytes were allowed to reach confluence and were used for experiments between passages 1 and 2.

Primary microglia culture

Primary microglia were prepared from mixed glial cultures obtained from postnatal day 0-2 (P0-P2) mouse pups (C57BL/6). The brains were dissected in cold phosphate-buffered saline (PBS, pH 7.4), and the meninges were carefully removed. The cortical tissue was minced into small pieces and digested in 0.05% Trypsin-EDTA at 37°C for 15 minutes with gentle agitation.

The digested tissue was triturated in Dulbecco's Modified Eagle Medium (DMEM) supplemented with 10% fetal bovine serum (FBS) and penicillin-streptomycin, and the suspension was filtered through a 70 µm cell strainer. The cells were plated in T75 flasks and maintained in DMEM supplemented with 10% FBS at 37°C with 5% CO₂.

After 7-10 days of culture, the microglia were separated by shaking the flasks at 180 rpm for 1 hour at 37°C. The detached microglia were collected, centrifuged, and resuspended in fresh DMEM supplemented with 10% FBS. The isolated microglia were seeded in appropriate plates or dishes for experiments and were typically used within 24-48 hours after isolation.

Detection of secreted Amyloid beta

SH-SY5Y/APP^{sw} or SH-SY5Y/APP^{sIPS1dE9} cell lines were transfected with target protein-expressing genes for 48 hours. The conditioned culture medium was then harvested and centrifuged at 3000 g for 15 minutes to remove cell debris. After debris removal, the conditioned medium was incubated overnight with anti-6E10 or anti-A β antibodies. The antibody-protein complexes were pulled down using Protein G beads, and the samples were subjected to SDS-PAGE.

For A β detection, the acrylamide gel was transferred onto a nitrocellulose (NC) membrane. The transferred membrane was heated in a pressure cooker for 15 minutes to perform heat-

induced epitope retrieval. The NC membrane was then blocked and incubated with anti-6E10 or anti-A β antibodies, followed by enhanced chemiluminescence (ECL) detection.

Detection of extracellular NAMPT

The conditioned culture medium from various cell types was harvested and centrifuged at 3000 g for 15 minutes to remove cell debris. After debris removal, the conditioned medium was incubated overnight with anti-NAMPT or anti-IgG control antibodies. Extracellular NAMPT was pulled down using Protein G beads, and the samples were boiled at 95°C in a heat block before being subjected to SDS-PAGE.

Immunoprecipitation of membrane protein

For immunoprecipitation of membrane proteins, harvested cells were fractionated using a fractionation buffer to enrich membrane proteins. The crude membrane fraction was solubilized by adding 0.5% DDM and incubating for 2 hours at 4°C. The solubilized fraction was then incubated with target antibodies, and the antibody-protein complexes were pulled down using Protein G beads. The pulled-down samples were subjected to SDS-PAGE for analysis.

Recombinant His-NAMPT purification

BL21-Rosetta bacterial strain was transformed with the pET28-His-NAMPT (mouse form) vector. Transformed bacteria were grown in LB broth containing kanamycin (50 μ g/mL) at 37°C until the culture reached an optical density (OD₆₀₀) of 0.5. Protein expression was induced by adding 1 mM isopropyl β -D-1-thiogalactopyranoside (IPTG), and the culture was further incubated at 18°C for 3 hours to optimize protein folding.

The bacterial culture was harvested by centrifugation at 3000 g for 10 minutes at 4°C, and the pellet was resuspended in lysis buffer (20 mM Tris-HCl, 500 mM NaCl, 10 mM imidazole,

pH 8.0). To ensure efficient cell lysis, the suspension was sonicated on ice for 2 hours (10-second pulse on, 10-second pulse off) at 30% amplitude. The lysate was clarified by centrifugation at 12,000 g for 30 minutes at 4°C to remove cellular debris.

The supernatant containing the His-tagged NAMPT protein was incubated with Ni-NTA agarose beads (Qiagen) pre-equilibrated in lysis buffer overnight at 4°C with gentle rotation. The beads were washed five times with wash buffer (20 mM Tris-HCl, 500 mM NaCl, 10 mM imidazole, pH 8.0) to remove non-specifically bound proteins. His-NAMPT was eluted using elution buffer (20 mM Tris-HCl, 500 mM NaCl, 400 mM imidazole, pH 8.0).

The purity of the eluted protein was confirmed by SDS-PAGE followed by Coomassie staining, and protein concentration was measured by comparing with a BSA standard curve. After dialysis in PBS (1:1000, two exchanges), the purified protein was aliquoted and stored at -80°C for further experiments.

Quantification and statistical analysis

ImageJ and image studio software were used for quantification of signal intensity of western blotting and fluorescence intensity of immunostaining. Graph Pad Prism (version 8) software was used for the statistical analysis. For statistical analysis of the data from animal models and human tissue samples, the mean \pm SEM of the number of subjects was used. For statistical analysis of the data from in vitro cell culture experiments, the mean \pm SD of the number of biological replicates was used. For analysis of statistical significance, either Student's t tests, One-way ANOVA or Two-way ANOVA was used. The significance was defined with P values of less than 0.05 and denoted as asterisk (* $p < 0.05$; ** $p < 0.01$; *** $p < 0.005$; **** $p < 0.001$).

References

- Abdullah A Alghasham and Youssef A Barakat (2008) Serum visfatin and its relation to insulin resistance and inflammation in type 2 diabetic patients with and without macroangiopathy. *Saudi Med J* 29, 185-192
- Akira Nakajima, Daisuke Ibi, Taku Nagai et al. (2014) Induction of interferon-induced transmembrane protein 3 gene expression by lipopolysaccharide in astrocytes. *Eur J Pharmacol* 745, 166-175
- Alexander N Garcia, Nancy G Casanova, Daniel G Valera, Xiaoguang Sun, Jin H Song et al. (2022) Involvement of eNAMPT/TLR4 signaling in murine radiation pneumonitis: protection by eNAMPT neutralization. *Transl Res* 239, 44-57
- Amantha Thathiah, Katrien Horre, An Snellinx, Elke Vandeweyer et al. (2013) β -arrestin 2 regulates A β generation and γ -secretase activity in Alzheimer's disease. *Nature Medicine* 19, 43-49
- Anastasiou, D., Yu, Y.M., Israelsen, W.J., Jiang, J.K., Boxer, M.B., Hong, B.S., Tempel, W., Dimov, S., Shen, M., Jha, A., et al. (2012). Pyruvate kinase M2 activators promote tetramer formation and suppress tumorigenesis (vol 8, pg 839, 2012). *Nat. Chem. Biol.* 8, 1008.
- Anusha Jayaraman, Christian J Pike et al. (2015) Alzheimer's Disease and Type 2 Diabetes: Multiple Mechanisms Contribute to Interactions. *Curr Diab Rep* 14, 476
- Badawi, Y., Ramamoorthy, P., and Shi, H. (2012). Hypoxia-inducible factor 1 protects hypoxic astrocytes against glutamate toxicity. *ASN Neuro* 4, 231–241.

- Bart De Strooper, Robert Vassar and Todd Golde. (2010) The secretases: enzymes with therapeutic potential in Alzheimer disease. *Nat Rev Neurol*
- Belinda L Sun, Xiaoguang Sun, Carrie L Kempf et al. (2023) Involvement of eNAMPT/TLR4 inflammatory signaling in progression of non-alcoholic fatty liver disease, steatohepatitis, and fibrosis. *FASEB J.* 37
- Bigl, M., Brückner, M.K., Arendt, T., Bigl, V., and Eschrich, K. (1999). Activities of key glycolytic enzymes in the brains of patients with Alzheimer's disease. *J. Neural Transm. (Vienna)* 106, 499–511.
- Bluemlein, K., Grüning, N.M., Feichtinger, R.G., Lehrach, H., Kofler, B., and Ralser, M. (2011). No evidence for a shift in pyruvate kinase PKM1 to PKM2 expression during tumorigenesis. *Oncotarget* 2, 393–400.
- Bruno P. Imbimbo and Giuseppe A.M. Giardina. (2011) Gamma-Secretase Inhibitors and Modulators for the Treatment of Alzheimer's Disease: Disappointments and Hopes. *Current Topics in Medicinal Chemistry* 11 (12), 1555-70
- Butterfield, D.A., Poon, H.F., St Clair, D., Keller, J.N., Pierce, W.M., Klein, J.B., and Markesbery, W.R. (2006). Redox proteomics identification of oxidatively modified hippocampal proteins in mild cognitive impairment: insights into the development of Alzheimer's disease. *Neurobiol. Dis.* 22, 223–232.
- Carroll, J.C., Rosario, E.R., Chang, L., Stanczyk, F.Z., Oddo, S., LaFerla, F.M., and Pike, C.J. (2007). Progesterone and estrogen regulate Alzheimer-like neuropathology in female 3xTg-AD mice. *J. Neurosci.* 27, 13357–13365.
- Chen, Z., and Zhong, C. (2013). Decoding Alzheimer's disease from perturbed cerebral

- glucose metabolism: implications for diagnostic and therapeutic strategies. *Prog. Neurobiol.* 108, 21–43.
- Chen, F., Hasegawa, H., Schmitt-Ulms, G., Kawarai, T., Bohm, C., Katayama, T., Gu, Y., Sanjo, N., Glista, M., Rogaeva, E., et al. (2006). TMP21 is a presenilin complex component that modulates gamma-secretase but not epsilon-secretase activity. *Nature* 440, 1208–1212.
- Christofk, H.R., Vander Heiden, M.G., Wu, N., Asara, J.M., and Cantley, L.C. (2008). Pyruvate kinase M2 is a phosphotyrosine-binding protein. *Nature* 452, 181–186.
- Clinton, L.K., Billings, L.M., Green, K.N., Caccamo, A., Ngo, J., Oddo, S., McGaugh, J.L., and LaFerla, F.M. (2007). Age-dependent sexual dimorphism in cognition and stress response in the 3xTg-AD mice. *Neurobiol. Dis.* 28, 76–82.
- Eduardo García-Fuentes, Jose M García-Almeida, Juan García-Arnés, Sara García-Serrano et al. (2007) Plasma visfatin concentrations in severely obese subjects are increased after intestinal bypass. *Obesity* 15, 2391-5
- Fabrizio Montecucco, Michele Cea, Antonia Cagnetta, Patrizia Damonte et al. (2013) Nicotinamide phosphoribosyltransferase as a target in inflammation-related disorders. *Curr Top Med Chem* 13, 2930-8
- Francisco J. Martínez-Morcillo, Joaquín Cantón-Sandoval, Teresa Martínez-Menchón, Raúl Corbalán-Vélez, Pablo Mesa-del-Castillo et al. (2021) Non-canonical roles of NAMPT and PARP in inflammation
- Gao, X., Wang, H., Yang, J.J., Liu, X., and Liu, Z.-R. (2012). Pyruvate kinase M2 regulates gene transcription by acting as a protein kinase. *Mol. Cell* 45, 598–609.

Giorgia Colombo, Cristina Travelli, Chiara Porta and Armando A Genazzani. (2022)

Extracellular nicotinamide phosphoribosyltransferase boosts IFN γ -induced macrophage polarization independently of TLR4. *iScience* 25

Glenner, G.G., and Wong, C.W. (1984). Alzheimer's disease: initial report of the purification and characterization of a novel cerebrovascular amyloid protein. *Biochem. Biophys. Res. Commun.* 120, 885–890.

Gwon, A.R., Park, J.S., Arumugam, T.V., Kwon, Y.K., Chan, S.L., Kim, S.H., Baik, S.H., Yang, S., Yun, Y.K., Choi, Y., et al. (2012). Oxidative lipid modification of nicastrin enhances amyloidogenic γ -secretase activity in Alzheimer's disease. *Aging Cell* 11, 559–568.

Haass, C., and Selkoe, D.J. (2007). Soluble protein oligomers in neurodegeneration: lessons from the Alzheimer's amyloid beta-peptide. *Nat. Rev. Mol. Cell Biol.* 8, 101–112.

Han, J., Jung, S., Jang, J., Kam, T.I., Choi, H., Kim, B.J., Nah, J., Jo, D.G., Nakagawa, T., Nishimura, M., and Jung, Y.K. (2014). OCIAD2 activates γ -secretase to enhance amyloid β production by interacting with nicastrin. *Cell. Mol. Life Sci.* 71, 2561–2576.

Harada, K., Saheki, S., Wada, K., and Tanaka, T. (1978). Purification of four pyruvate kinase isozymes of rats by affinity elution chromatography. *Biochim. Biophys. Acta* 524, 327–339.

Hasegawa, S., Furuichi, T., Yoshida, T., Endoh, K., Kato, K., Sado, M., Maeda, R., Kitamoto, A., Miyao, T., Suzuki, R., et al. (2009). Transgenic up-regulation of alpha-CaMKII in forebrain leads to increased anxiety-like behaviors and aggression. *Mol. Brain* 2, 6.

- Hoshino, A., Hirst, J.A., and Fujii, H. (2007). Regulation of cell proliferation by interleukin-3-induced nuclear translocation of pyruvate kinase. *J. Biol. Chem.* 282, 17706–17711.
- Hsiao, K., Chapman, P., Nilsen, S., Eckman, C., Harigaya, Y., Younkin, S., Yang, F., and Cole, G. (1996). Correlative memory deficits, Abeta elevation, and amyloid plaques in transgenic mice. *Science* 274, 99–102.
- Ji-Yeun Hur, Georgia R. Frost, Xianzhong Wu, Christina Crump, Si Jia Pan et al. (2020) The innate immunity protein IFITM3 modulates γ -secretase in Alzheimer's disease. *Nature* 586, 735–740
- Jing Z, Xing J, Chen X, et al. (2014) Neuronal NAMPT is released after cerebral ischemia and protects against white matter injury. *J Cereb Blood Flow Metab* 34:1613–21
- Kam, T.I., Song, S., Gwon, Y., Park, H., Yan, J.J., Im, I., Choi, J.W., Choi, T.Y., Kim, J., Song, D.K., et al. (2013). FcγRIIb mediates amyloid- β neurotoxicity and memory impairment in Alzheimer's disease. *J. Clin. Invest.* 123, 2791–2802.
- Kazi Rahman, Charles A Coomer, Saliha Majdoul, Selena Y Ding et al. (2020) Homology-guided identification of a conserved motif linking the antiviral functions of IFITM3 to its oligomeric state. *eLife*
- Kress, S., Stein, A., Maurer, P., Weber, B., Reichert, J., Buchmann, A., Huppert, P., and Schwarz, M. (1998). Expression of hypoxia-inducible genes in tumor cells. *J. Cancer Res. Clin. Oncol.* 124, 315–320.
- Leger, M., Quiedeville, A., Bouet, V., Haelewyn, B., Boulouard, M., Schumann-Bard, P., and Freret, T. (2013). Object recognition test in mice. *Nat. Protoc.* 8, 2531–2537.
- Li, L., Zhang, X., Yang, D., Luo, G., Chen, S., and Le, W. (2009). Hypoxia increases A β generation by altering beta- and gamma-cleavage of APP. *Neurobiol. Aging* 30, 1091–

1098.

Li Qin Zhang, Djanybek M Adyshev, Patrick Singleton, Hailong Li et al. (2009) Interactions between PBEF and oxidative stress proteins-a potential new mechanism underlying PBEF in the pathogenesis of acute lung injury. *FEBS Lett* 582, 1802-1808

Liya Qin, Xuefei Wu, Michelle L Block, Yuxin Liu, George R Breese et al. (2010) Systemic LPS Causes Chronic Neuroinflammation and Progressive Neurodegeneration. *Glia* 55, 4530462

Luo, W., and Semenza, G.L. (2012). Emerging roles of PKM2 in cell metabolism and cancer progression. *Trends Endocrinol. Metab.* 23, 560–566.

Luo, W., Hu, H., Chang, R., Zhong, J., Knabel, M., O’Meally, R., Cole, R.N., Pandey, A., and Semenza, G.L. (2011). Pyruvate kinase M2 is a PHD3-stimulated coactivator for hypoxia-inducible factor 1. *Cell* 145, 732–744.

Masters, C.L., Simms, G., Weinman, N.A., Multhaup, G., McDonald, B.L., and Beyreuther, K. (1985). Amyloid plaque core protein in Alzheimer disease and Down syndrome. *Proc. Natl. Acad. Sci. USA* 82, 4245–4249.

Matrone, C., Ciotti, M.T., Mercanti, D., Marolda, R., and Calissano, P. (2008). NGF and BDNF signaling control amyloidogenic route and A β production in hippocampal neurons. *Proc. Natl. Acad. Sci. USA* 105, 13139–13144.

Mazurek, S. (2011). Pyruvate kinase type M2: a key regulator of the metabolic budget system in tumor cells. *Int. J. Biochem. Cell Biol.* 43, 969–980.

Mazurek, S., Zwerschke, W., Jansen-Dürr, P., and Eigenbrodt, E. (2001). Metabolic

cooperation between different oncogenes during cell transformation: interaction between activated ras and HPV-16 E7. *Oncogene* 20, 6891–6898.

Mazurek, S., Boschek, C.B., Hugo, F., and Eigenbrodt, E. (2005). Pyruvate kinase type M2 and its role in tumor growth and spreading. *Semin. Cancer Biol.* 15, 300–308.

Miao-Pei Chen, Fu-Mei Chung, Dao-Ming Chang, Jack C.-R. Tsai, Han-Feng Huang et al. (2006) Elevated Plasma Level of Visfatin/Pre-B Cell Colony-Enhancing Factor in Patients with Type 2 Diabetes Mellitus. *The Journal of Clinical Endocrinology & Metabolism* 91, 295-299

Michael S Wolfe. (2013) Alzheimer's γ -secretase under arrestin. *Nature Medicine* 19, 22-24

Noguchi, T., Inoue, H., and Tanaka, T. (1986). The M1- and M2-type isozymes of rat pyruvate kinase are produced from the same gene by alternative RNA splicing. *J. Biol. Chem.* 261, 13807–13812.

Noguchi, T., Yamada, K., Inoue, H., Matsuda, T., and Tanaka, T. (1987). The L- and R-type isozymes of rat pyruvate kinase are produced from a single gene by use of different promoters. *J. Biol. Chem.* 262, 14366–14371.

N P E Kadoglou, N Sailer, A Moutzouoglou, A Kapelouzou, H Tsanikidis et al. (2009) Visfatin (nampt) and ghrelin as novel markers of carotid atherosclerosis in patients with type 2 diabetes. *Exp Clin Endocrinol Diabetes* 118, 75-80

Nyabi, O., Bentahir, M., Horre, K., Herreman, A., Gottardi-Littell, N., Van Broeckhoven, C., Merchiers, P., Spittaels, K., Annaert, W., and De Strooper, B. (2003). Presenilins mutated at Asp-257 or Asp-385 restore Pen-2 expression and Nicastrin glycosylation but remain catalytically inactive in the absence of wild-type Presenilin. *J. Biol. Chem.*

278, 43430–43436.

Oakley, H., Cole, S.L., Logan, S., Maus, E., Shao, P., Craft, J., Guillozet-Bongaarts, A., Ohno, M., Disterhoft, J., Van Eldik, L., et al. (2006). Intraneuronal beta-amyloid aggregates, neurodegeneration, and neuron loss in transgenic mice with five familial Alzheimer's disease mutations: potential factors in amyloid plaque formation. *J. Neurosci.* 26, 10129–10140.

Oddo, S., Caccamo, A., Shepherd, J.D., Murphy, M.P., Golde, T.E., Kaye, R., Metherate, R., Mattson, M.P., Akbari, Y., and LaFerla, F.M. (2003). Triple-transgenic model of Alzheimer's disease with plaques and tangles: intracellular A β and synaptic dysfunction. *Neuron* 39, 409–421.

Ohta, K., Mizuno, A., Li, S., Itoh, M., Ueda, M., Ohta, E., Hida, Y., Wang, M.X., Furoi, M., Tsuzuki, Y., et al. (2011). Endoplasmic reticulum stress enhances γ -secretase activity. *Biochem. Biophys. Res. Commun.* 416, 362–366.

Periz, G., and Fortini, M.E. (2004). Functional reconstitution of gamma-secretase through coordinated expression of presenilin, nicastrin, Aph-1, and Pen2. *J. Neurosci. Res.* 77, 309–322.

Querfurth, H.W., and Laferla, F.M. (2010). Alzheimer's Disease REPLY. *N. Engl. J. Med.* 362, 1844–1845.

Roberson, E.D., and Mucke, L. (2006). 100 years and counting: prospects for defeating Alzheimer's disease. *Science* 314, 781–784.

Schägger, H., Cramer, W.A., and von Jagow, G. (1994). Analysis of molecular masses and oligomeric states of protein complexes by blue native electrophoresis and isolation of

- membrane protein complexes by two-dimensional native electrophoresis. *Anal. Biochem.* 217, 220–230.
- Selkoe, D.J., and Wolfe, M.S. (2007). Presenilin: running with scissors in the membrane. *Cell* 131, 215–221.
- Shen, C., Chen, Y., Liu, H., Zhang, K., Zhang, T., Lin, A., and Jing, N. (2008). Hydrogen peroxide promotes A β production through JNK-dependent activation of γ -secretase. *J. Biol. Chem.* 283, 17721–17730.
- Simone Torretta, Giorgia Colombo, Cristina Travelli, Sara Boumya et al. (2020) The Cytokine Nicotinamide Phosphoribosyltransferase (eNAMPT; PBEF; Visfatin) Acts as a Natural Antagonist of C-C Chemokine Receptor Type 5 (CCR5). *Cells* 9, 496
- Soucek, T., Cumming, R., Dargusch, R., Maher, P., and Schubert, D. (2003). The regulation of glucose metabolism by HIF-1 mediates a neuroprotective response to amyloid beta peptide. *Neuron* 39, 43–56.
- Steták, A., Veress, R., Ovádi, J., Csermely, P., Kéri, G., and Ullrich, A. (2007). Nuclear translocation of the tumor marker pyruvate kinase M2 induces programmed cell death. *Cancer Res.* 67, 1602–1608.
- Sun, X., He, G., Qing, H., Zhou, W., Dobie, F., Cai, F., Staufenbiel, M., Huang, L.E., and Song, W. (2006). Hypoxia facilitates Alzheimer's disease pathogenesis by up-regulating BACE1 gene expression. *Proc. Natl. Acad. Sci. USA* 103, 18727–18732.
- Thathiah, A., Spittaels, K., Hoffmann, M., Staes, M., Cohen, A., Horr , K., Vanbrabant, M., Coun, F., Baekelandt, V., Delacourte, A., et al. (2009). The orphan G protein-coupled receptor 3 modulates amyloid-beta peptide generation in neurons. *Science* 323, 946–

951.

Thathiah, A., Horré, K., Snellinx, A., Vandewyer, E., Huang, Y., Ciesielska, M., De Kloe, G., Munck, S., and De Strooper, B. (2013). β -arrestin 2 regulates A β generation and γ -secretase activity in Alzheimer's disease. *Nat. Med.* 19, 43–49.

Villa, J.C., Chiu, D., Brandes, A.H., Escorcía, F.E., Villa, C.H., Maguire, W.F., Hu, C.J., de Stanchina, E., Simon, M.C., Sisodia, S.S., et al. (2014). Nontranscriptional role of Hif-1 α in activation of γ -secretase and notch signaling in breast cancer. *Cell Rep.* 8, 1077–1092.

Wang, R., Zhang, Y.-W., Zhang, X., Liu, R., Zhang, X., Hong, S., Xia, K., Xia, J., Zhang, Z., and Xu, H. (2006). Transcriptional regulation of APH-1A and increased γ -secretase cleavage of APP and Notch by HIF-1 and hypoxia. *FASEB J.* 20, 1275–1277.

Wang, H.-J., Hsieh, Y.-J., Cheng, W.-C., Lin, C.-P., Lin, Y.S., Yang, S.-F., Chen, C.-C., Izumiya, Y., Yu, J.-S., Kung, H.-J., and Wang, W.C. (2014). JMJD5 regulates PKM2 nuclear translocation and reprograms HIF-1 α -mediated glucose metabolism. *Proc. Natl. Acad. Sci. USA* 111, 279–284.

Weiyi Xu, Le Li, Lilei Zhang. (2020) NAD⁺ Metabolism as an Emerging Therapeutic Target for Cardiovascular Diseases Associated with Sudden Cardiac Death (vol 11). *Front. Physiol*

Wilson, W.R., and Hay, M.P. (2011). Targeting hypoxia in cancer therapy. *Nat. Rev. Cancer* 11, 393–410.

X.-Q. ZHANG, J.-T. LU, W.-X. JIANG, Y.-B. LU, et al. (2015) Nampt inhibitor and metabolite protect mouse brain from cryo injury through distinct mechanism.

Neuroscience 291, 230-240

Yamada, K., and Noguchi, T. (1999). Nutrient and hormonal regulation of pyruvate kinase gene expression. *Biochem. J.* 337, 1–11.

Yang, W., Xia, Y., Hawke, D., Li, X., Liang, J., Xing, D., Aldape, K., Hunter, T., Alfred Yung, W.K., and Lu, Z. (2012). PKM2 phosphorylates histone H3 and promotes gene transcription and tumorigenesis. *Cell* 150, 685–696.

Yang Deng, Rui Duan, Wangli Ding, Qiuchen Gu et al. (2022) Astrocyte-derived exosomal nicotinamide phosphoribosyltransferase (Nampt) ameliorates ischemic stroke injury by targeting AMPK/mTOR signaling to induce autophagy. *Cell Death Dis* 13, 1057

Yash B. Joshi, Phillip F. Giannopoulos, Jin Chu, and Domenico Praticò. (2013) Modulation of LPS-induced memory insult, γ -secretase and neuroinflammation in 3xTg mice by 5-Lipoxygenase. *Neurobiol Aging* 35, 1024-1031

Zetterberg, H., Mörtberg, E., Song, L., Chang, L., Provuncher, G.K., Patel, P.P., Ferrell, E., Fournier, D.R., Kan, C.W., Campbell, T.G., et al. (2011). Hypoxia due to cardiac arrest induces a time-dependent increase in serum amyloid β levels in humans. *PLoS ONE* 6, e28263.

Zhongjie Sun, Han Lei and Zhong Zhang. (2013) Pre-B cell colony enhancing factor (PBEF), a cytokine with multiple physiological functions. *Cytokine growth factor rev* 24, 433-442

Zwerschke, W., Mazurek, S., Massimi, P., Banks, L., Eigenbrodt, E., and Jansen-Dürr, P. (1999). Modulation of type M2 pyruvate kinase activity by the human papillomavirus type 16 E7 oncoprotein. *Proc. Natl. Acad. Sci. USA* 96, 1291–1296.

국문초록

알츠하이머병(Alzheimer's disease, AD)은 감마 세크리테이즈(γ -secretase) 복합체에 의해 매개되는 아밀로이드 베타(A β)의 축적이 특징적이다. 감마 세크리테이즈는 아밀로이드 베타 생성에 핵심적 역할을 하지만, 저산소증 및 신경염증과 같은 병리학적 조건 하에서 그 조절 기작은 잘 알려져 있지 않다. 본 연구에서는 감마 세크리테이즈의 두 가지 새로운 조절자인 pyruvate kinase M2 (PKM2)와 nicotinamide phosphoribosyltransferase (NAMPT)를 탐구하여 저산소증에 의한 스트레스 매개 유전자 발현과 염증 경로가 아밀로이드 베타 생성 과정에 어떻게 관여하는지에 대한 분자적 기전을 규명하였다.

PKM2는 감마 세크리테이즈의 핵심 구성 요소인 A β -1a의 전사 조절을 통해 감마 세크리테이즈 활성을 조절하는 것으로 나타났다. PKM2의 핵 내 이합체는 전사 공동활성인자로 작용하여 히스톤 변형 및 HDAC3 억제를 통해 A β -1a 전사를 조절하였다. 시험관 실험과 생체 실험을 통해 감마 세크리테이즈 활성 증가, 아밀로이드 베타 생성 및 알츠하이머병 모델 마우스에서의 기억력 손상에서 PKM2의 역할이 확인되었다. 특히 PKM2의 조절 역할은 대사적 기능과는 독립적이며, 알츠하이머병 병리에서 PKM2의 전사 조절 역할을 강조한다.

NAMPT는 인간 시크리션 유전자 집합을 이용한 스크리닝을 통하여 동정되었으며, 알파 세크리테이즈 (α -secretase) 또는 베타 세크리테이즈 (β -secretase) 및 Notch 절단에 영향을 미치지 않고 감마 세크리테이즈 활성을 선택적으로 증가시

키는 것으로 나타났다. 알츠하이머병 마우스 모델과 환자 뇌척수액에서 NAMPT 수준은 질병 진행과 상관관계를 보이며 증가하였다. 분자기전으로 NAMPT는 presenilin 조절자인 IFITM3와 상호작용하며, 세포외 NAMPT(extracellular NAMPT)는 NF- κ B 신호 경로를 통해 IFITM3 발현을 유도하였다. 이러한 결과는 NAMPT가 염증 매개자이자 감마 세크리테이즈 조절자로서의 역할을 수행함을 강조한다.

결론적으로, 본 연구는 PKM2와 NAMPT가 알츠하이머병 병리학에서 각각 스트레스 매개 유전자 발현과 염증 경로를 통하여 감마 세크리테이즈를 조절하는 새로운 활성 조절자임을 밝히고 있다. 이 연구 결과는 감마 세크리테이즈 조절에 대한 새로운 통찰을 제공하며, PKM2와 NAMPT가 알츠하이머병 치료의 잠재적 표적이 될 수 있음을 제안한다.

주요어: 알츠하이머병, 감마 세크리테이즈, 아밀로이드 베타, PKM2, NAMPT, 저산소증, 신경염증

학번: 2017-25409